Naval Command,
Control and Ocean
Surveillance Center RDT&E Division San Diego, CA
92152-5001

Technical Document 2496
May 1993

A Discrepancy in the CCIR Report 322-3 Radio Noise Model

The Probable Cause and a Recommended Solution

David B. Sailors

Technical Document 2496
May 1993

A Discrepancy in the CCIR Report 322-3 Radio Noise Model

The Probable Cause and a Recommended Solution

David B. Sailors

NAVAL COMMAND, CONTROL AND
OCEAN SURVEILLANCE CENTER
RDT&E DIVISION
San Diego, California 92152-5001

J. D. FONTANA, CAPT, USN
Commanding Officer

R. T. SHEARER
Executive Director

ADMINISTRATIVE INFORMATION

This work was funded by the Space and Naval Warfare Systems Command (SPAWAR) and the Office of Naval Research (ONR) under program elements 0601153N and OMN, respectively.

Released by
J. A. Ferguson, Head
Ionospheric Branch

Under authority of
J. H. Richter, Head
Ocean and Atmospheric
Sciences Division

LH

SUMMARY

OBJECTIVE

Determine the probable cause for a discrepancy in the Consultative Committee International Radio (CCIR) Report 322-3 radio noise model and recommend a course of action to overcome the discrepancy.

RESULTS

The basis for this discrepancy was found to be in the procedure used to prepare the measured noise data for the determination of a global numerical representation of the 1-MHz data. The procedure followed in the development of the model was to determine correction factors to the old CCIR model for each measurement site, to interpolate these corrections to a 100-latitude by 84-longitude grid for each time block/season, to add the correction factors at each grid point to corresponding values for the old CCIR model, and finally to numerically map the resulting data for each time block and season. Nineteen locations were used in the final model. Four sites used in the original CCIR model were not used. These include Bill, Wyoming; Byrd Station, Antarctica; Ibadan, Nigeria; and Thule, Greenland. As no correction factors were obtained for these locations nor a correction factor of zero used, the interpolation algorithm used to obtain the 100-latitude by 84-longitude grid of correction factors supplied other values. For Bill, Wyoming, the result is not too serious; but for the other three sites, the error is at some seasons and time of day serious. For Thule, Greenland, the maximum and minimum errors in the correction contours were 10.1 and −10.8 dB, respectively. For Ibadan, Nigeria, the maximum and minimum errors were 12.5 and −1.5 dB, respectively. For Byrd Station, Antarctica, the maximum and minimum errors were 12.0 and 3.0 dB, respectively. Examination of the geographical extent of these errors reveals that the error is not confined to the measurement location but in fact is very large. It was found that the error as a function of frequency was diurnally dependent. An error of 10 dB at 1 MHz was more serious at another frequency during local daytime than at night. Finally, the absence of the data locations affected the accuracy of the interpolation itself.

RECOMMENDATIONS

1. Use the CCIR Report 322-3 atmospheric noise model with caution, especially in the northern and southern high latitudes, the Arabian Peninsula, northern Africa, and the mid-Atlantic Ocean area. In these areas, consider using the original CCIR Report 322 model.

2. A three-step process should be followed to develop a new 1-MHz atmospheric noise model.

3. First, obtain correction factors for additional locations to increase the accuracy of the interpolation.

4. Second, test the method of interpolation against a benchmark.

5. Third, use the Zacharisen and Jones numerical mapping technique applied in local time to develop the final model.

6. Consider using a latitude transformation to increase the accuracy of the numerical mapping technique.

7. Submit a corrected model to the CCIR.

CONTENTS

FIGURES

CONTENTS (continued)

CONTENTS (continued)

CONTENTS (continued)

CONTENTS (continued)

CONTENTS (continued)

CONTENTS (continued)

TABLES

CONTENTS (continued)

1.0 INTRODUCTION

Recently, Bowen and Fraser-Smith (1992) made a comparison of measured 32-kHz radio noise amplitudes with the current CCIR Report 322-3 noise model predictions (CCIR, 1988). They found that the greatest discrepancies between the measured and predicted amplitudes were observed at the two northern high-latitude stations (Søndre Strømfjord and Thule, Greenland), where on some occasions the predicted values were nearly five times greater than the measured values. On the other hand, there was moderately good agreement between the measured and predicted values at a southern high-latitude site (Arrival Heights, Antarctica). The best agreement was observed at middle to low latitudes. The data used to make these comparisons were measured by a ELF/VLF measurement system (Fraser-Smith et al., 1987).

CCIR Report 322-3 is an output document of the CCIR XVIth Plenary Assembly held in Dubrovnik, Yugoslavia, in 1986. It was produced by the International Working Party (IWP) 6/2 of CCIR Study Group 6. It was based on the work of Spaulding and Washburn (1985).

Because of the worldwide acceptance of the CCIR Report 322-3 radio noise model, an attempt was made to determine the cause of this discrepancy. It was found that the basis for this error was in the procedure used to prepare the measured noise data for the determination of a global numerical representation of the 1-MHz data. Since the contour plots of the 1-MHz radio noise in CCIR Report 322-3 were in turn generated from the numerical representation thus developed, they are also in error.

The purpose of this report is to present the probable cause of the CCIR 322-3 radio noise model. First, a description of how CCIR Report 322 (CCIR, 1964) noise models have been and are currently used is presented to provide an understanding on how a systematic error in a 1-MHz noise model could appear at other frequencies. Second, the development process of the current CCIR Report 322-3 model is presented so that the cause of the error can be fully understood. Then the cause itself of the error in the 1-MHz model along with the frequency dependence of this error for three measurement sites are presented. Next, a proposed process to develop a corrected 1-MHz noise model is discussed. Finally, conclusions and recommendations are made. Primary among these recommendations is that the CCIR 322-3 radio noise model should be used with caution until a replacement for the 1-MHz model has been developed. In particular the northern and southern high latitudes, the Arabian Peninsula, northern Africa, and the mid-Atlantic appear to be the most inaccurate areas. Europe, Asia, the Indian Ocean, Australia, and the western Pacific from Asia to the date line appear to be the most accurate areas.

2.0 THE CCIR 322 NOISE MODEL

The CCIR Report 322 radio noise model is based upon measurements of average power levels (f_a) of atmospheric noise on a worldwide basis starting in 1957 by the Central Radio Propagation Laboratory (CRPL). Figure 1 shows the locations of the 16 identical recording stations used to measure this data. At most of the sites the data continued to be measured until 1966. Measurements of F_a, the external noise figure defined as 10 log f_a; V_d, the dB difference between the average voltage and the rms voltage; and L_d, the dB difference between the antilog of the envelope voltage and the rms voltage, were made using a bandwidth of 200 Hz. The measurements were made on frequencies of essentially 0.013, 0.051, 0.160, 0.495, 2.5, 5, 10, and 20 MHz. Amplitude probability distribution (APD) measurements were made at some of the sites. These data were analyzed and published in a series of reports known as the NBS Technical Note Series 18 (Crichlow et al., 1959; Crichlow, Disney, & Jenkins, 1967). For each frequency and location, the month-hour median value of F_a along with D_u and D_l, the upper and lower decile values, were given. The median values of V_d and L_d were also given. In addition, the corresponding season-time block values of these parameters were given for the four seasons, winter (December, January, and February), spring (March, April, May), summer (June, July, August), and fall (September, October, and November), and six 4-hour time blocks (0000–0400, etc.). The atmospheric noise data used to develop CCIR Report 322 were the data from July 1957 through October 1961.

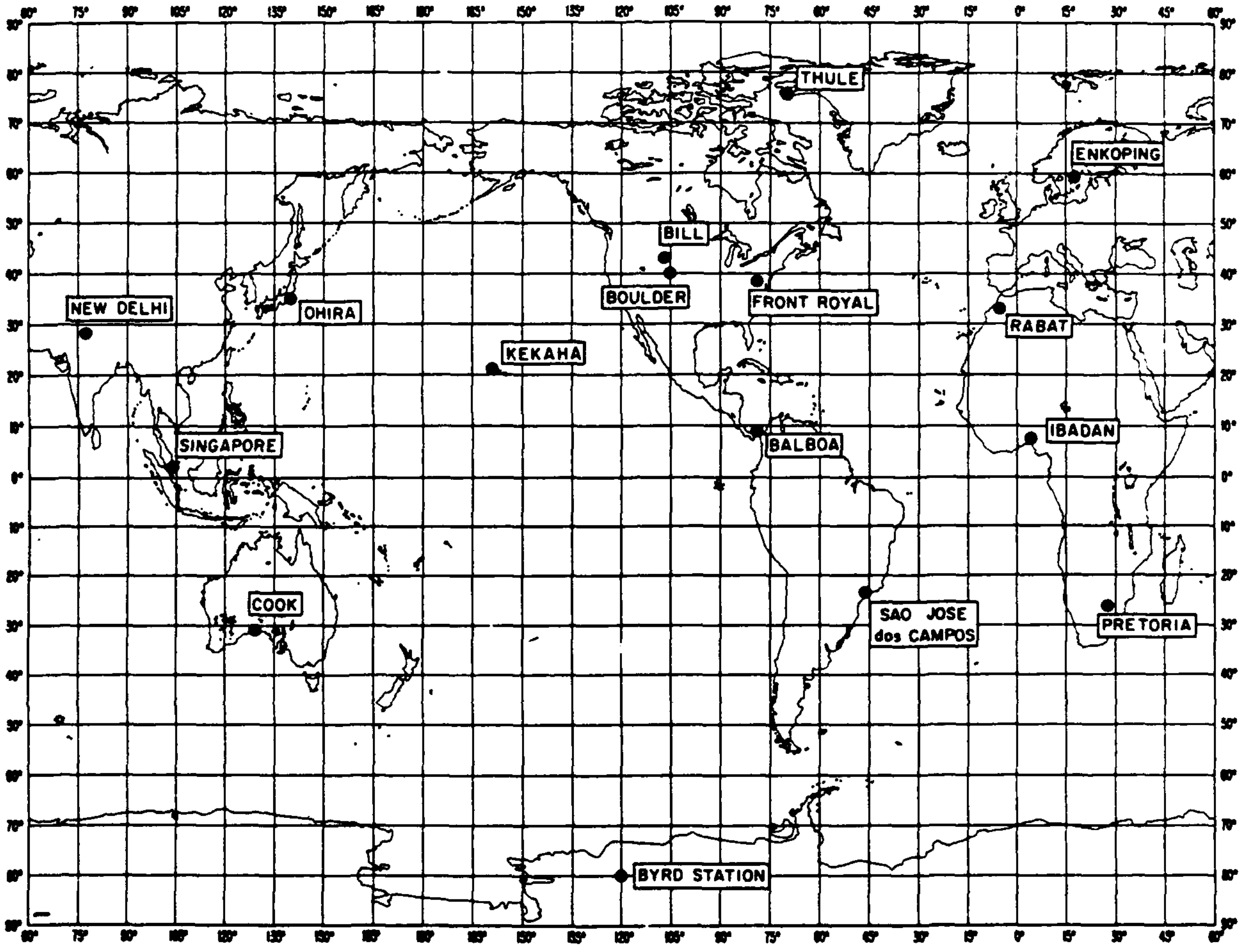

Figure 1. Radio noise recording stations used to obtain data used to develop the original CCIR Report 322.

The CCIR Report 322 radio noise model consists basically of two parts: a 1-MHz model and a frequency-dependence model. Figure 2 shows figure 5A of CCIR Report 322. This figure gives F_{am}, the median noise figure, at 1 MHz as a function of latitude and longitude for the winter season and the time block 1200–1600. Since this map is for a particular season, there is a discontinuity at the equator (corresponding to winter being 6 months apart in the northern and southern hemispheres). To obtain F_{am} at a particular frequency, figure 3 (figure 5B of CCIR Report 322) is used to convert the 1-MHz value to any frequency between 10 kHz and 30 MHz. Finally, the median value of V_d, V_{dm}, and the statistical variations of F_a about its median value F_{am}, are given also in figure 3 (figure 5C in CCIR Report 322).

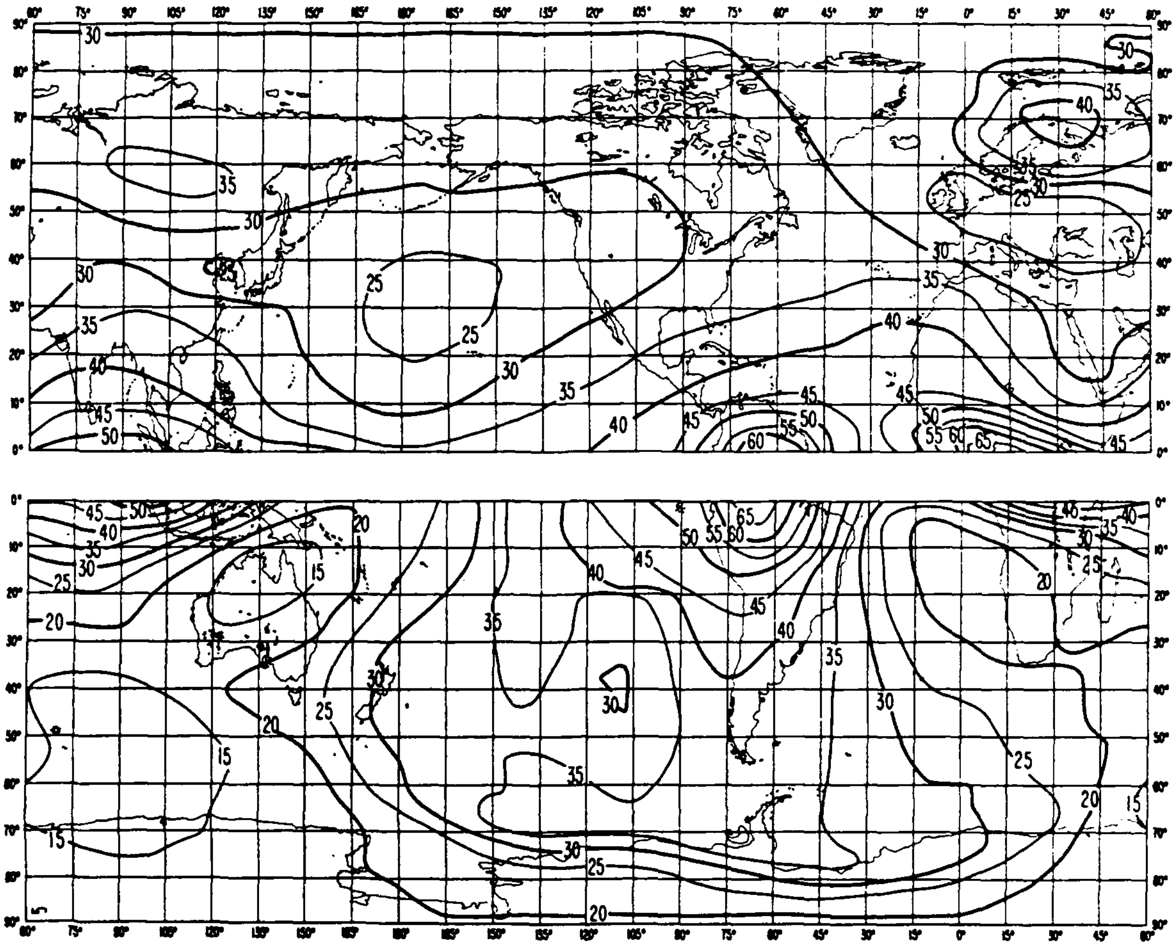

FIGURE 5A

Expected values of atmospheric radio noise, F_{am},
(db above kT_0b at 1 Mc/s)
(Winter; 1200–1600 h.)

Figure 2. Figure 5A from CCIR Report 322.

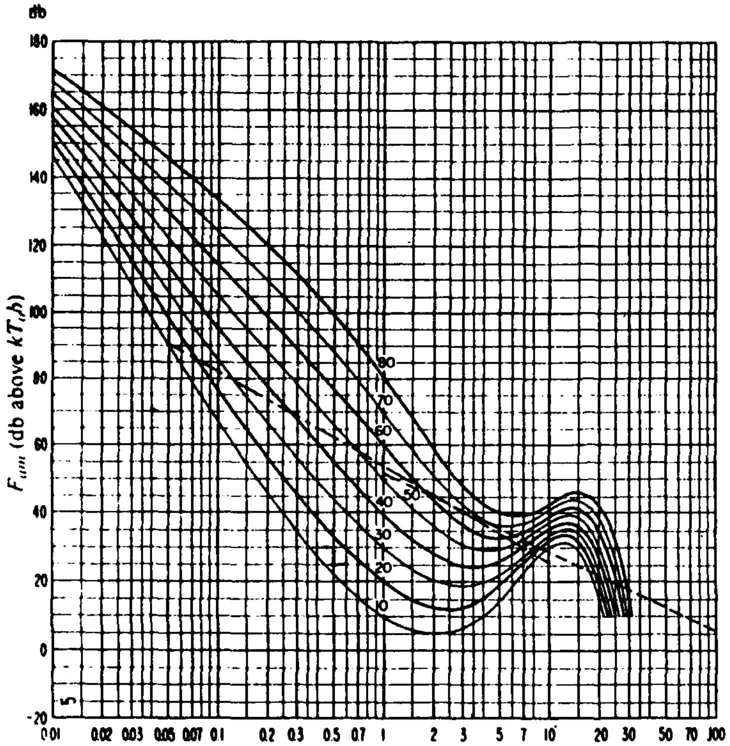

Frequency (Mc/s)

FIGURE 5B

Variation of radio noise with frequency
(Winter; 1200–1600 h.)

——— Expected values of atmospheric noise
—·—·— Expected values of man-made noise at a quiet receiving location
- - - - Expected values of galactic noise

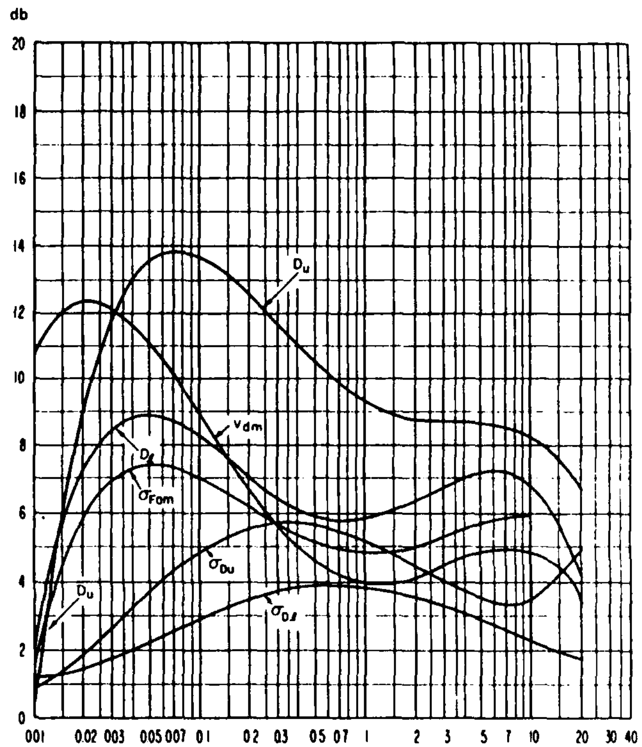

Frequency (Mc/s)

FIGURE 5C

Data on noise variability and character
(Winter; 1200–1600 h.)

σ_{Fam} = Standard deviation of values of F_{am}
D_u = Ratio of upper decile to median value, F_{am}
σ_{Du} = Standard deviation of values of D_u
D_l = Ratio of median value, F_{am}, to lover decile
σ_{Dl} = Stantard deviation of value of D_l
V_{dm} = Expected value of median deviation of average voltage. The values shown are for a bandwidth of 200 c/s.

Figure 3. Figure 5B and 5C from CCIR Report 322.

Numerical representation of CCIR Report 322 is available. The first by Lucas and Harper (1965) covers the frequency range from 10 kHz to 30 MHz. This representation was obtained by numerically mapping values obtained from the CCIR 322 1-MHz maps themselves, rather than by numerically mapping the original data points (84-longitude by 100-latitude grid points) that produced the CCIR Report 322 maps. Spaulding and Washburn (1985) report an rms error of 2 dB with maximum errors up to approximately 10 dB for the Lucas and Harper model due to the method of obtaining the representation. The Lucas and Harper numerical representation of the frequency variation of F_{am}, D_u, and D_l are "precise," as these numerical routines were used to produce these particular parts of CCIR Report 322. World maps of 1-MHz atmospheric noise in universal time are available (Zacharisen & Jones, 1970). These universal time maps were obtained by numerical mapping using the "original" Report 322 data. Also, using the original data to plot the contour maps in Report 322, Sailors and Brown (1982, 1983) developed a simplified atmospheric noise model suitable for use on minicomputers.

3.0 THE PROCESS USED TO DEVELOP THE CCIR REPORT 322-3 RADIO NOISE MODEL

CCIR Report 322 was developed using data available through October 1961. Since then much additional data has become available. Data from the original worldwide network continued to be measured through 1966. Many years of data from 10 Soviet measurement locations became available along with data from Thailand for March 1966 through February 1968 (Chindahporn and Younker, 1968). All of this data was analyzed and updated set of atmospheric radio noise estimates produced, essentially in the CCIR Report 322 format (Spaulding and Washburn, 1985). These estimates are new 1-MHz contour maps corresponding to figure 2. This model was submitted to the CCIR IWP 6/2 by the United States as a replacement for CCIR Report 322-2 (CCIR Report 322 reprinted with a revised text and title, but with the same atmospheric noise estimates). This became CCIR Report 322-3.

This section attempts to describe the process used to develop the new CCIR Report 322-3. It is based on the work of Spaulding and Washburn (1985) and Spaulding (1992*).

3.1 THE NEW DATA

The worldwide network locations and new locations are given in table 1 (table 1 in Spaulding and Washburn (1985)). Figure 4 (figure 7 in Spaulding and Washburn (1985)) is a repeat of figure 1, but with the new locations added.

In the development of the new noise model, data from Thule, Greenland, and Byrd Station, Anarctica, were not used. These data were not used because it was assumed that the data were generally contaminated by high levels of man-made noise.

For a number of years, the Soviet Union operated a network of 10 noise measurement stations. Data from these measurement locations within the old Soviet Union were available from the World Data Center (National Oceanic and Atmospheric Administration, Boulder, CO). Raw data were available on microfilm for periods of time from mid-1958 through 1965, coincident with the measurements of the worldwide network. The parameters that were measured were different from those discussed for the worldwide network above. The analysis and use of the Soviet data are discussed next.

* Spaulding, A. D., private communication, May 1992.

Table 1. Atmospheric noise measurement locations.

WORLDWIDE NETWORK LOCATIONS (CCIR 322).

Balboa, Canal Zone	79.5W,	9.0N
Bill, Wyoming	105.2W,	43.2N
Boulder, Colorado	105.1W,	40.1N
Byrd Station, Antarctia	120.0W,	80.0S
Cook, Australia	130.4E,	30.6S
Enkoping, Sweden	17.3E,	59.5N
Front Royal, Virginia	78.2W,	38.8N
Ibadan, Nigeria	3.9E,	7.4N
Kekaha, Hawaii	159.7W,	22.0N
New Delhi, India	77.3E,	28.8N
Ohira, Japan	140.5E,	35.6N
Pretoria, South Africa	28.3E,	25.8S
Rabat, Morocco	6.8W,	33.9N
San Jose, Brazil	45.8W,	23.3S
Singapore	103.8E,	1.3N
Thule, Greenland	68.7W,	76.6N

NEW LOCATIONS

Alma Ata, USSR	76.92E,	43.25N
Ashkhabad, USSR	8.3E,	37.92N
Irkutsk, USSR	104.5E,	52.0N
Khabarovsk, USSR	135.0E,	50.0N
Kiev, USSR	30.3E,	50.72N
Laem Chabang, Thailand	100.9E,	13.05N
Moscow, USSR	37.32E,	55.47N
Murmansk, USSR	35.0e,	69.0N
Simferopol, USSR	34.03E,	45.02N
Sverdlovsk, USSR	61.07E,	56.73N
Tbilisi, USSR	40.0E,	41.72N

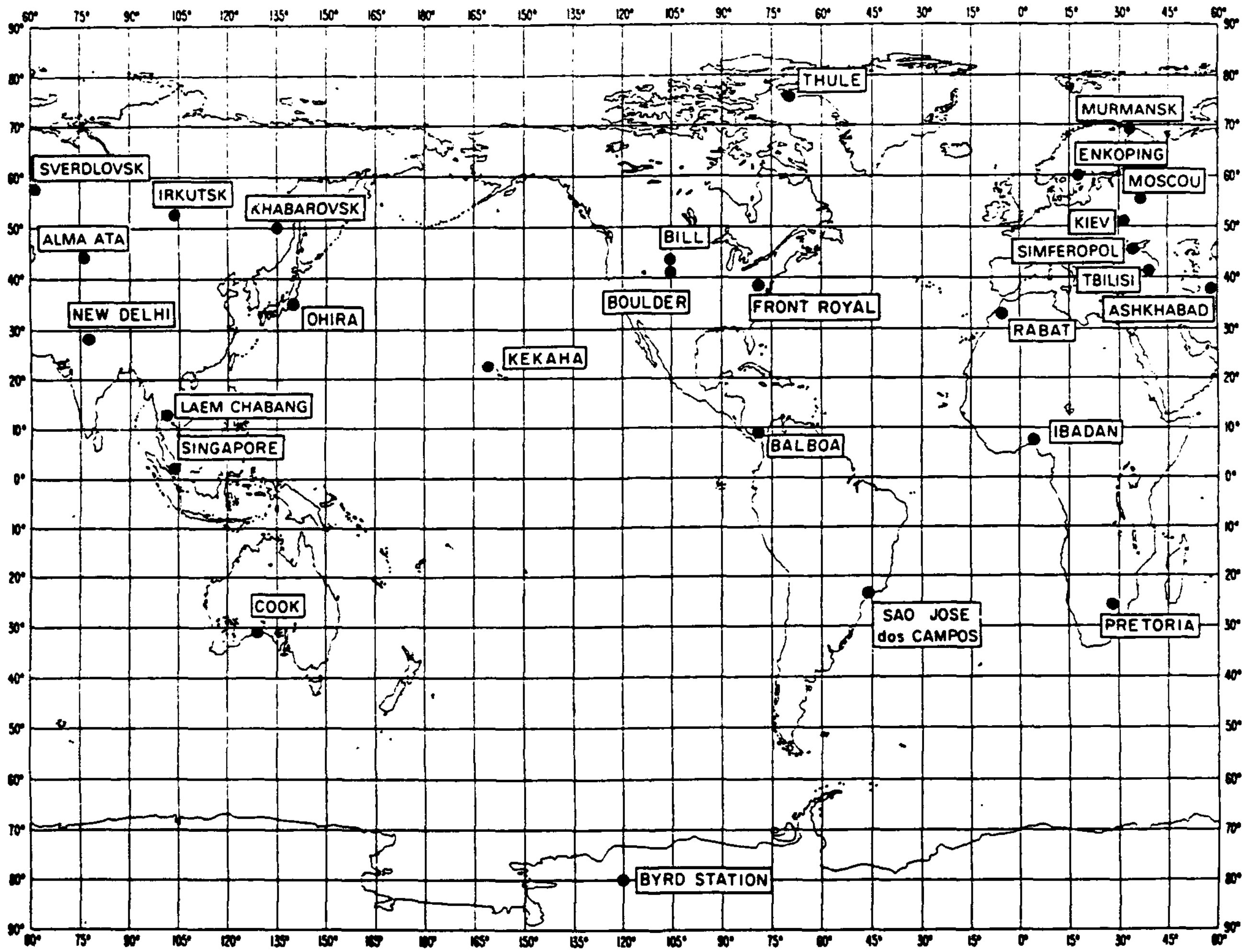

Figure 4. Radio noise recording locations used by Spaulding and Washburn (1985).

3.2 ANALYSIS OF THE SOVIET DATA

The Soviet atmospheric noise measurement program was organized and controlled by Dr. Ja. I. Likhter (Izmiran, P. O., Akademgorodok, Moscow Region, USSR). Dr. Likhter supplied to Dr. A. Donald Spaulding of the Institute for Telecommunication Sciences in Boulder, Colorado, detailed information on the measurement equipment used and the definitions of the various parameters measured. On each measurement frequency, a measurement lasted approximately 2 minutes, and measurements were taken 3 hours apart each day. On many days, no measurements were made. The voltage levels (given in field strength, µV/m) that were exceeded 2, 10, 20, 30, 40, 50, 60, 70, 80, and 90 percent of the time were recorded. On the microfilm, these are noted by $E_{0.02}$ to $E_{0.9}$. Because of averaging in the receiving and, perhaps, the short

measurement time, this set of measurements, unfortunately, did not appear to Dr. Spaulding to be APD measurements, and they did not seem to correspond to other Soviet APD results. Also, most of the energy in the atmospheric noise process is contained at levels that occur less than 2 percent of the time. The peak value was also recorded and appears on the microfilm. Also on the microfilm is another parameter noted as E_{on}. This parameter has no physical meaning in itself but is a level set by the equipment operator, below which the other levels ($E_{0.02}$, etc.) were recorded. Spaulding and Washburn (1985) determined that E_{on} would serve as a good approximation to the rms level (f_a), and the parameter E_{on} was used by them in the analysis of the Soviet data.

The median value of E_{on} was determined for all measurements at a given location and for a given measurement frequency for the hours and months within each of the twenty-four 3-month/4-hour time blocks. This median value of E_{on} is in μV/m. The antennas used at the Soviet measurement sites were 5-meter vertical rods over a ground plane. To go from field strength to F_{am}, therefore, it was necessary to use equation 1, the equation for the vertical component of the rms field strength for a short ($h << \lambda$) grounded vertical monopole,

$$E_n = F_a + 20 \log f_{MHz} + B - 95.5 \text{ dB } (1\ \mu\text{V/m}) \quad (1)$$

where E_n is the field strength [dB (1 μV/m)] in bandwidth b (Hz), f_{MHz} is the center frequency in MHz, and $B = 10 \log b$. The bandwidths used were approximately 250 Hz at frequencies below 1.5 MHz, and 1000 Hz at frequencies at or above 1.5 MHz, with some variation at some of the measurement sites. For example, a 1000-Hz bandwidth was sometimes used at 0.750 and 1 MHz. Throughout the Soviet data, there were missing months, time, frequencies, some months with only a few days of measurements. All in all, there was a large body of usable data. Some of the data was analyzed by The Institute for Telecommunication Sciences (ITS) in Boulder, Colorado, but most of the data were analyzed by the Naval Ocean Systems Center (NOSC)* in San Diego, California.

The measurement frequencies and other information are summarized in Spaulding and Washburn (1985) for each of the Soviet measurement locations.

The analysis involved determining, at each frequency, for each 3-month period and 4–hour time block, the median value of all the data. These median values at the various frequencies were then used to determine the approximate 1-MHz F_{am} value. This value was then used to obtain a correction value to the CCIR Report 322 value. Figure 5 (figure 8 in Spaulding and Washburn (1985)) shows an example for Moscow for June, July, August (Northern Hemisphere summer) and 1600–2000 hours. Note that the noise curve for a quiet receiving location falls considerably below the analyzed median values. A computer algorithm was developed that determined the atmospheric noise

* Now the RDT&E Division of the Naval Command, Control and Ocean Surveillance Center.

frequency variation curve that "best" fit the data. However, since the median value at some frequencies was based on much more data than the value of the other frequencies for a location, time block, and season (due to missing data and some frequencies being stressed at some locations); "fitting" process was generally done by hand (visually). On figure 5, the "best" fitting frequency law curve was determined to be 72 dB. The CCIR Report 322 value is 65 dB. Hence, a value of +7 dB can be used to correct the atmospheric noise predicted by CCIR Report 322 at Moscow during the summer at 1600–2000 hours. Figure 6 (figure 9 in Spaulding and Washburn (1985)) shows an example for Moscow for the period November, December, January, 0800–1200 hours. Atmospheric noise would be expected to be low during this period (winter morning) and could possibly be contaminated by man-made noise at the higher frequencies. For the higher frequencies, 350 kHz and above, the figure shows a typical man-made noise curve at a level to be expected for a quiet receiving site. Because of this contamination possibility, the lower frequencies are used to determine the frequency law curve. In this case, the frequency law curve for 31 dB was determined. The CCIR Report 322 value was 29 dB, resulting in a required correction of +2 dB.

3.3 CORRECTIONS TO CCIR REPORT 322 1-MHz F_{am} VALUES

The procedure illustrated above for figures 5 and 6 for determining the corrections to be made to CCIR Report 322 was followed by Spaulding and Washburn (1985) to obtain corrections for each location and for each 3-month/4-hour time block. Tables 2 through 5 give the corrections determined using this procedure for each of the four seasons. Each table contains a correction for each time block and for each station in table 1 except for those noted below. The "correction" is the difference between the CCIR Report 322 1-MHz F_{am} value and the corresponding value determined using the above procedure from the data.

For certain stations listed in table 1, no corrections were determined. No correction values were obtained for Thule, Greenland, and Byrd Station, Antarctica, because it was assumed that the data were contaminated by man-made noise. Since there were no data from Ibadan, Nigeria, beyond the data used in the development of CCIR Report 322, no correction was used for Ibadan. Because the corrections for Bill, Wyoming, and Boulder, Colorado, were essentially identical, only corrections for Boulder were used. Corrections were used for only 6 Soviet locations rather than 10. Simferopol, Sverdlovsk, Tbilisi, and Kiev either had only small amounts of usable low-frequency data necessary to determine the proper 1-MHz F_{am} value or were close to other measurement locations. The data at these four Soviet locations were analyzed to ascertain that the corrections agreed with those used at nearby locations, namely Moscow and Ashkhabad. For Murmansk for the March, April, May season and for the four time blocks 0400–0800, 0800–1200, 1200–1600, and 1600–2000 hours, the data were highly irregular and confusing. Hence, Spaulding and Washburn (1985) decided not to attempt to obtain any correction values for Murmansk for these four periods (see table 3).

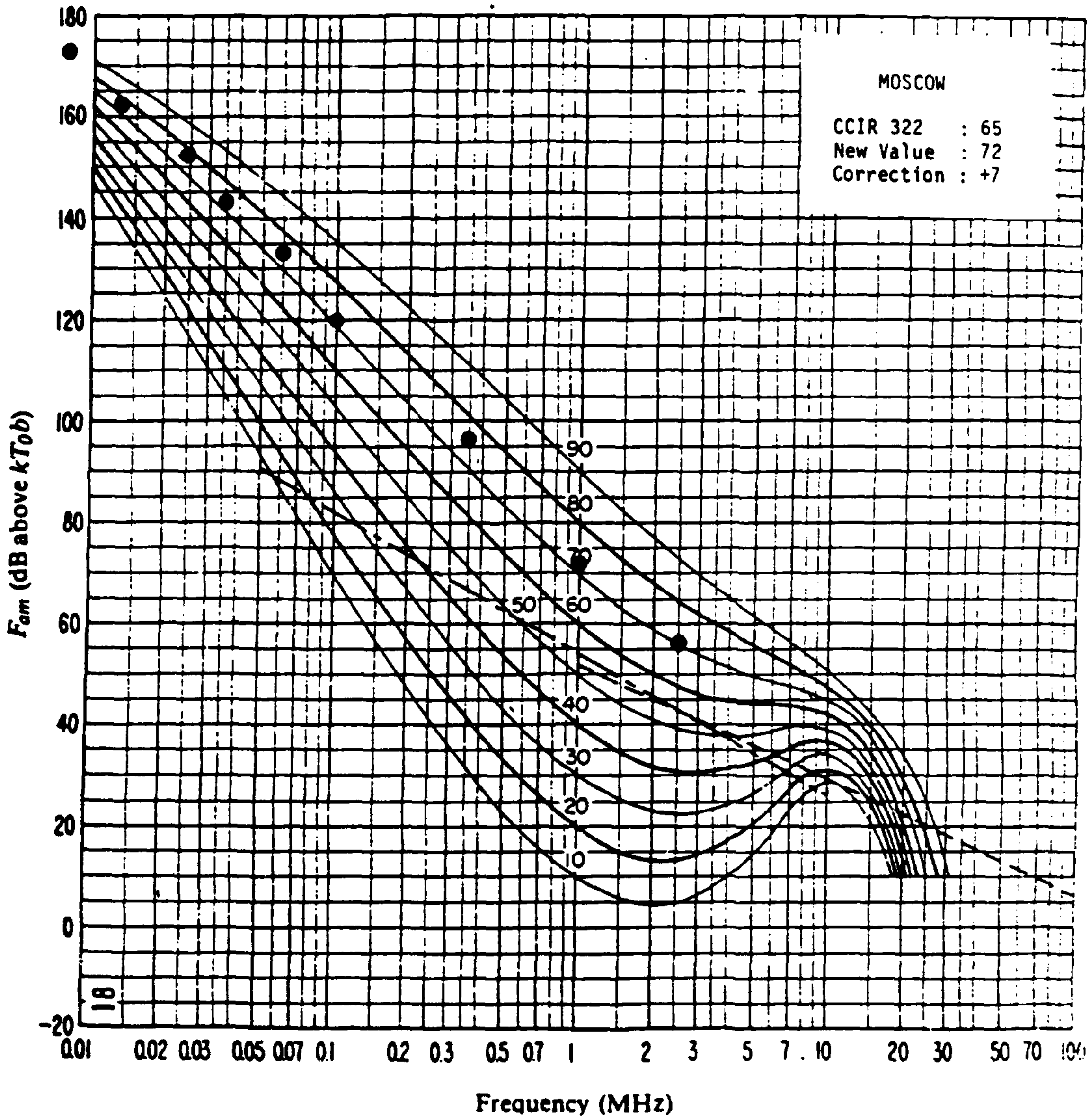

Figure 5. Determination of 1-MHz F_{am} value for Moscow, June, July, August, 1600–2000 hours (Spaulding and Washburn, 1985).

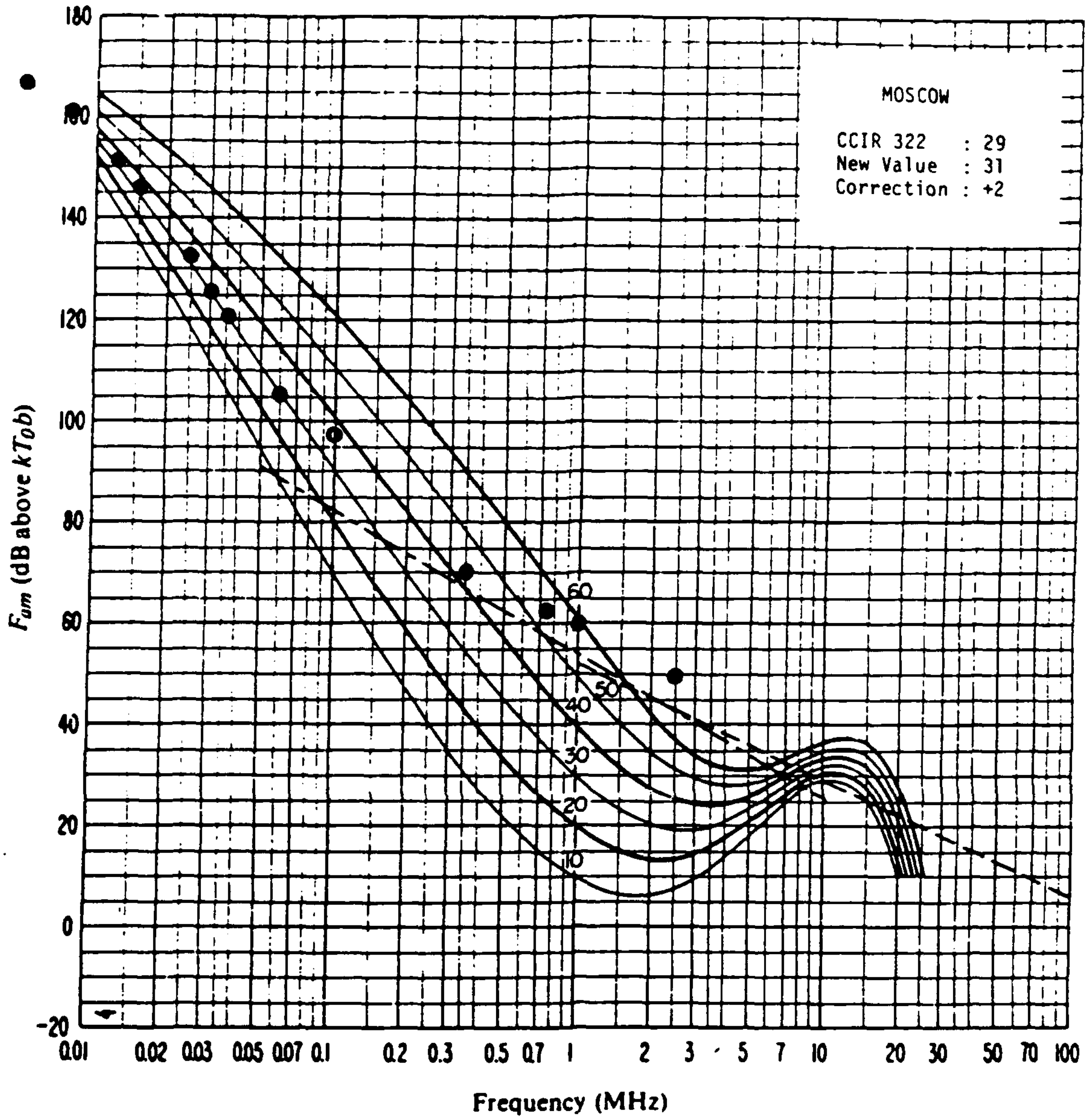

Figure 6. Determination of 1-MHz F_{am} value for Moscow, December, January, February, 1000–1200 hours (Spaulding and Washburn, 1985).

Because the original contour maps in CCIR Report 322 were produced directly from a grid of equally spaced 84-longitude by 100-latitude points for each time block/season, the next step in the analysis was to translate the correction data for the 19 sites to this same 84-by-100 lattice. Then data for a new noise model were found simply by adding the corrections point-by-point for the grid point of original data.

To do this, Spaulding and Washburn (1985) used an interpolation method due to Dr. Charles L. Lawson (1982, 1984) for interpolating scattered data over a sphere. This method first constructs a triangular grid over a surface (in this case the Earth)

using a given set of points as vertices (in this case the 19 data points in tables 2 through 5). Then continuous first partial derivatives are estimated by the method at each vertex using local quadratic least squares approximations to given data values at nearby vertices. The method for interpolation then uses six Hermite cubic interpolations along arcs of great circles. Figures 7 through 30 are the resultant contour maps of the 24 (four 3-month periods, six 4-hour time blocks) 100-by-84 correction grids produced by Spaulding and Washburn. These maps show the changes to the CCIR Report 322 to be made. There are substantial corrections in some areas as could also be seen by examining tables 2 through 5. The correction maps are presented in terms of 3-month periods rather than as season (which results in a discontinuity at the equator) as in CCIR Report 322.

Table 2. Corrections (dB) to CCIR Report 322 1-MHz F_{am} values for December, January, and February (Spaulding and Washburn (1985)).

PLACE	LOCATION	LOCAL TIME					
		00–04	04–08	08–12	12–16	16–20	20–24
Alma Ata	76.9E, 43.2N	−7	−6	+6	+5	−3	−6
Irkutsk	104.5E, 52.0N	−21	−25	−7	−15	−25	−25
Khabarovsk	135.0E, 50.0N	−19	−15	−8	−7	−20	−20
New Delhi	77.3E, 28.8N	−13	+7	+17	+17	+8	+11
Ohira	140.5E, 35.6N	+7	+7	+8	+12	+11	11
Thailand	100.9E, 13.0N	+14	+15	+24	+18	+17	+15
Singapore	103.8E, 1.3N	0	+6	12	+9	+5	+1
Kekaha	159.7W, 22.0N	+5	+10	+8	+15	+5	+5
Boulder	105.1W, 40.1N	+5	+4	+7	+14	+7	+8
Front Royal	78.2W, 38.8N	−1	+2	+3	+8	0	0
Balboa	79.5W, 9.0N	+3	+6	+7	+9	+7	+2
Rabat	6.8W, 33.9N	+2	+4	+3	+8	+2	+4
Enkoping	17.3E, 59.5N	+12	+10	−1	+8	+7	+7
Murmansk	35.0E, 69.0N	+8	+5	+7	+9	+7	+7
Moscow	37.3E, 55.5N	+4	+3	+2	+4	0	−1
Ashkabad	58.3E, 37.9N	−9	−1	−5	−5	−6	−12
Cook	130.4E, 30.6S	+2	−3	+6	+1	+6	+3
San Jose	45.8W, 23.3S	+2	0	+2	+2	+4	+3
Pretoria	28.3E, 25.8S	−4	+8	−4	+1	+5	−8

Table 3. Corrections (dB) to CCIR Report 322 1-MHz F_{am} values for March, April, and May (Spaulding and Washburn (1985)).

PLACE	LOCAL TIME	LOCATION					
		00–04	04–08	08–12	12–16	16–20	20–24
Alma Ata	76.9E, 43.2N	–7	–4	–5	–8	–2	–5
Irkutsk	104.5E, 52.0N	–12	–7	–5	+5	+4	–14
Khabarovsk	135.0E, 50.0N	–15	–6	–7	+1	–1	–21
New Delhi	77.3E, 28.8N	+6	+10	+15	+9	+12	+7
Ohira	140.5E, 35.6N	+2	+4	+15	+12	+7	+2
Thailand	100.9E, 13.0N	+6	+9	+14	+17	+10	+8
Singapore	103.8E, 1.3N	+3	+5	+16	+13	+10	+5
Kekaha	159.7W, 22.0N	+6	+8	+11	+13	+5	+6
Boulder	105.1W, 40.1N	+3	+5	+7	+2	+8	+3
Front Royal	78.2W, 38.8N	–3	–1	–5	–5	–3	+1
Balboa	79.5W, 9.0N	+4	+5	+9	+5	+6	+4
Rabat	6.8W, 33.9N	+1	+4	+3	–5	0	0
Enkoping	17.3E, 59.5N	0	0	+3	–1	–5	+2
Murmansk	35.0E, 69.0N	+3					+4
Moscow	37.3E, 55.5N	+4	0	0	–2	0	–4
Ashkabad	58.3E, 37.9N	+2	+1	–3	+2	–4	+2
Cook	130.4E, 30.6S	+3	+9	+5	+8	+4	+5
San Jose	45.8W, 23.3S	+2	+3	+5	+7	+3	+7
Pretoria	28.3E, 25.8S	+3	+2	+11	+9	+11	–1

Table 4. Corrections (dB) to CCIR Report 322 1-MHz F_{am} values for June, July, and August (Spaulding and Washburn (1985)).

PLACE	LOCATION	LOCAL TIME					
		00–04	04–08	08–12	12–16	16–20	20–24
Alma Ata	76.9E, 43.2N	–4	0	–8	–6	–2	–3
Irkutsk	104.5E, 52.0N	–20	–6	–11	0	–4	–15
Khabarovsk	135.0E, 50.0N	–10	–4	–8	+1	+2	–12
New Delhi	77.3E, 28.8N	+8	+17	+11	+4	+10	+8
Ohira	140.5E, 35.6N	+2	+5	+11	+10	+9	+3
Thailand	100.9E, 13.0N	+11	+15	+15	+18	+13	+8
Singapore	103.8E, 1.3N	+4	+11	+15	+15	+10	+2
Kekaha	159.7W, 22.0N	+9	+6	+2	+2	–6	+4
Boulder	105.1W, 40.1N	+2	+8	+7	+10	+12	+6
Front Royal	78.2W, 38.8N	–8	–4	+4	–11	–10	–1
Balboa	79.5W, 9.0N	–10	+9	+12	+1	+3	+4
Rabat	6.8W, 33.9N	0	+3	+2	–16	–4	0
Enkoping	17.3E, 59.5N	+5	+6	–4	–7	–4	–7
Murmansk	35.0E, 69.0N	–2	+8	–1	+5	+10	–2
Moscow	37.3E, 55.5N	–2	0	–2	+2	+7	–6
Ashkabad	58.3E, 37.9N	+2	–4	–7	–8	–3	–3
Cook	130.4E, 30.6S	+5	+7	+12	+11	+10	+6
San Jose	45.8W, 23.3S	–4	+5	+11	+10	+9	0
Pretoria	28.3E, 25.8S	+12	+11	+20	+22	+16	+17

Table 5. Corrections (dB) to CCIR Report 322 1-MHz F_{am} values for September, October, and November (Spaulding and Washburn (1985)).

PLACE	LOCATION	LOCAL TIME					
		00–04	04–08	08–12	12–16	16–20	20–24
Alma Ata	76.9E, 43.2N	–4	–3	–2	–8	–7	–9
Irkutsk	104.5E, 52.0N	–22	–20	–15	–15	–20	–20
Khabarovsk	135.0E, 50.0N	–19	–10	–8	–9	–12	–18
New Delhi	77.3E, 28.8N	+5	+8	+9	–4	+6	+5
Ohira	140.5E, 35.6N	+6	+4	+12	+9	+9	+7
Thailand	100.9E, 13.0N	+5	+11	+20	+12	+9	+7
Singapore	103.8E, 1.3N	+7	+11	+20	+14	+7	+7
Kekaha	159.7W, 22.0N	+1	+5	0	+2	0	+2
Boulder	105.1W, 40.1N	+2	+7	+12	+10	+9	+3
Front Royal	78.2W, 38.8N	–2	+3	+4	–1	–2	–1
Balboa	79.5W, 9.0N	0	+4	+14	+12	+5	0
Rabat	6.8W, 33.9N	+5	+9	+11	+3	+6	+5
Enkoping	17.3E, 59.5N	+2	+4	0	+4	0	+3
Murmansk	35.0E, 69.0N	–5	+2	–2	+3	+1	–2
Moscow	37.3E, 55.5N	0	+3	+3	–2	–2	+2
Ashkabad	58.3E, 37.9N	+3	+5	–6	–4	–2	0
Cook	130.4E, 30.6S	–1	+2	+11	+10	+4	+4
San Jose	45.8W, 23.3S	+4	+6	+12	+6	+3	+2
Pretoria	28.3E, 25.8S	+3	+9	+9	+6	+8	+4

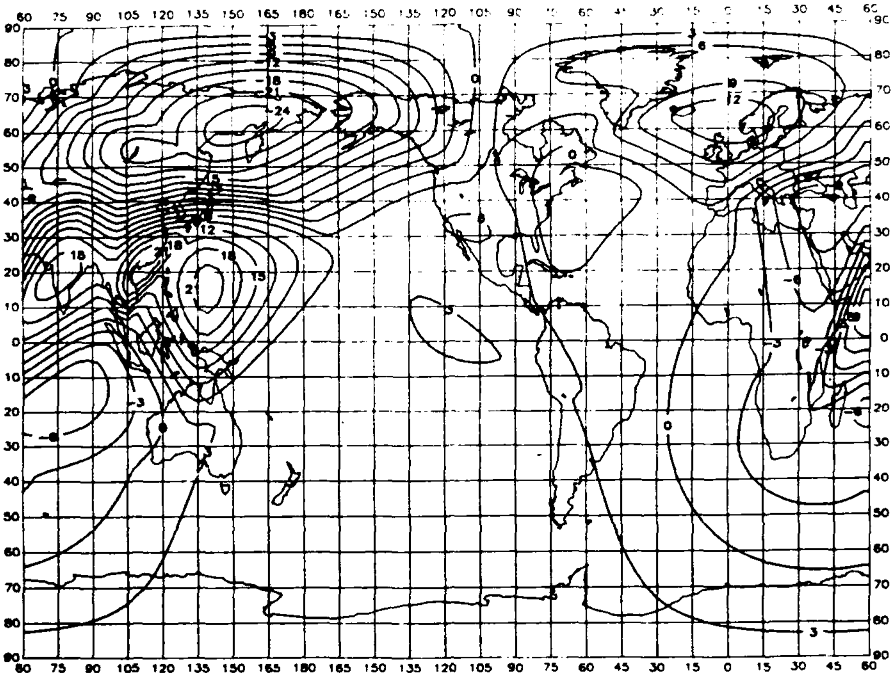

Figure 7. Corrections (dB) to original CCIR Report 322 1-MHz F_{am} estimates, December, January, February, 0000-0400 hours (Spaulding and Washburn, 1985).

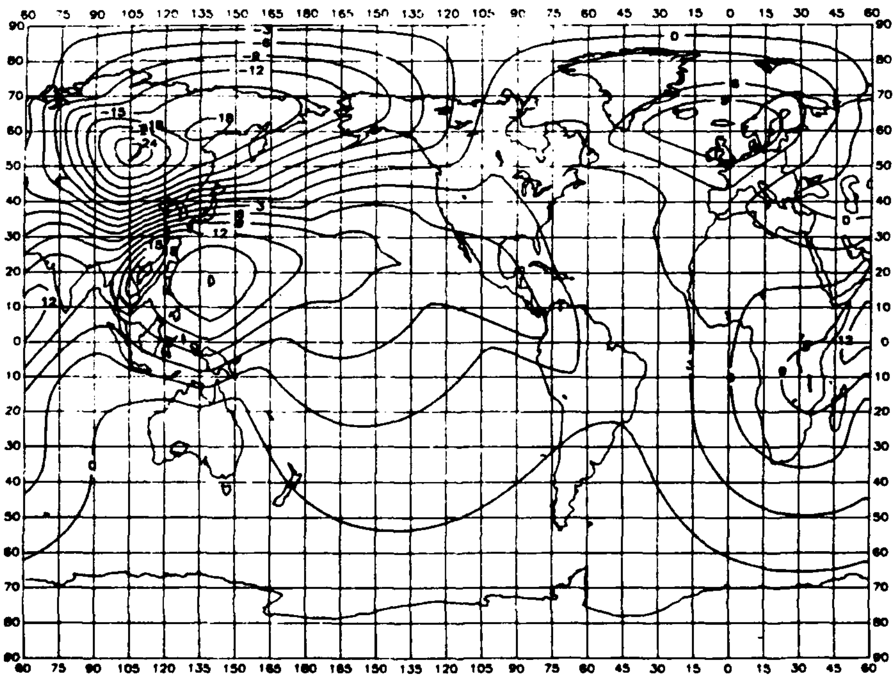

Figure 8. Corrections (dB) to original CCIR Report 322 1-MHz F_{am} estimates, December, January, February, 0400-0800 hours (Spaulding and Washburn, 1985).

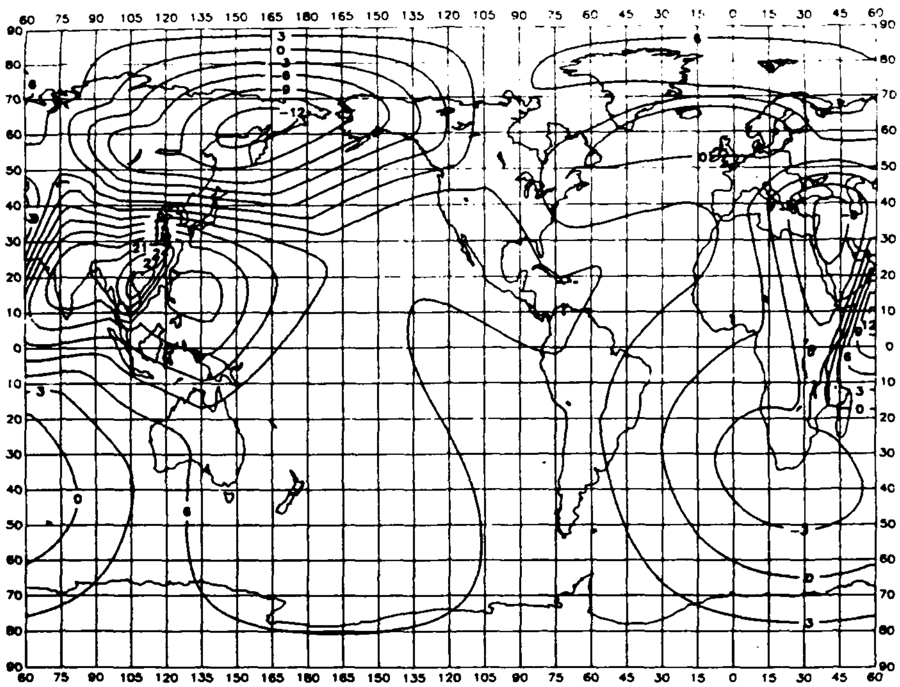

Figure 9. Corrections (dB) to original CCIR Report 322 1-MHz F_{am} estimates, December, January, February, 0800–1200 hours (Spaulding and Washburn, 1985).

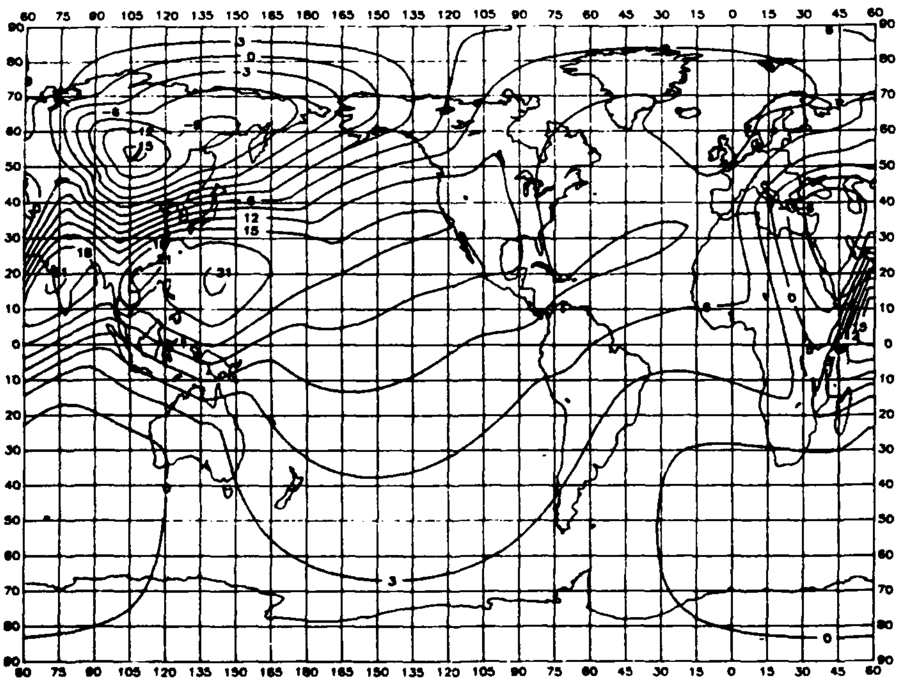

Figure 10. Corrections (dB) to original CCIR Report 322 1-MHz F_{am} estimates, December, January, February, 1200–1600 hours (Spaulding and Washburn, 1985).

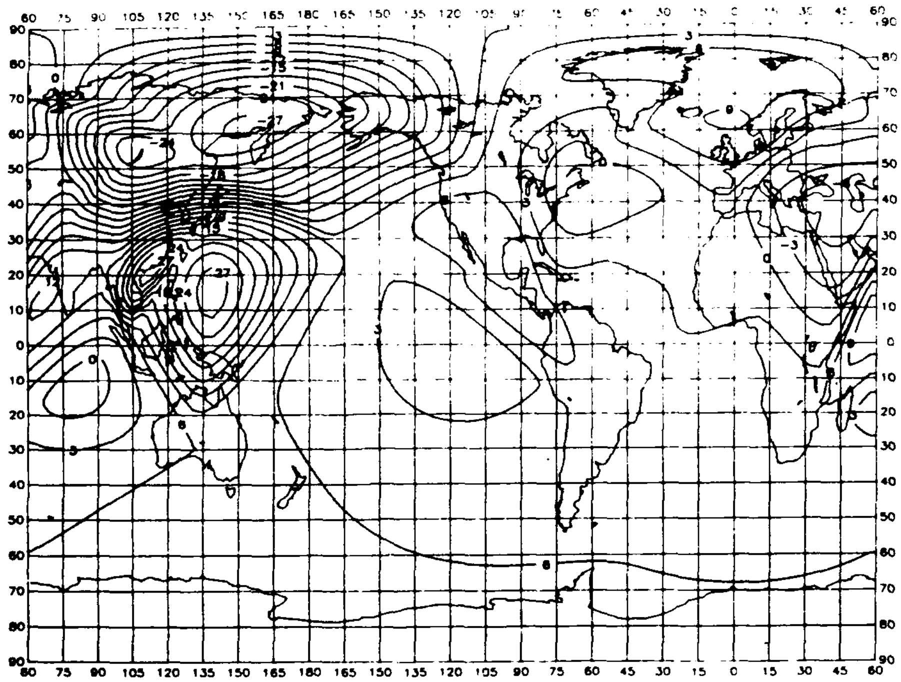

Figure 11. Corrections (dB) to original CCIR Report 322 1-MHz F_{am} estimates, December, January, February, 1600–2000 hours (Spaulding and Washburn, 1985).

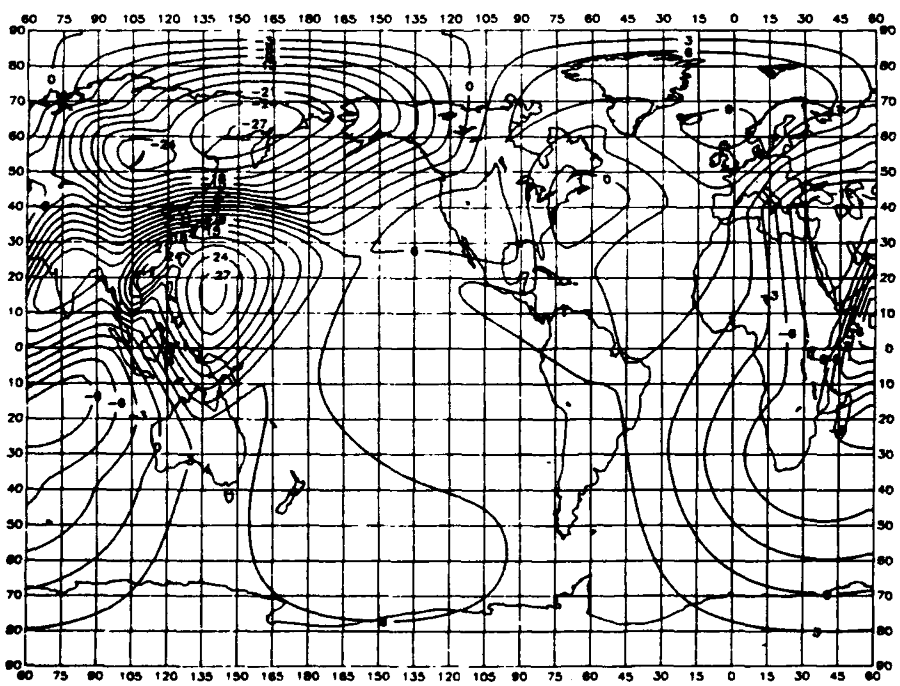

Figure 12. Corrections (dB) to original CCIR Report 322 1-MHz F_{am} estimates, December, January, February, 2000–2400 hours (Spaulding and Washburn, 1985).

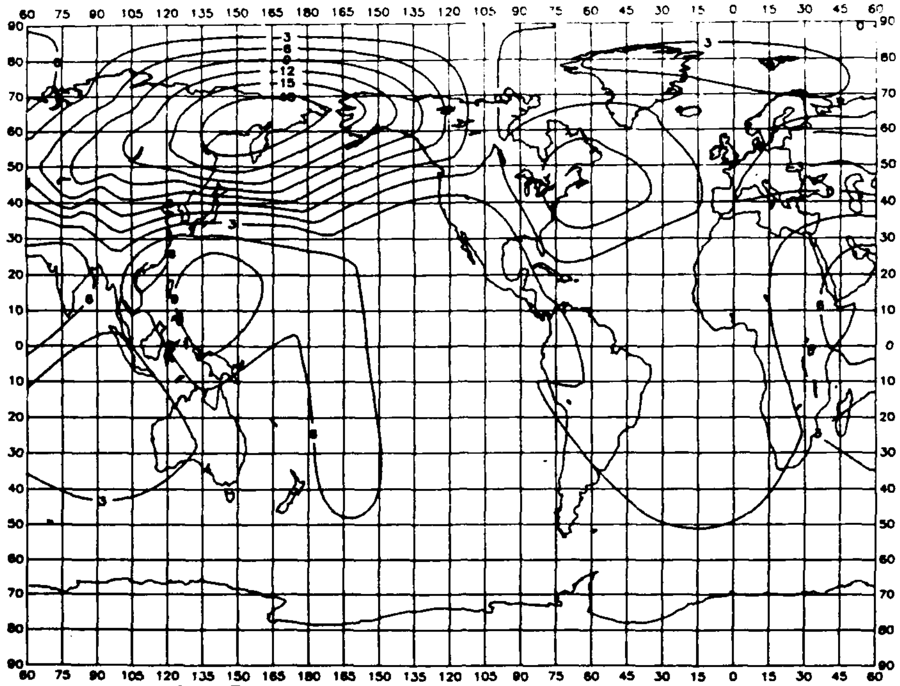

Figure 13. Corrections (dB) to original CCIR Report 322 1-MHz F_{am} estimates, March, April, May, 0000–0400 hours (Spaulding and Washburn, 1985).

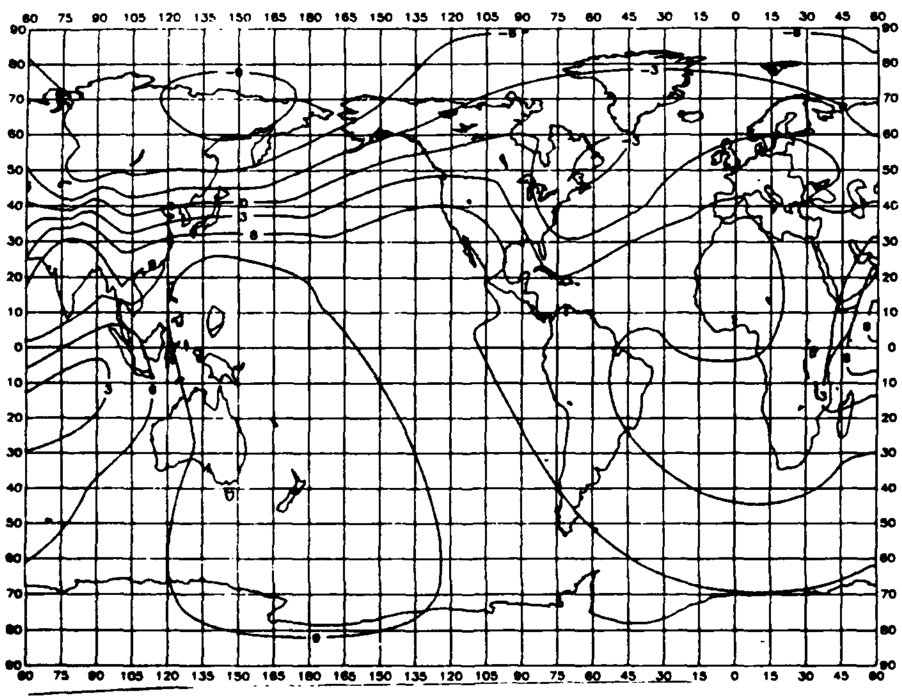

Figure 14. Corrections (dB) to original CCIR Report 322 1-MHz F_{am} estimates, March, April, May, 0400–0800 hours (Spaulding and Washburn, 1985).

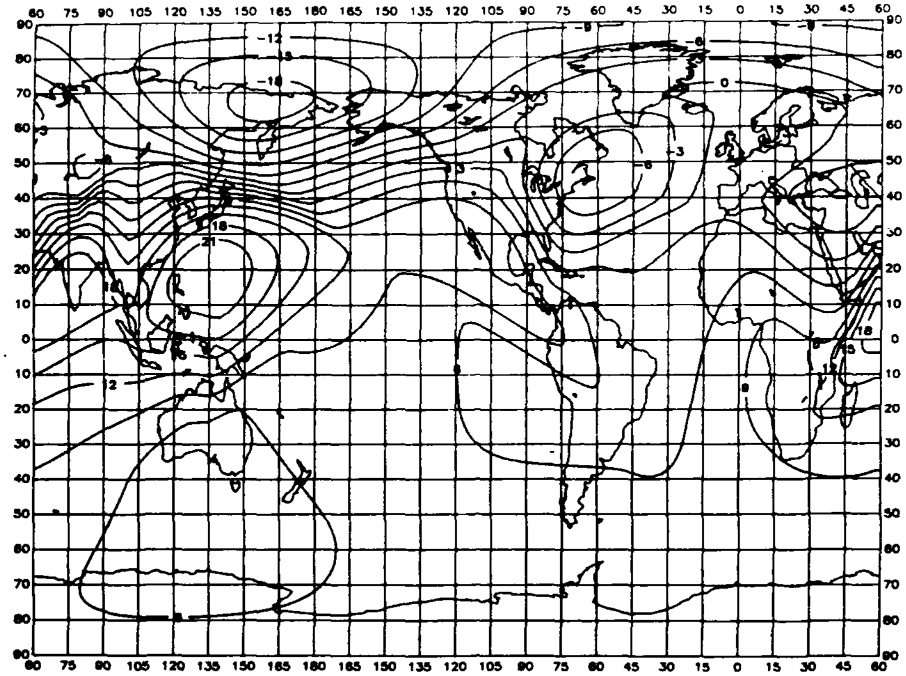

Figure 15. Corrections (dB) to original CCIR Report 322 1-MHz F_{am} estimates, March, April, May, 0800–1200 hours (Spaulding and Washburn, 1985).

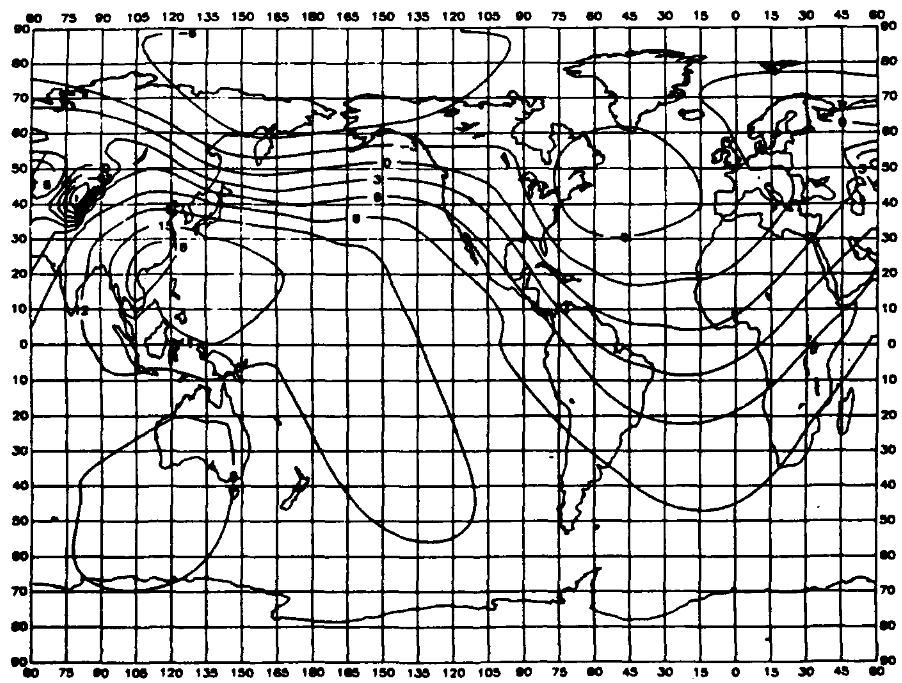

Figure 16. Corrections (dB) to original CCIR Report 322 1-MHz F_{am} estimates, March, April, May, 1200–1600 hours (Spaulding and Washburn, 1985).

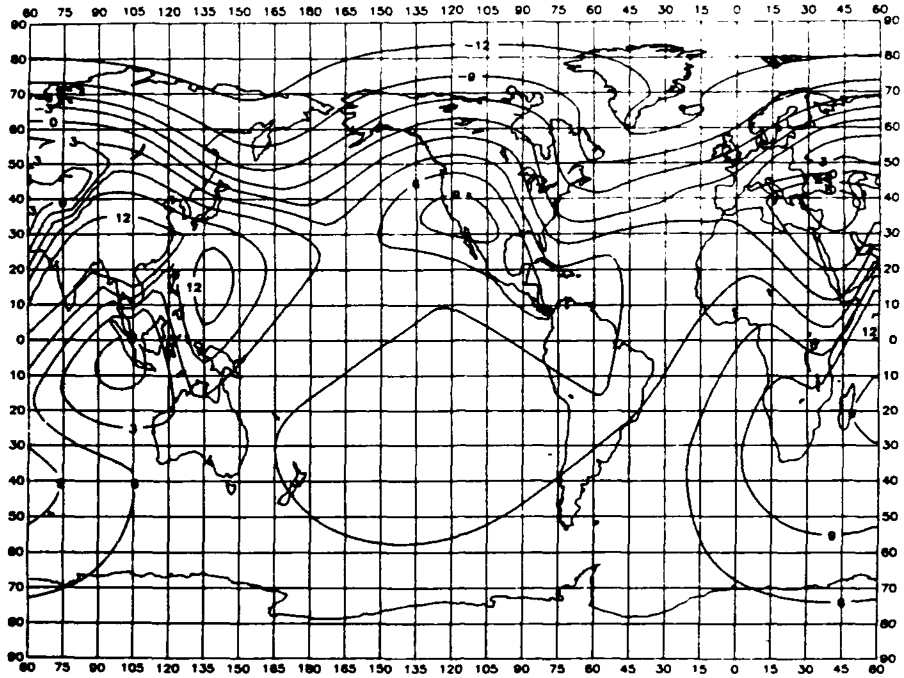

Figure 17. Corrections (dB) to original CCIR Report 322 1-MHz F_{am} estimates, March, April, May, 1600-2000 hours (Spaulding and Washburn, 1985).

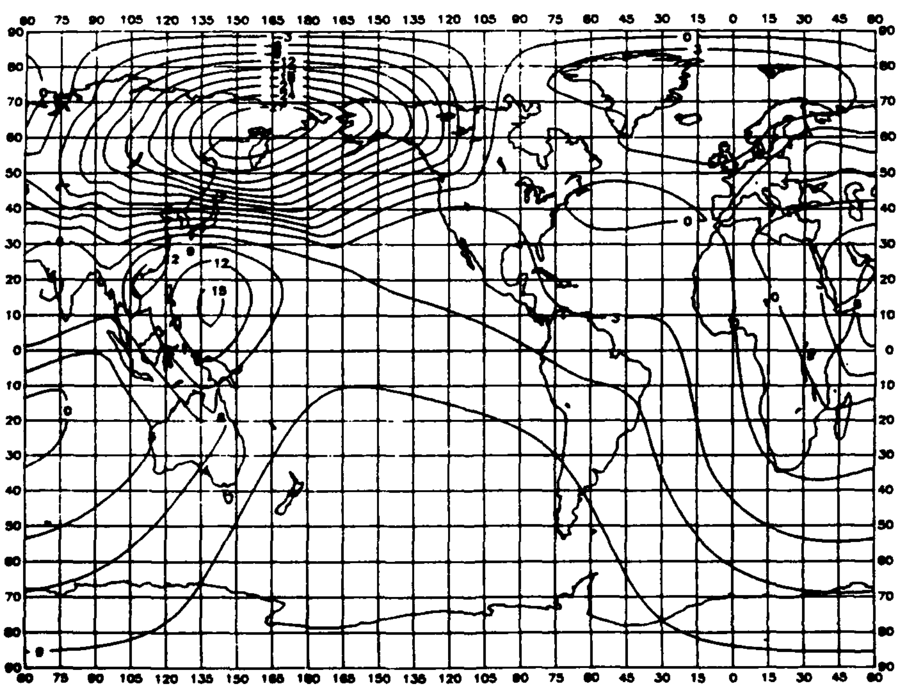

Figure 18. Corrections (dB) to original CCIR Report 322 1-MHz F_{am} estimates, March, April, May, 2000-2400 hours (Spaulding and Washburn, 1985).

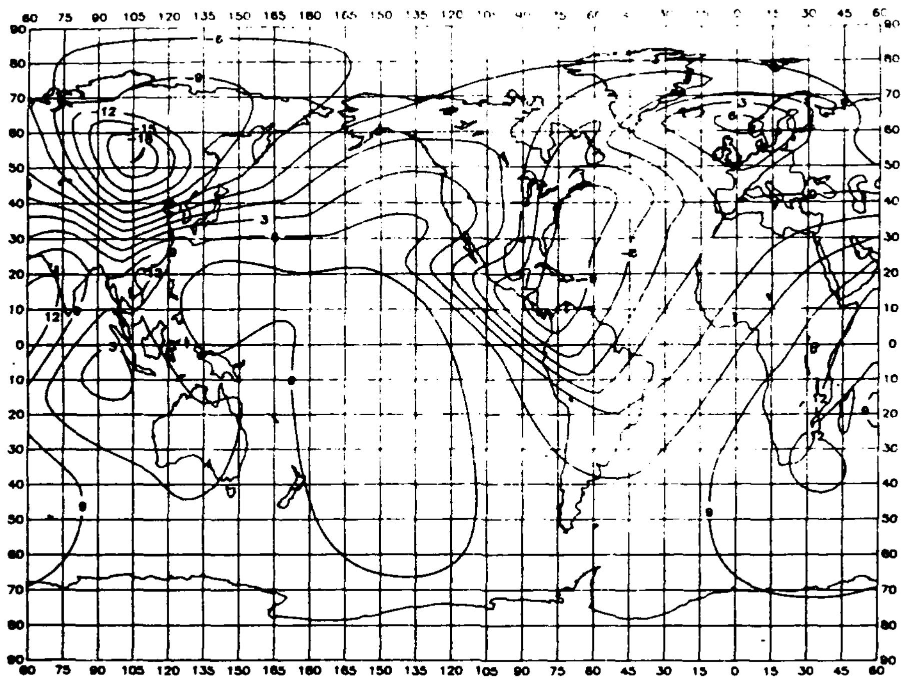

Figure 19. Corrections (dB) to original CCIR Report 322 1-MHz F_{am} estimates, June, July, August, 0000–0400 hours (Spaulding and Washburn, 1985).

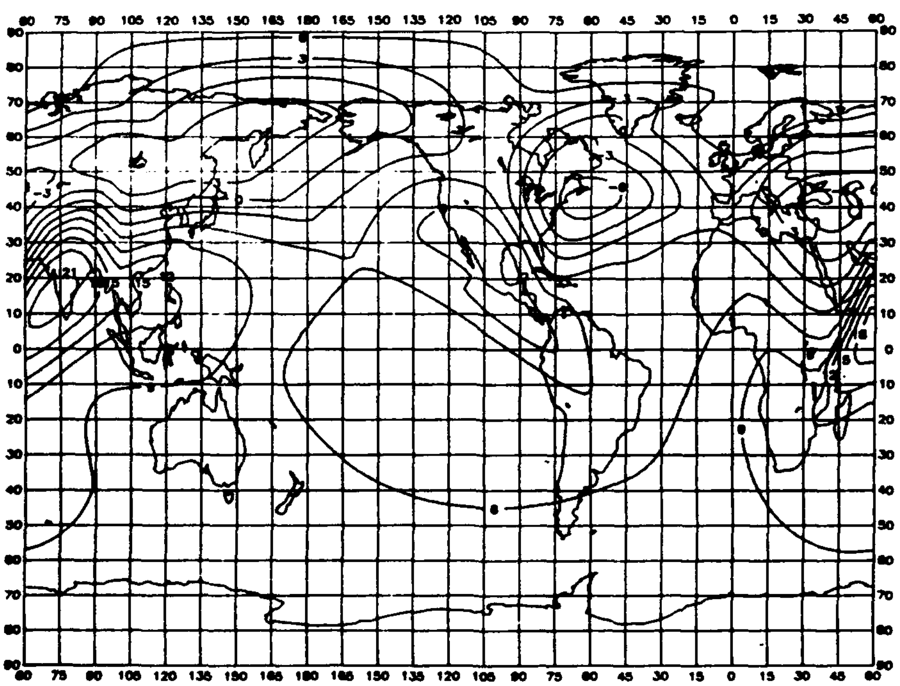

Figure 20. Corrections (dB) to original CCIR Report 322 1-MHz F_{am} estimates, June, July, August, 0400–0800 hours (Spaulding and Washburn, 1985).

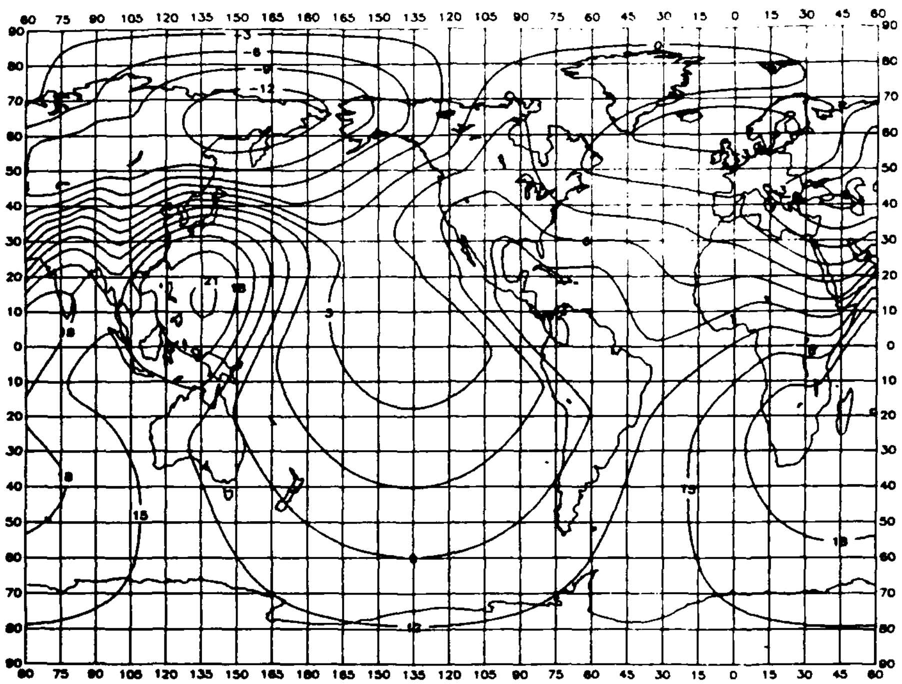

Figure 21. Corrections (dB) to original CCIR Report 322 1-MHz F_{am} estimates, June, July, August, 0800–1200 hours (Spaulding and Washburn, 1985).

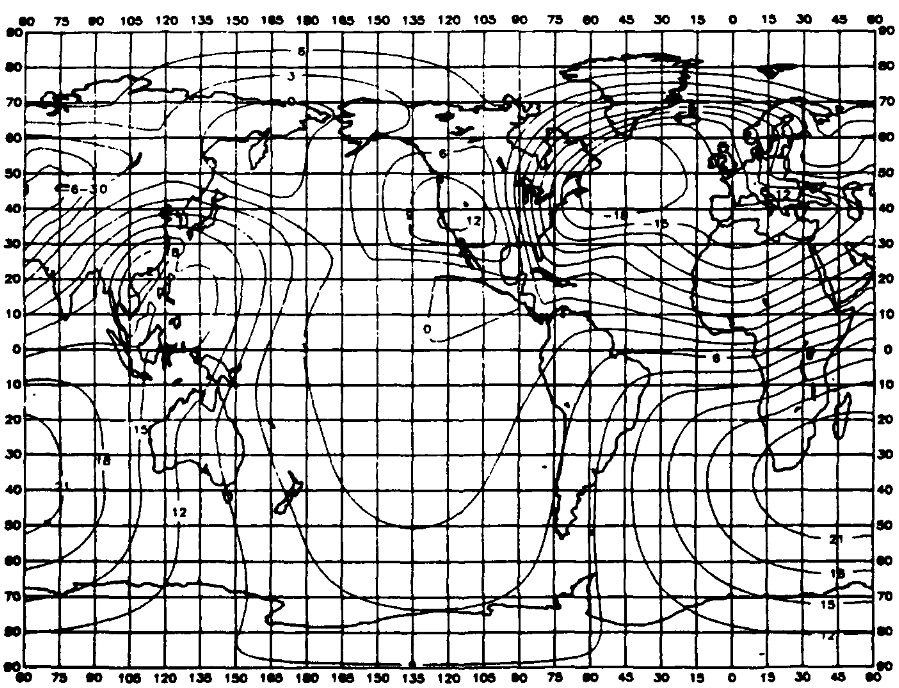

Figure 22. Corrections (dB) to original CCIR Report 322 1-MHz F_{am} estimates, June, July, August, 1200–1600 hours (Spaulding and Washburn, 1985).

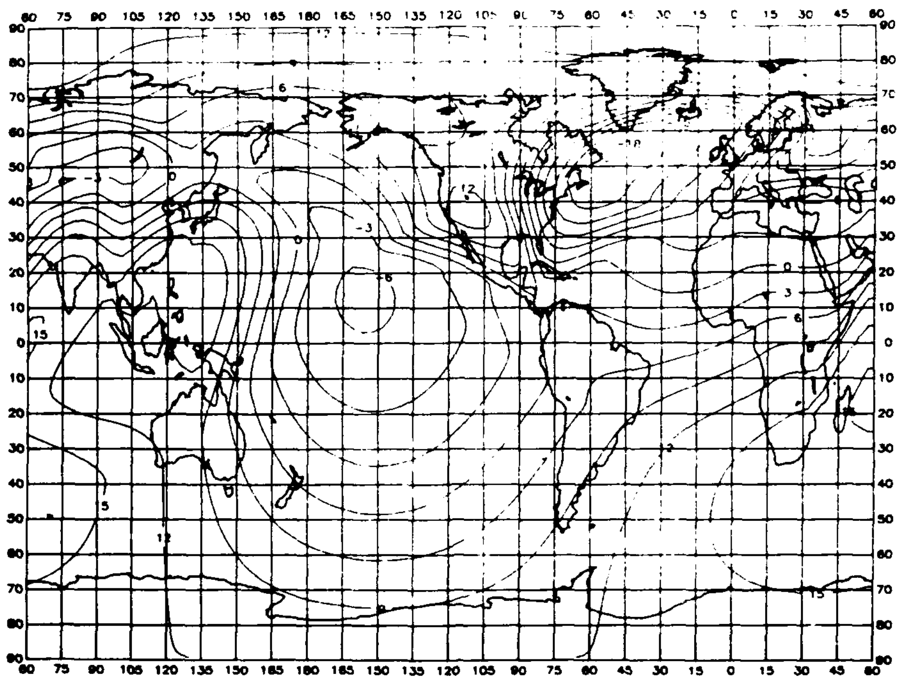

Figure 23. Corrections (dB) to original CCIR Report 322 1-MHz F_{am} estimates, June, July, August, 1600–2000 hours (Spaulding and Washburn, 1985).

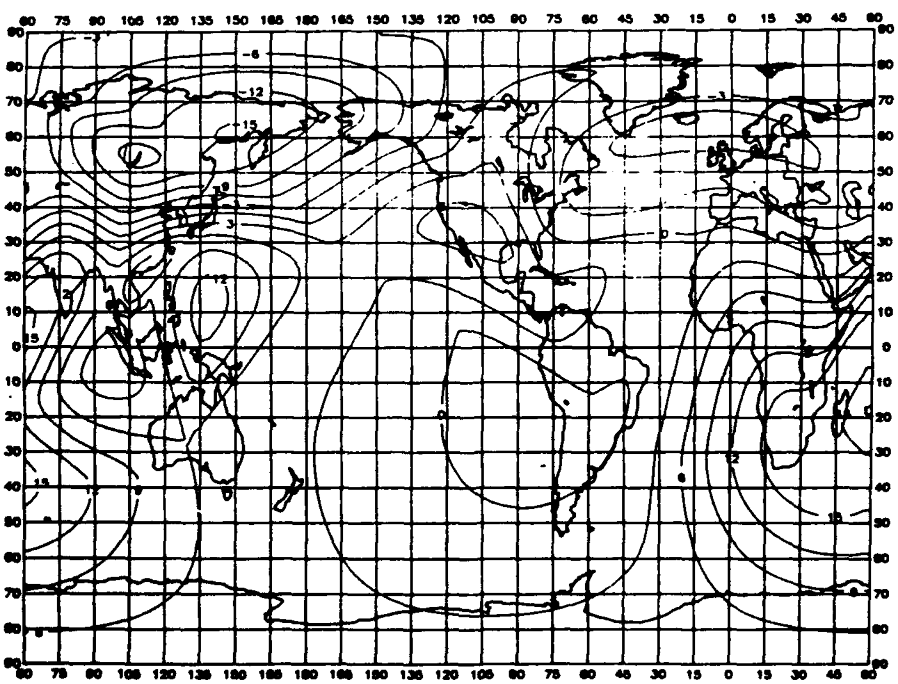

Figure 24. Corrections (dB) to original CCIR Report 322 1-MHz F_{am} estimates, June, July, August, 2000–2400 hours (Spaulding and Washburn, 1985).

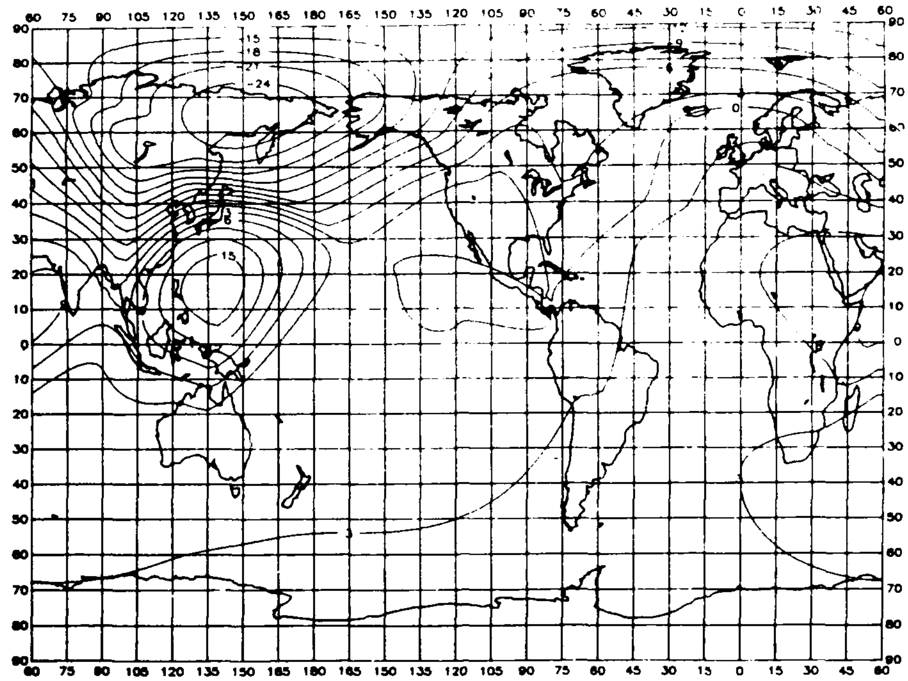

Figure 25. Corrections (dB) to original CCIR Report 322 1-MHz F_{am} estimates, September, October, November, 0000-0400 hours (Spaulding and Washburn, 1985).

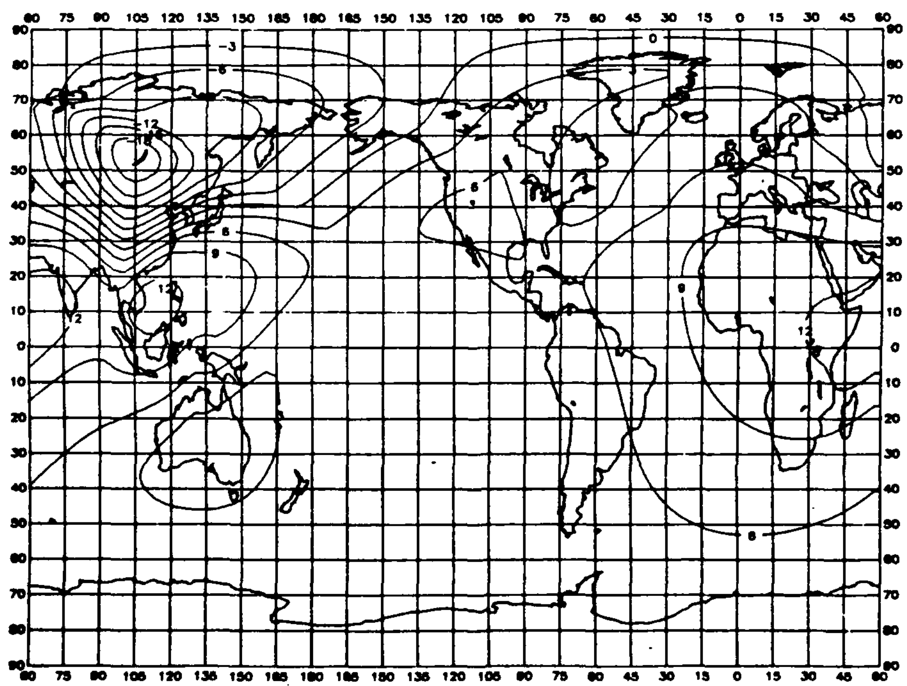

Figure 26. Corrections (dB) to original CCIR Report 322 1-MHz F_{am} estimates, September, October, November, 0400-0800 hours (Spaulding and Washburn, 1985).

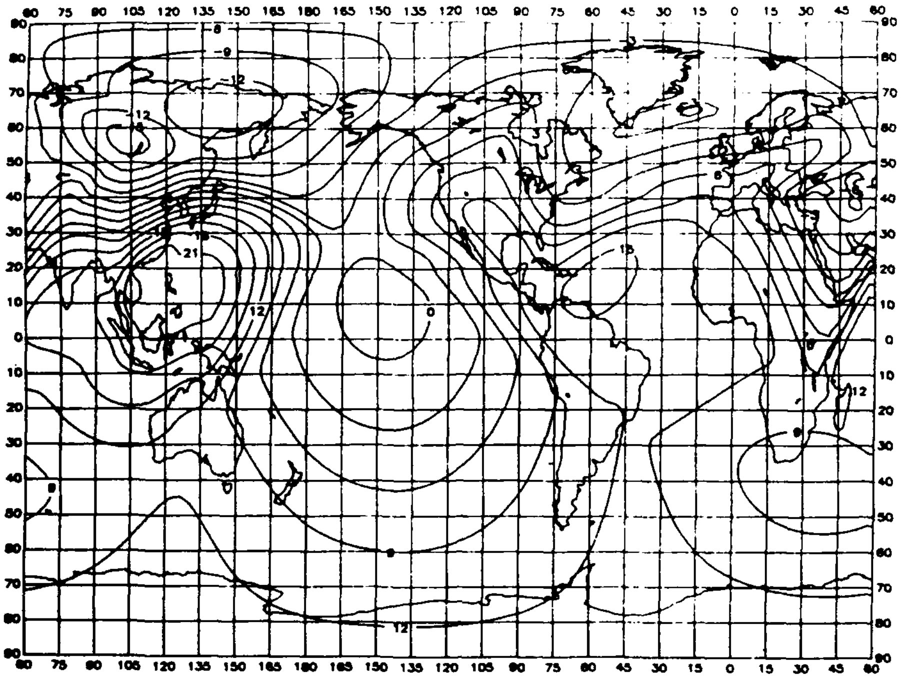

Figure 27. Corrections (dB) to original CCIR Report 322 1-MHz F_{am} estimates, September, October, November, 0800–1200 hours (Spaulding and Washburn, 1985).

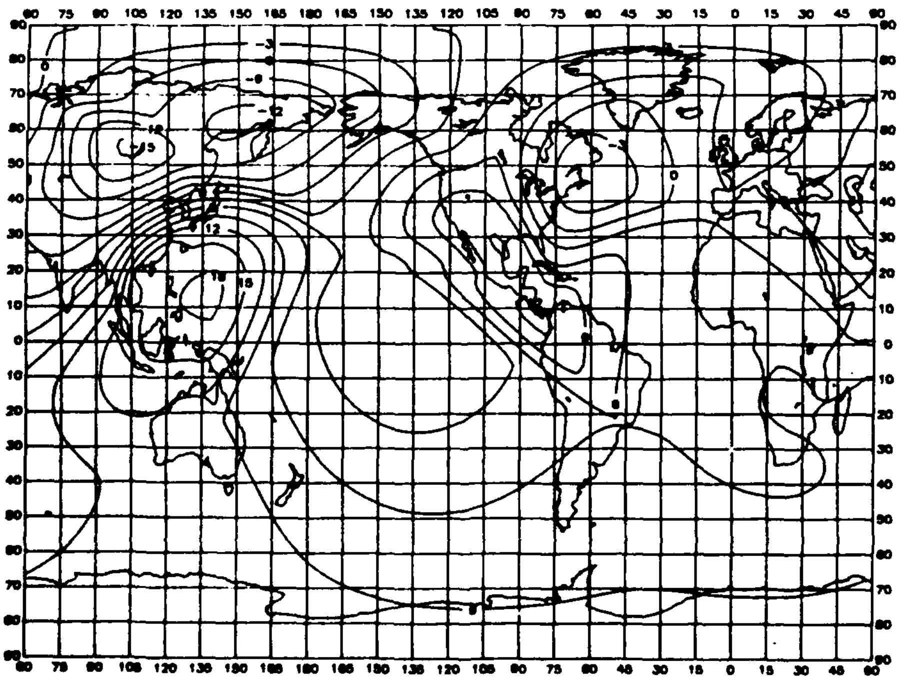

Figure 28. Corrections (dB) to original CCIR Report 322 1-MHz F_{am} estimates, September, October, November, 1200–1600 hours (Spaulding and Washburn, 1985).

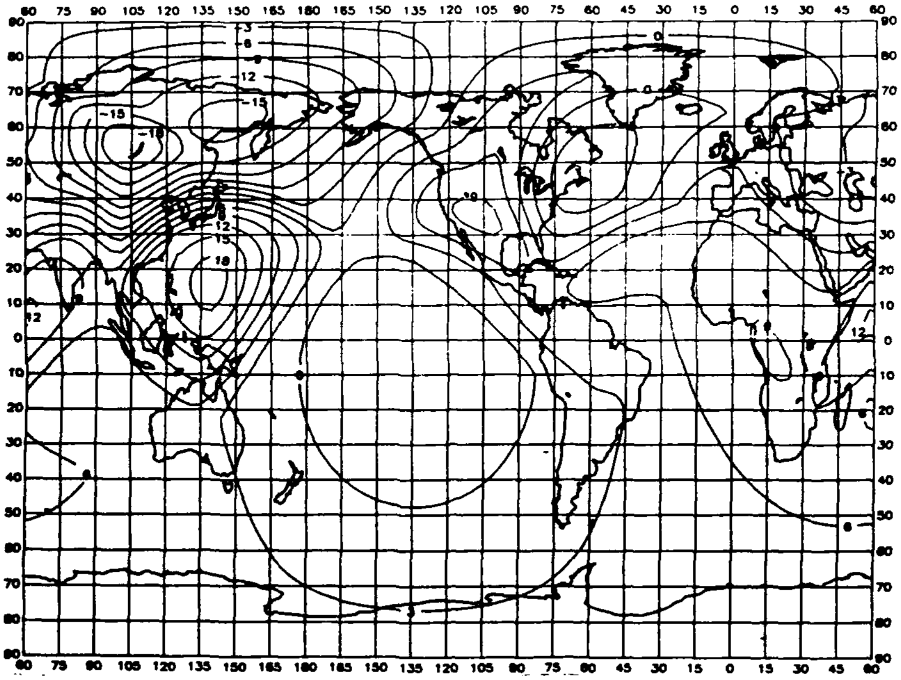

Figure 29. Corrections (dB) to original CCIR Report 322 1-MHz F_{am} estimates, September, October, November, 1600-2000 hours (Spaulding and Washburn, 1985).

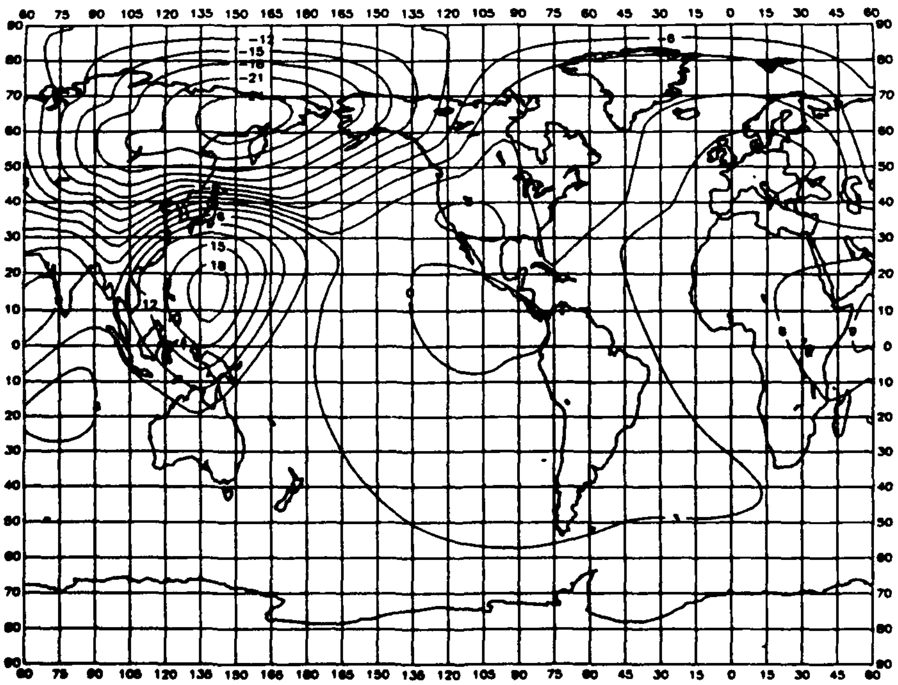

Figure 30. Corrections (dB) to original CCIR Report 322 1-MHz F_{am} estimates, September, October, November, 2000-2400 hours (Spaulding and Washburn, 1985).

3.4 THE NEW 1-MHz F_{am} VALUES

The new 1-MHz F_{am} data values for constructing a new 1-MHz noise model were obtained by Spaulding and Washburn (1985) by adding each of the 84-longitude by 100-latitude grid of correction values to the corresponding original 84-longitude by 100-latitude grid data values from which CCIR Report 322 was constructed.

In developing a numerical representation for these new 1-MHz F_{am} maps, Spaulding and Washburn used the method used by Lucas and Harper (1965). The resulting sets of numerical coefficients could then be used with existing programs developed to obtain the 1-MHz F_{am} noise value from the Lucas and Harper representation of the CCIR Report 322 noise model. Spaulding and Washburn give details on how these coefficients were obtained.

Spaulding and Washburn (1985) compared the numerical representation thus obtained for each of the 8400 original data points (84 $\times$ 100 grids) for each of the 24 numerical maps. They found an rms variation that ranged from 0.88 dB to 2.37 dB over the 24 maps with an average rms variation of 1.52 dB and with a maximum deviation of 6.7 dB (all maps considered, i.e., 24 $\times$ 8400 points).

These numerical maps represent a "smoothed" version of the original data and are the new 1-MHz F_{am} worldwide atmospheric noise estimates. Figures 31 through 54 (figures 34 through 57 from Spaulding and Washburn (1985)) are contour plots of these estimates.

The contour plots in CCIR Report 322-3 are similar, except the CCIR IWP 6/2 gathered the plots together by season rather than by months as in figures 31 through 54. This resulted in the discontinuity at the equator in CCIR Report 322-3.

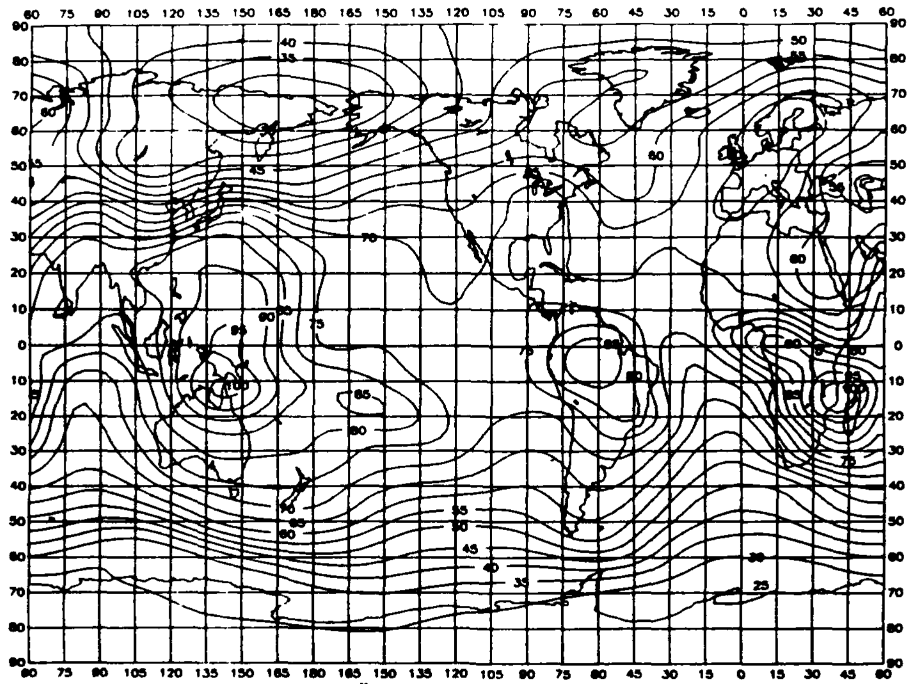

Figure 31. Expected values of atmospheric radio noise at 1 MHz, F_{am} (dB above kT_0b), for December, January, February, 0000-0400 hours (Spaulding and Washburn, 1985).

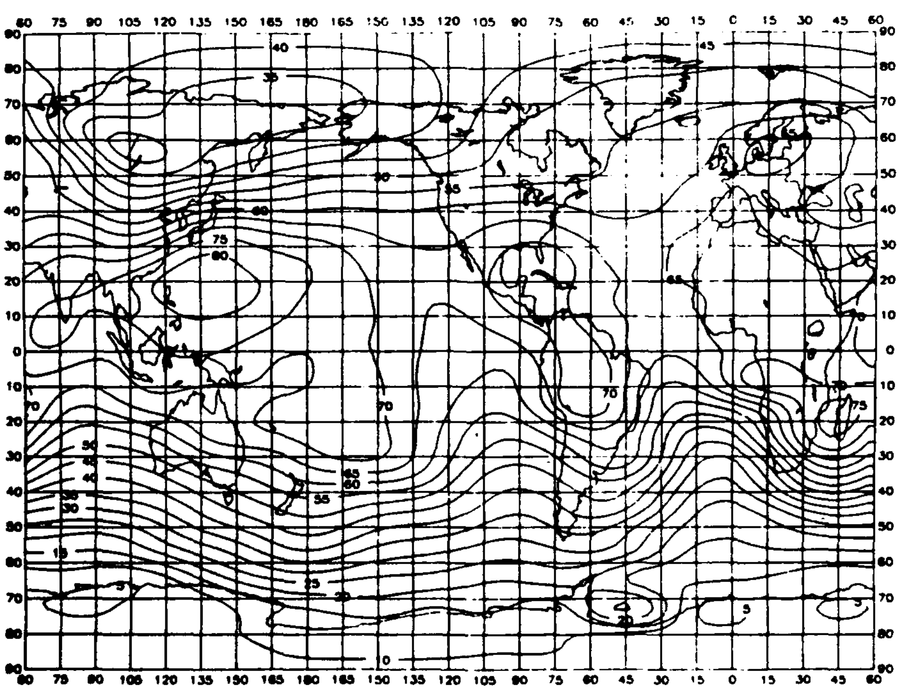

Figure 32. Expected values of atmospheric radio noise at 1 MHz, F_{am} (dB above kT_0b), for December, January, February, 0400-0800 hours (Spaulding and Washburn, 1985).

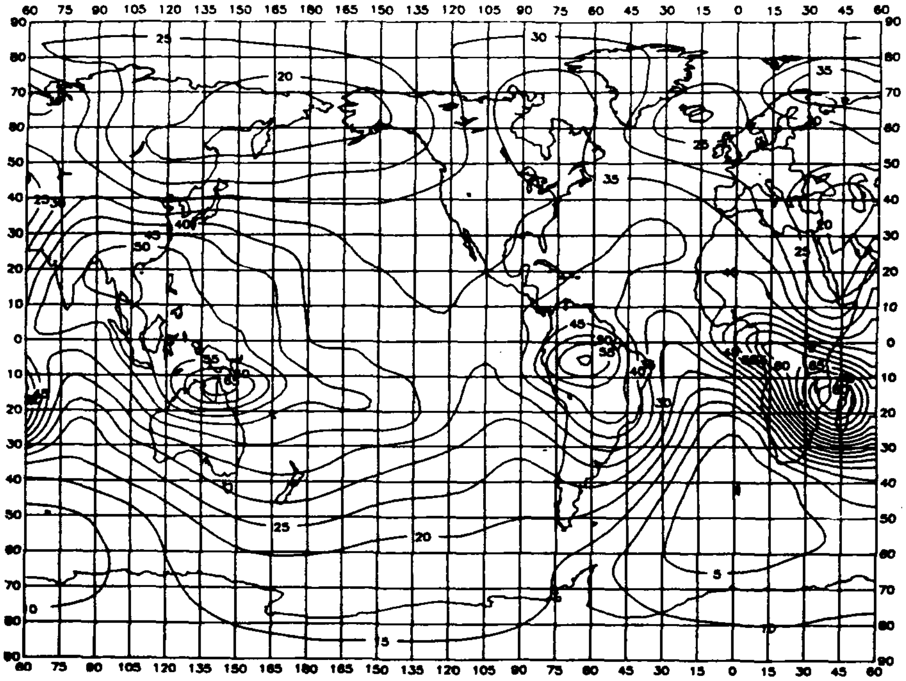

Figure 33. Expected values of atmospheric radio noise at 1 MHz, F_{am} (dB above kT_0b), for December, January, February, 0800–1200 hours (Spaulding and Washburn, 1985).

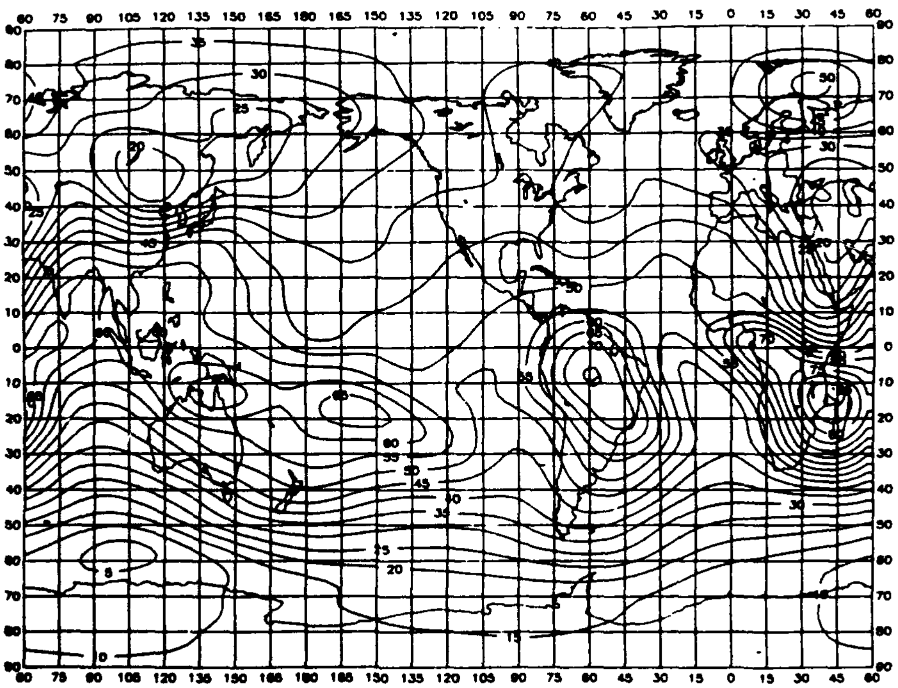

Figure 34. Expected values of atmospheric radio noise at 1 MHz, F_{am} (dB above kT_0b), for December, January, February, 1200–1600 hours (Spaulding and Washburn, 1985).

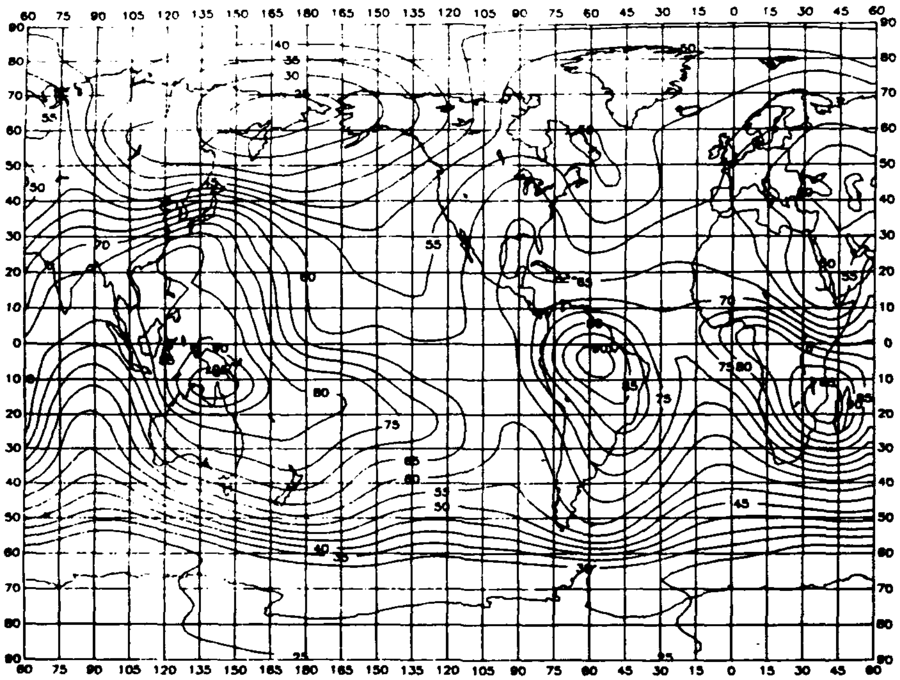

Figure 35. Expected values of atmospheric radio noise at 1 MHz, F_{am} (dB above kT_0b), for December, January, February, 1600-2000 hours (Spaulding and Washburn, 1985).

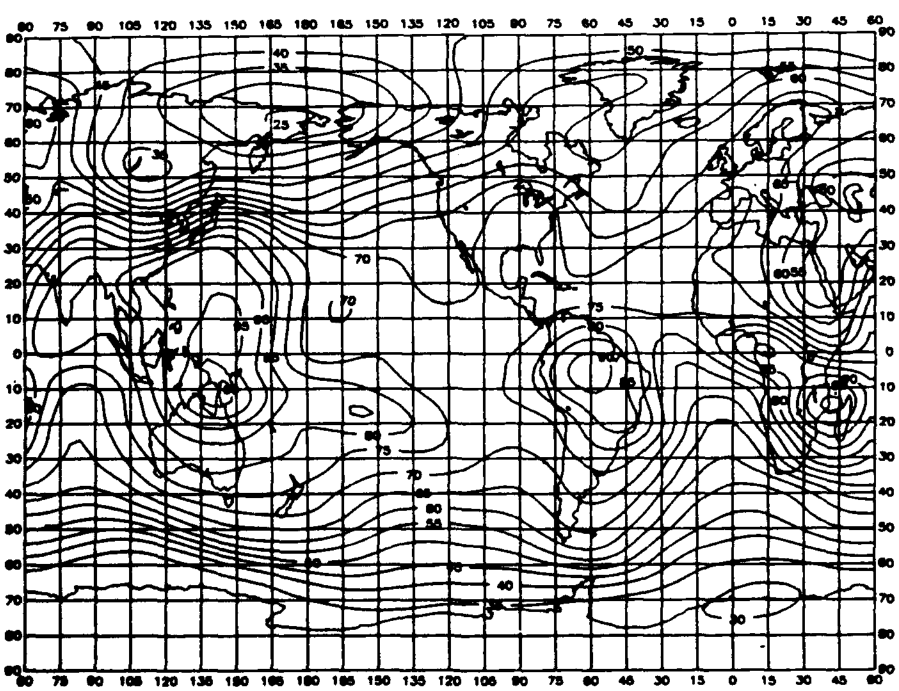

Figure 36. Expected values of atmospheric radio noise at 1 MHz, F_{am} (dB above kT_0b), for December, January, February, 2000-2400 hours (Spaulding and Washburn, 1985).

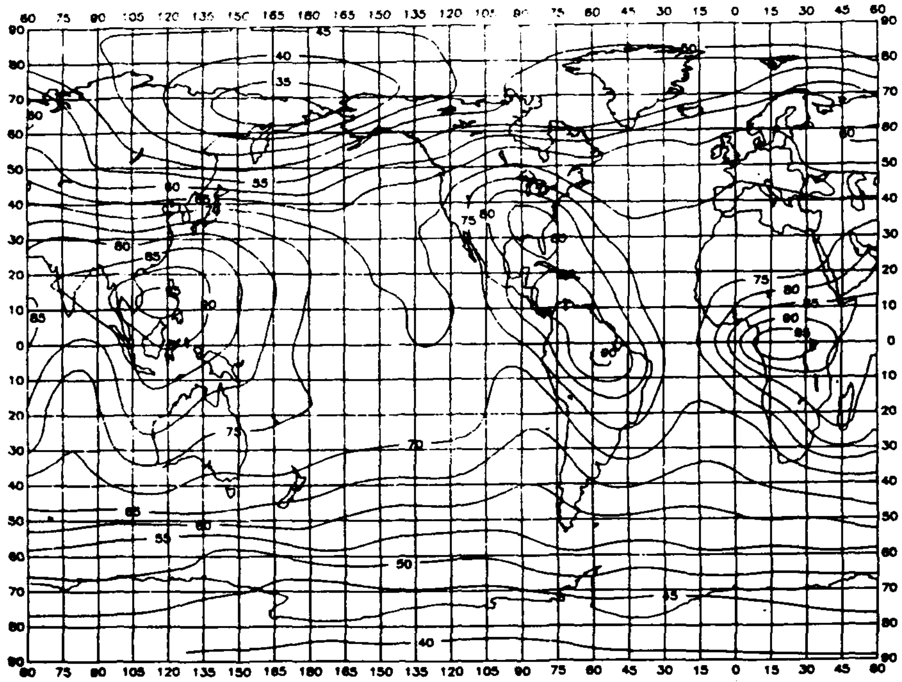

Figure 37. Expected values of atmospheric radio noise at 1 MHz, F_{am} (dB above kT_0b), for March, April, May, 0000-0400 hours (Spaulding and Washburn, 1985).

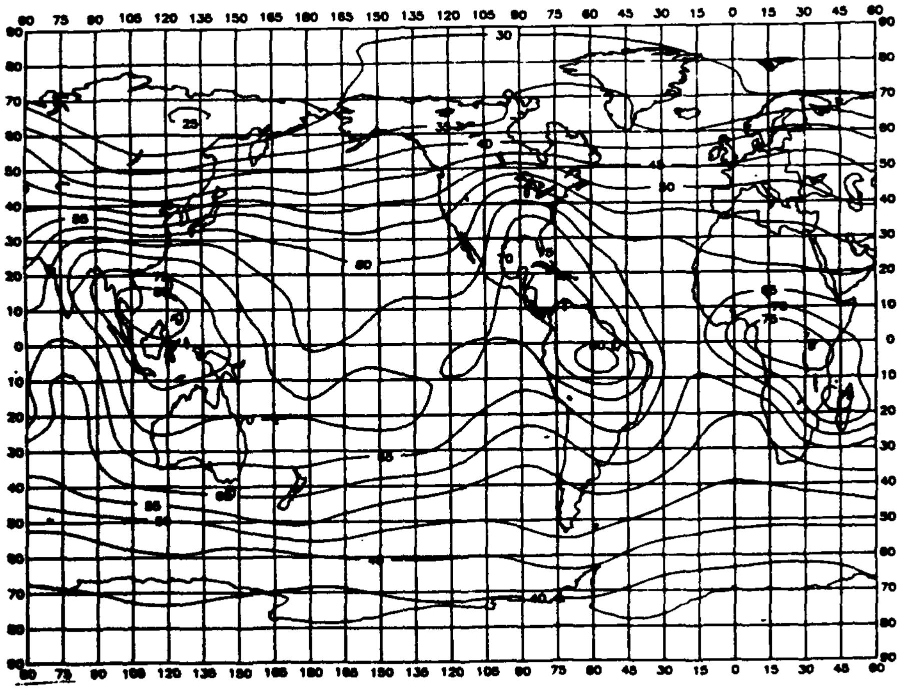

Figure 38. Expected values of atmospheric radio noise at 1 MHz, F_{am} (dB above kT_0b), for March, April, May, 0400-0800 hours (Spaulding and Washburn, 1985).

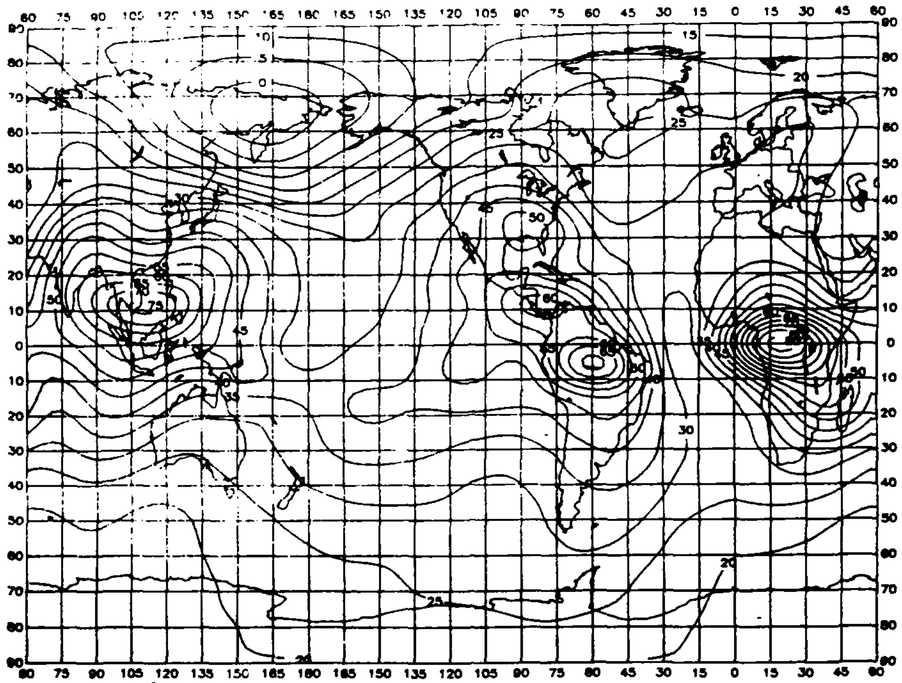

Figure 39. Expected values of atmospheric radio noise at 1 MHz, F_{am} (dB above kT_0b), for March, April, May, 0800-1200 hours (Spaulding and Washburn, 1985).

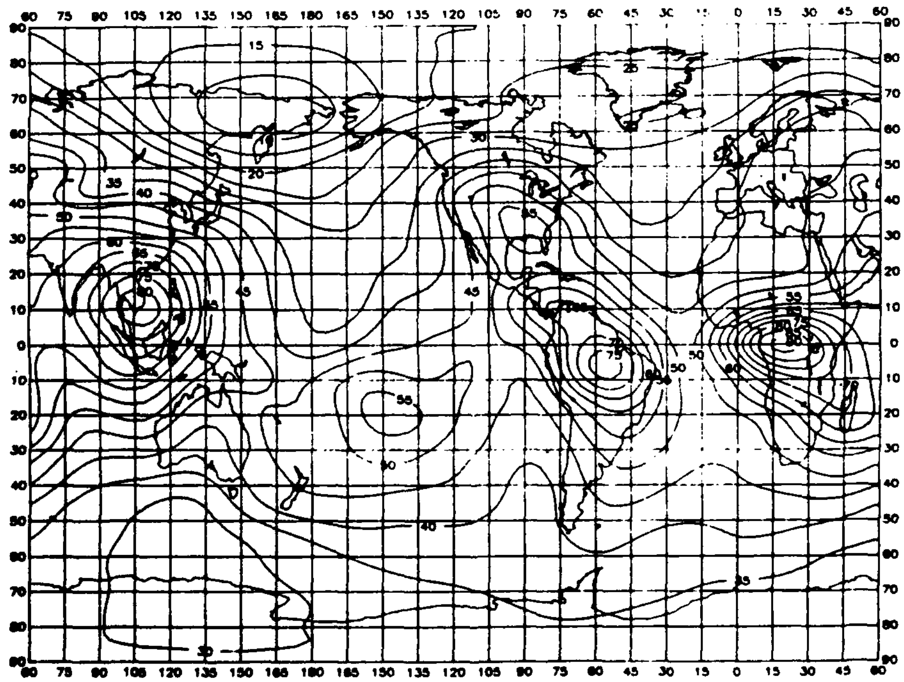

Figure 40. Expected values of atmospheric radio noise at 1 MHz, F_{am} (dB above kT_0b), for March, April, May, 1200-1600 hours (Spaulding and Washburn, 1985).

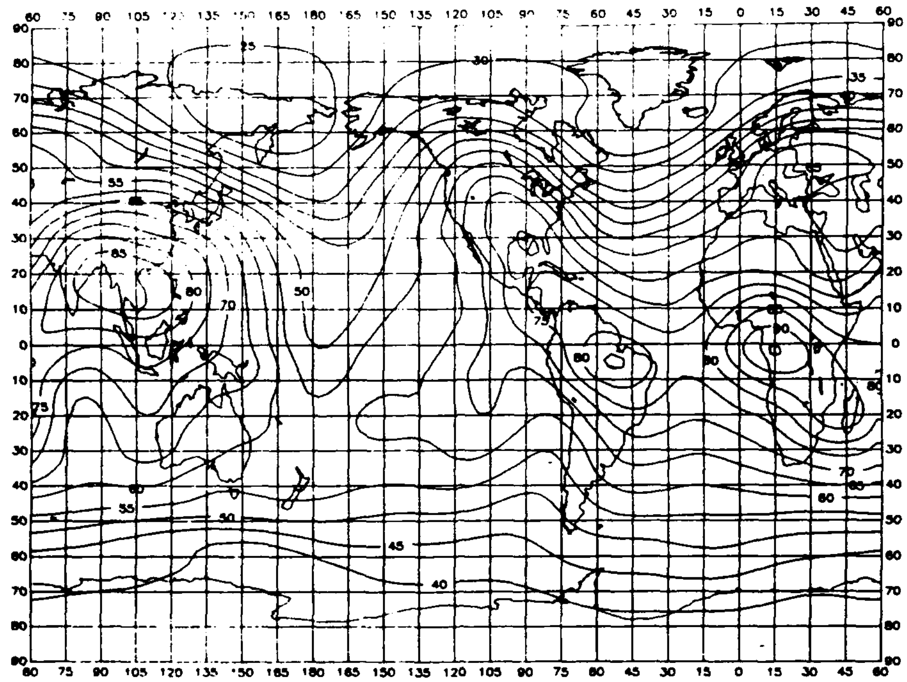

Figure 41. Expected values of atmospheric radio noise at 1 MHz, F_{am} (dB above kT_0b), for March, April, May, 1600-2000 hours (Spaulding and Washburn, 1985).

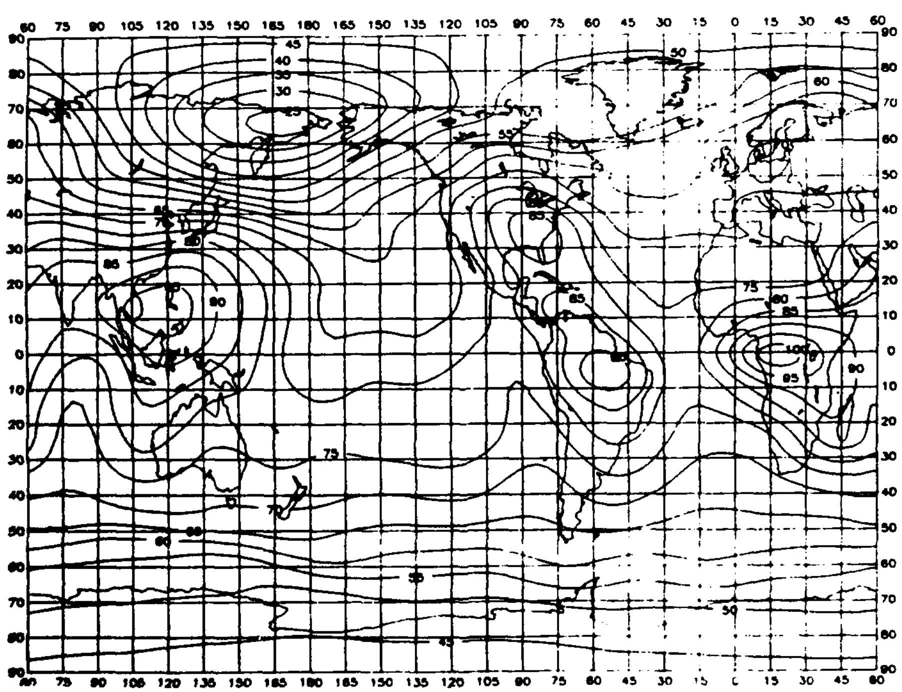

Figure 42. Expected values of atmospheric radio noise at 1 MHz, F_{am} (dB above kT_0b), for March, April, May, 2000-2400 hours (Spaulding and Washburn, 1985).

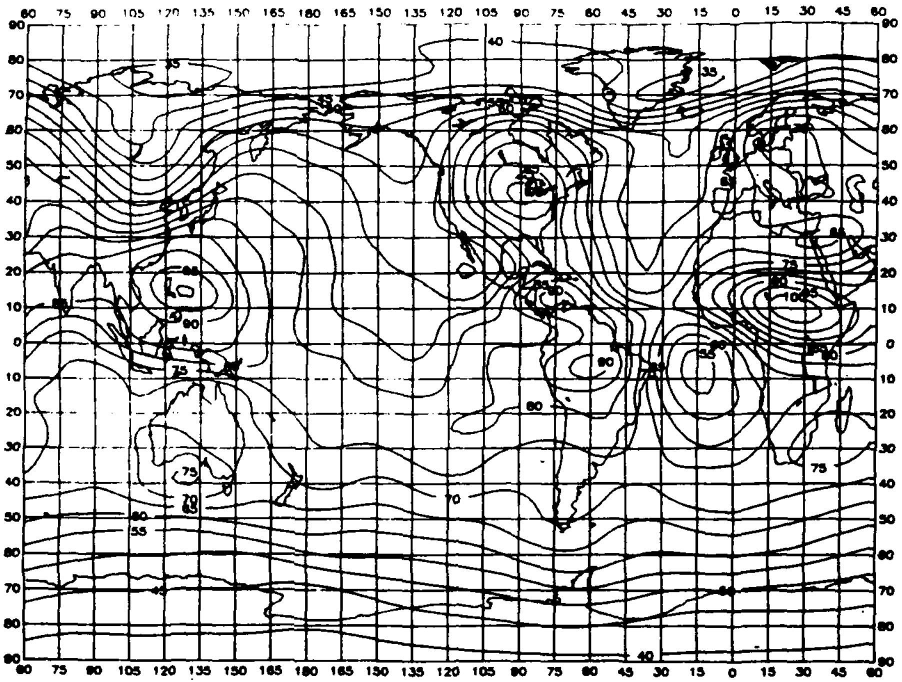

Figure 43. Expected values of atmospheric radio noise at 1 MHz, F_{am} (dB above kT_0b), for June, July, August, 0000-0400 hours (Spaulding and Washburn, 1985).

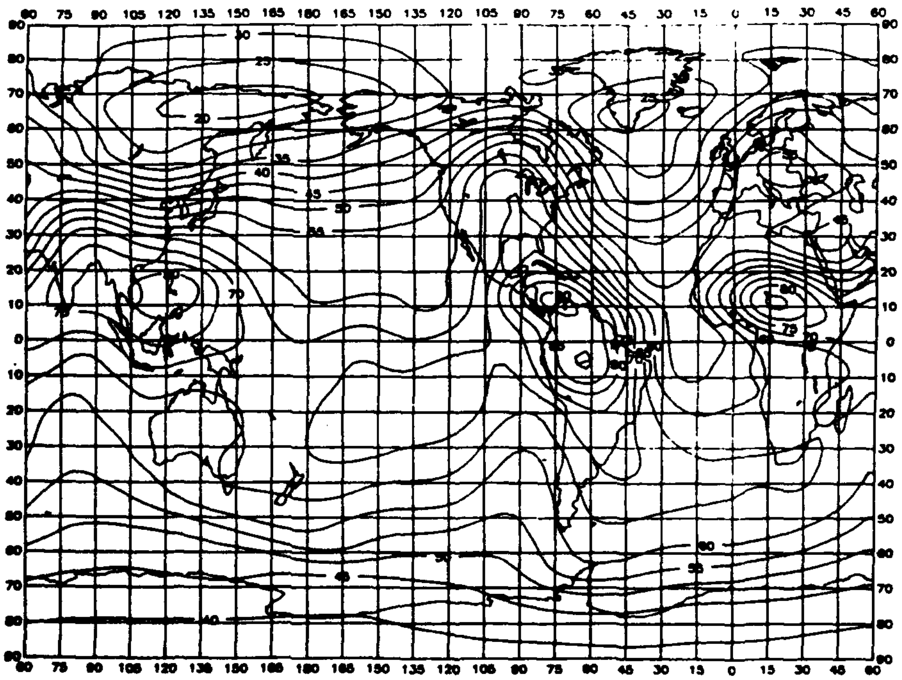

Figure 44. Expected values of atmospheric radio noise at 1 MHz, F_{am} (dB above kT_0b), for June, July, August, 0400-0800 hours (Spaulding and Washburn, 1985).

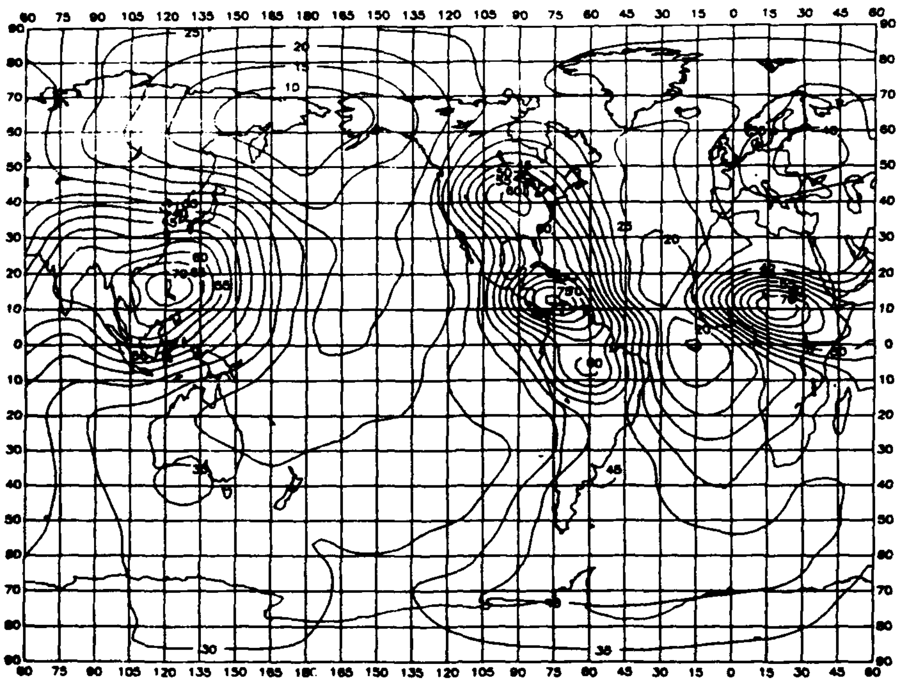

Figure 45. Expected values of atmospheric radio noise at 1 MHz, F_{am} (dB above kT_0b), for June, July, August, 0800–1200 hours (Spaulding and Washburn, 1985).

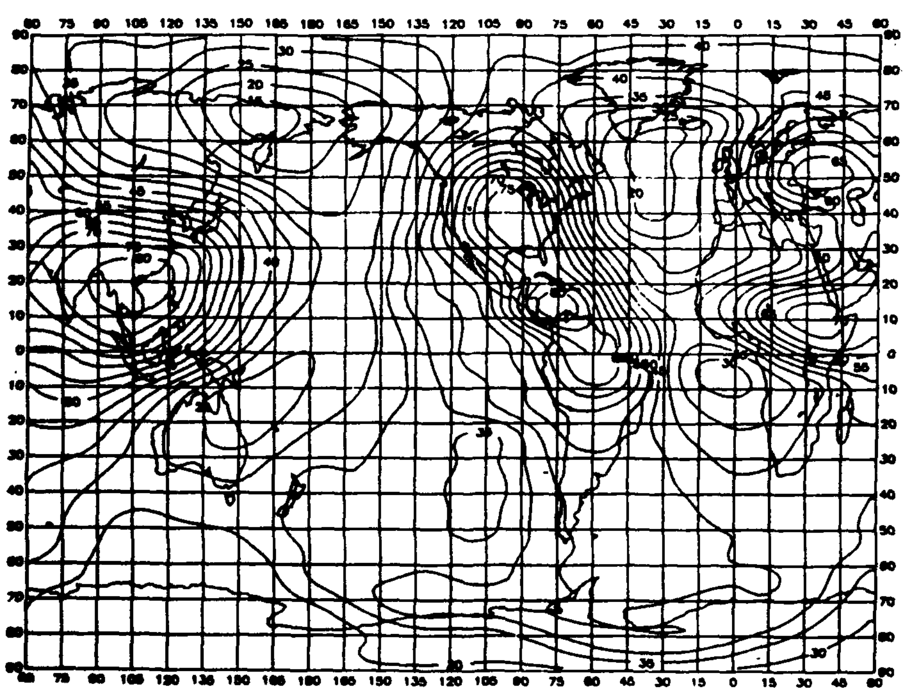

Figure 46. Expected values of atmospheric radio noise at 1 MHz, F_{am} (dB above kT_0b), for June, July, August, 1200–1600 hours (Spaulding and Washburn, 1985).

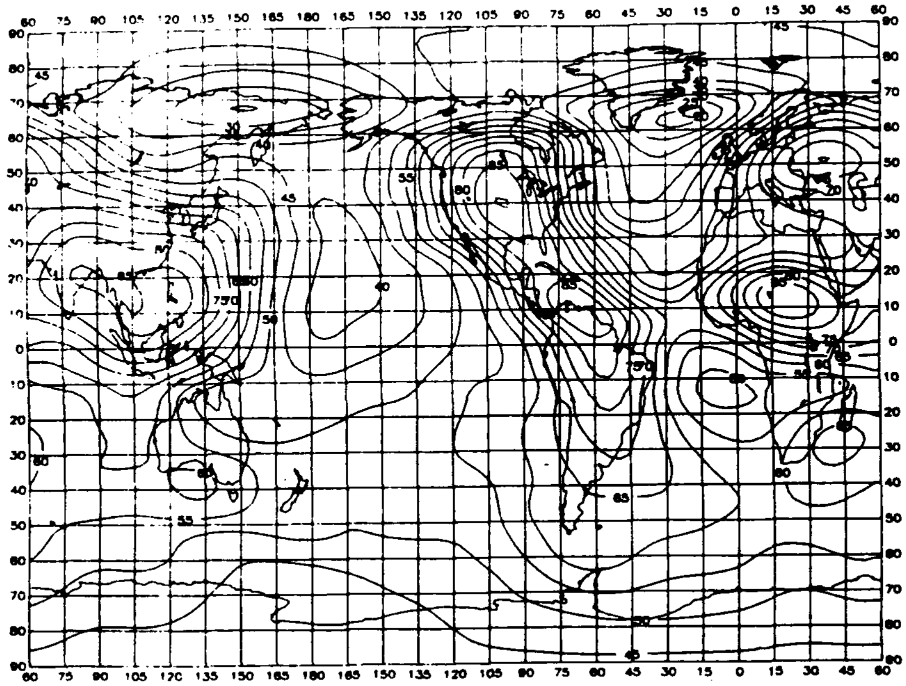

Figure 47. Expected values of atmospheric radio noise at 1 MHz, F_{am} (dB above kT_0b), for June, July, August, 1600–2000 hours (Spaulding and Washburn, 1985).

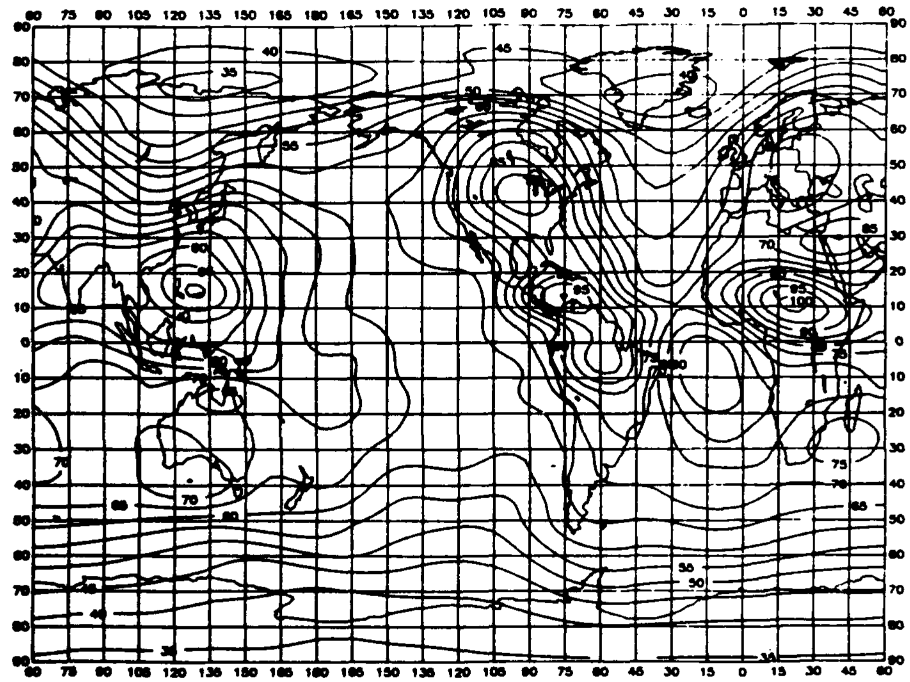

Figure 48. Expected values of atmospheric radio noise at 1 MHz, F_{am} (dB above kT_0b), for June, July, August, 2000–2400 hours (Spaulding and Washburn, 1985).

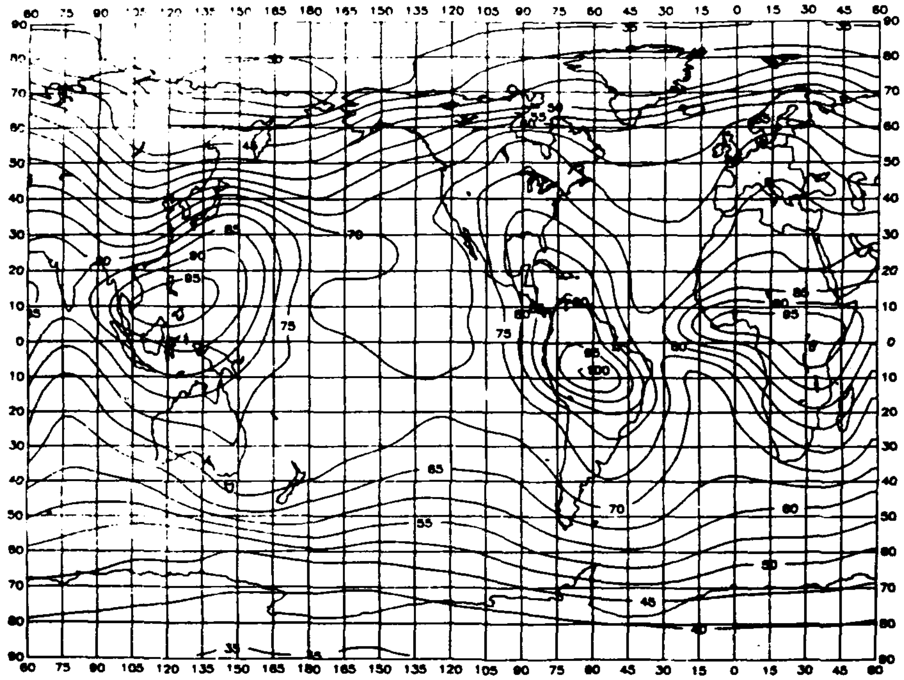

Figure 49. Expected values of atmospheric radio noise at 1 MHz, F_{am} (dB above kT_0b), for September, October, November, 0000-0400 hours (Spaulding and Washburn, 1985).

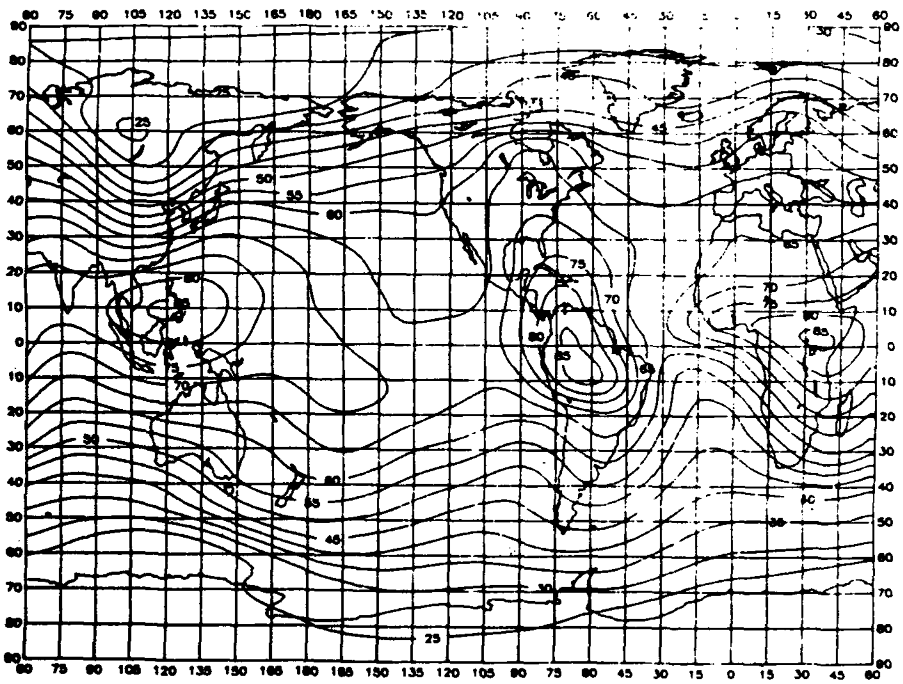

Figure 50. Expected values of atmospheric radio noise at 1 MHz, F_{am} (dB above kT_0b), for September, October, November, 0400-0800 hours (Spaulding and Washburn, 1985).

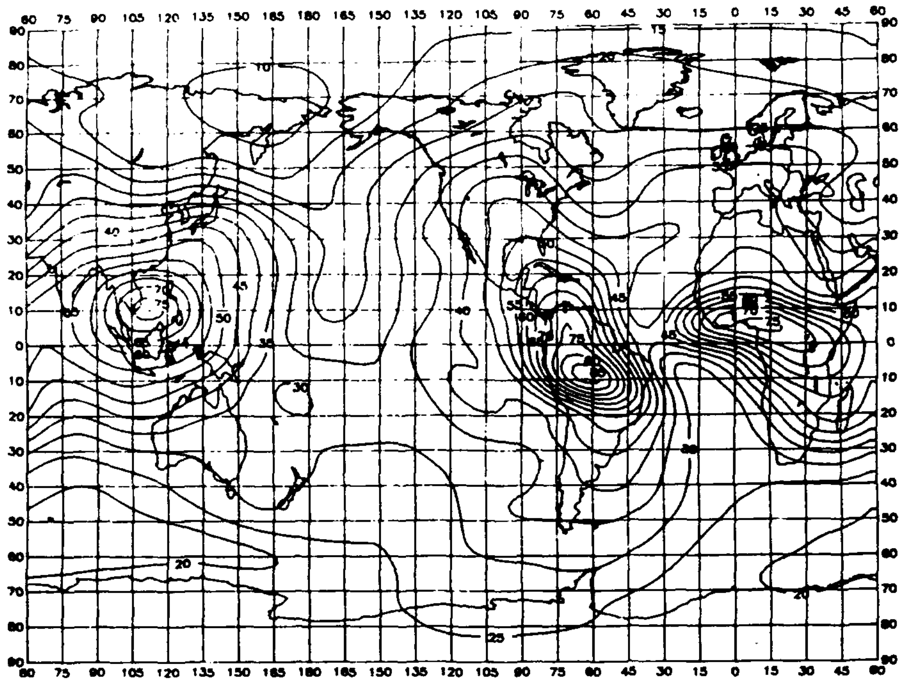

Figure 51. Expected values of atmospheric radio noise at 1 MHz, F_{am} (dB above kT_0b), for September, October, November, 0800–1200 hours (Spaulding and Washburn, 1985).

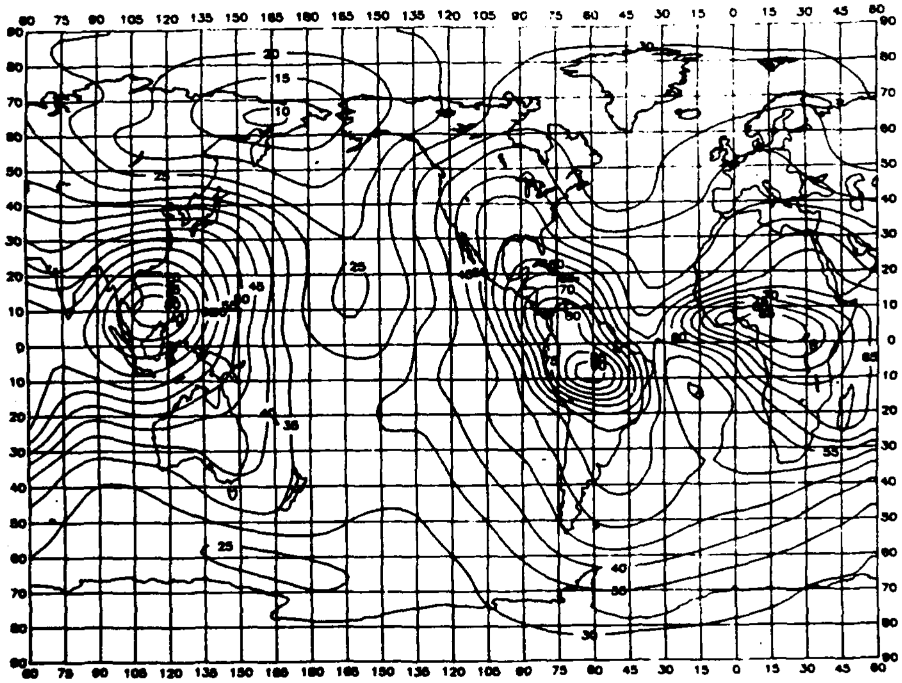

Figure 52. Expected values of atmospheric radio noise at 1 MHz, F_{am} (dB above kT_0b), for September, October, November, 1200–1600 hours (Spaulding and Washburn, 1985).

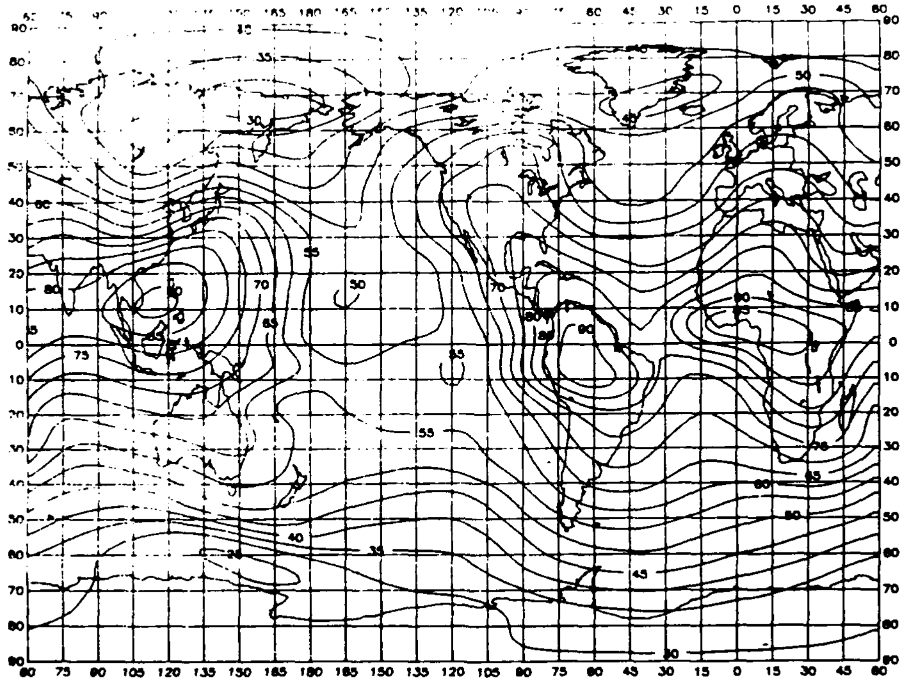

Figure 53. Expected values of atmospheric radio noise at 1 MHz, F_{am} (dB above kT_0b), for September, October, November, 1600-2000 hours (Spaulding and Washburn, 1985).

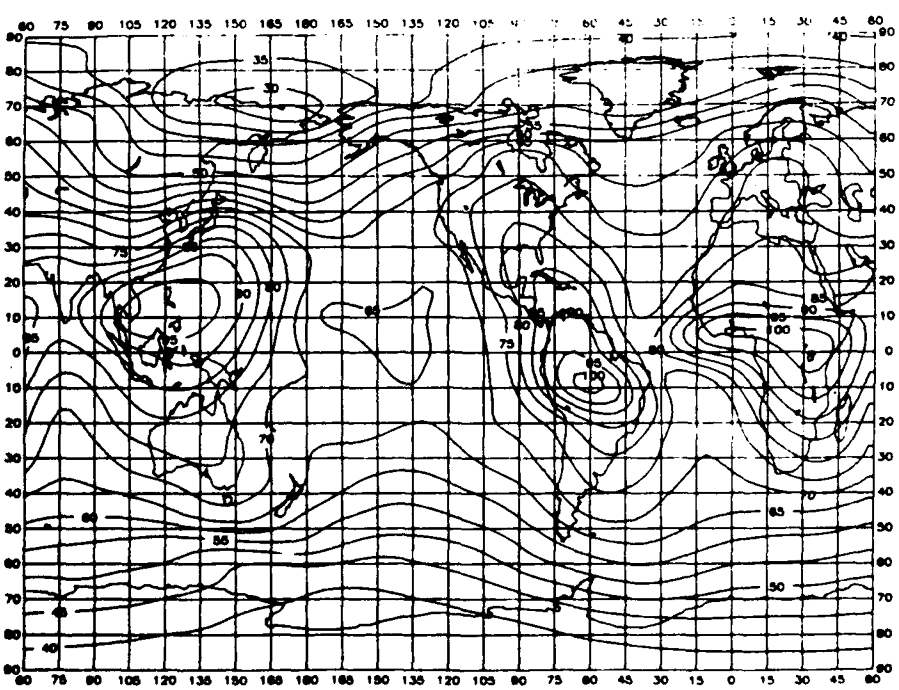

Figure 54. Expected values of atmospheric radio noise at 1 MHz, F_{am} (dB above kT_0b), for September, October, November, 2000-2400 hours (Spaulding and Washburn, 1985).

4.0 THE PROBABLE SOURCE OF THE ERROR IN THE CCIR RADIO NOISE MODEL

The probable source of the error in the CCIR radio noise model is most likely due to the nonuse of correction factors for Thule, Greenland; Byrd Station, Antarctica; Ibadan, Nigeria; and Bill, Wyoming. In the case of Thule and Byrd Station, data from these sites were not used because of possible contamination from man-made noise at these two locations. However, these same two locations were used in the original CCIR noise model. One would anticipate that if the data were contaminated by man-made noise that a negative correction factor would be the likely case. Thus, it would seem desirable to determine correction factors for these sites as was done for the other sites. That is, the data at lower frequencies could have been used to obtain correction factors at 1 MHz. Certainly, there is evidence that the measurements at Thule at 2.5 and 5.0 MHz were contaminated by man-made noise (Herman, 1962). However, Herman (1963) showed that Byrd Station is an exceptionally quiet location and would be a good site for making a variety of radio measurements requiring a low-noise background. At Thule, man-made noise on 2.5 and 5.0 MHz appeared to be 57 and 49 dB above kTB, respectively, while at Byrd Station the values were about 20 and 12 dB, respectively (Herman, 1964). These values were estimated from data taken during a PCA, when atmospheric noise was absent. The corresponding values for a quiet rural site at 2.5 and 5.0 MHz are 43 and 34 dB, respectively. Both sites are affected by galactic noise at 10.0 and 20.0 MHz. In the case of Ibadan, no additional data were available beyond the last date for data used in the original CCIR 322 noise model. Not even a correction factor of zero to maintain the status quo was used for these three sites. In the case of Bill, Wyoming, data were not included because the correction factors obtained for it were nearly the same as for Boulder, Colorado, which was in close proximity to Bill, Wyoming.

The net result of not including correction factors (not even zero to maintain the status quo) for these four locations was that the interpolation algorithm used to determine the 100-latitude by 84-longitude data points supplied erroneous correction factors at these sites. Tables 6 through 9 give the error in the correction factor for these four sites. For Thule, Byrd Station, and Ibadan, the error is the difference between the correction factors given in figures 7 through 30 and zero for the status quo. For Bill, Wyoming, the error is the difference between those given in these figures and the correction factor input for Boulder, Colorado. It was anticipated that the errors at Thule and Byrd Station might be large, but it was a surprise to see the magnitude of the errors at Ibadan. For Thule the maximum and minimum errors in the correction contours from zero status quo were 10.1 and −10.8 dB, respectively. For Ibadan the maximum and minimum errors were 12.5 and −1.5 dB, respectively. For Byrd Station the maximum and minimum errors were 12.0 and 3 dB, respectively. The error for Bill, Wyoming, is within the rms error of the numerical maps of CCIR Report 322-3.

Table 6. Interpolation errors (dB) for select measurement locations for December, January, and February.

LOCATION NAME	LOCAL TIME					
	00–04	04–08	08–12	12–16	16–20	20–24
Thule	7.0	3.5	6.0	6.0	3.0	6.0
Ibadan	–0.4	6.0	0.6	5.5	3.0	–1.5
Bill	–0.8	–0.6	–1.0	–0.3	–1.0	–1.0
Byrd Station	3.0	0.0	5.5	2.0	6.0	5.5

Table 7. Interpolation errors (dB) for select measurement locations for March, April, and May.

LOCATION NAME	LOCAL TIME					
	00–04	04–08	08–12	12–16	16–20	20–24
Thule	3.0	–3.0	–3.0	–4.1	–10.8	3.0
Ibadan	3.0	3.0	8.2	0.8	5.0	0.0
Bill	–1.0	–0.9	–1.0	–0.5	–1.0	–0.6
Byrd Station	4.0	8.0	12.0	7.3	10.2	7.0

Table 8. Interpolation errors (dB) for select measurement locations for June, July, and August.

LOCATION NAME	LOCAL TIME					
	00–04	04–08	08–12	12–16	16–20	20–24
Thule	–1.3	6.0	1.5	6.0	10.1	0.0
Ibadan	5.3	7.4	10.6	0.0	4.5	8.0
Bill	–0.5	–1.0	–1.0	–1.0	–1.0	–0.7
Byrd Station	8.3	8.0	12.0	7.3	10.2	7.0

Table 9. Interpolation errors (dB) for select measurement locations for September, October, November.

LOCATION NAME	LOCAL TIME					
	00–04	04–08	08–12	12–16	16–20	20–24
Thule	–6.0	3.0	0.0	3.0	3.0	–2.5
Ibadan	5.5	10.7	12.5	5.2	8.8	5.3
Bill	–1.4	–1.0	–1.0	–1.0	–0.7	–0.6
Byrd Station	3.0	4.9	12.0	9.0	3.0	3.0

4.1 GEOGRAPHICAL EFFECTS

To see the geographical effects of these errors, contour plots were made of the errors for each time block and season. For the 19 locations used to determine the correction factor contours in figures 7 through 30, the error was assumed to be zero. That is, it was assumed that the interpolation process gives values for the correction factors at these sites as were input into the interpolation process. The values given in tables 6 through 9 were used for the other four sites. The commercial graphics program for personal computers, Axum[1], was used to plot the errors for the irregularly spaced data points. Axum rarely was able to determine a grid spacing greater than 50 by 50 for its internal interpolation for the contour plotting. The results are presented in figures 55 through 78. Note that the longitudes are positive for degrees east of Greenwich (zero degree) and negative for degrees west of zero degree. This longitude convention was used so that the contour plots produced by Axum would have the eastward direction on the right-hand side as is the convention for maps. Postive latitudes are northern latitudes, and negative latitudes are southern latitudes. The locations of the four sites for which no correction factors were used in the interpolation are approximately given in the figures. Examination of these figures reveals that the geographical extent of the error is not confined to the measurement location but in fact in some cases is very large. This is especially true in the northern and southern high latitudes, the Arabian Peninsula, northern Africa, and the mid-Atlantic areas.

4.2 FREQUENCY-DEPENDENCE EFFECTS

As the CCIR Report 322-3 atmospheric noise model can be used at frequencies from 10 kHz through 30 MHz, it is important to be able to translate an error in the 1-MHz model to an error at any frequency in this frequency range. To determine this relationship, the frequency-dependence model was used, assuming no error inherit in it. This model obtains the noise at any frequency by inputing the 1-MHz value for a particular time block and season into a set of curves parametric in the 1-MHz value (see figure 3). For each time block and season, there is a range of possible input 1-MHz values for which the atmospheric noise can be obtained depending on the location of the receive site. To obtain the error at an arbitrary frequency, time block, and season, each of the parametric values was perturbed by errors of 10 and -10 dB, and the resultant errors, respectively, were determined. The statistical average, high, and low values were then obtained. It was found that the error at each of the 35 frequencies from 10 kHz through 30 MHz used did not depend significantly on the parametric curve value. However, the error was diurnally dependent. The maximum errors for each frequency occurred during the local time daytime, and the minimum-error errors occurred during the nighttime. Figure 79 shows the average, high, and low error as a function of frequency and 1-MHz error. The figure shows the error for -10 dB to be a mirror image of that for a 10-dB error.

[1] trademark of TriMetrix, Inc.

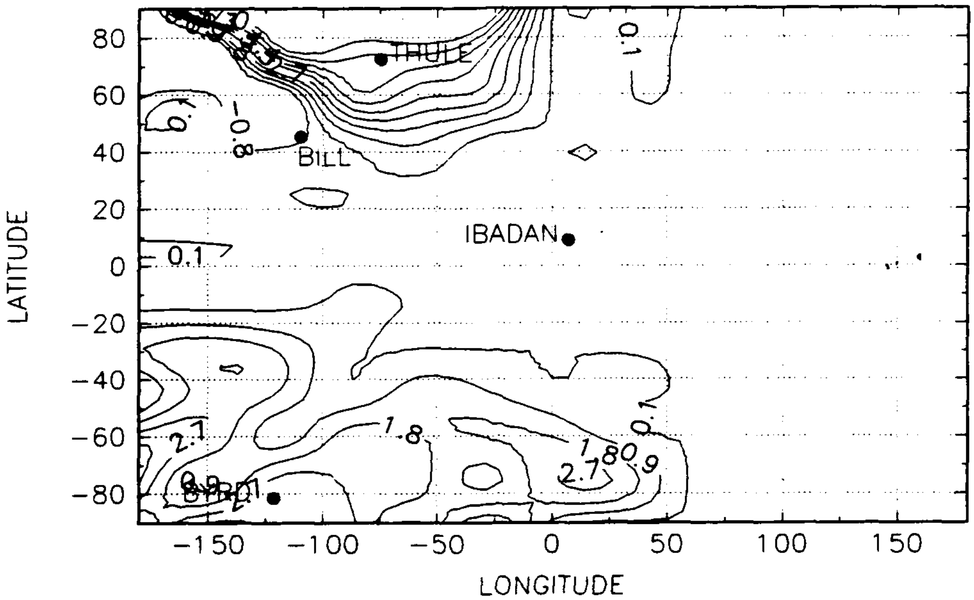

Figure 55. Geographical 1-MHz atmospheric noise model error, December, January, February, 0000–0400 hours.

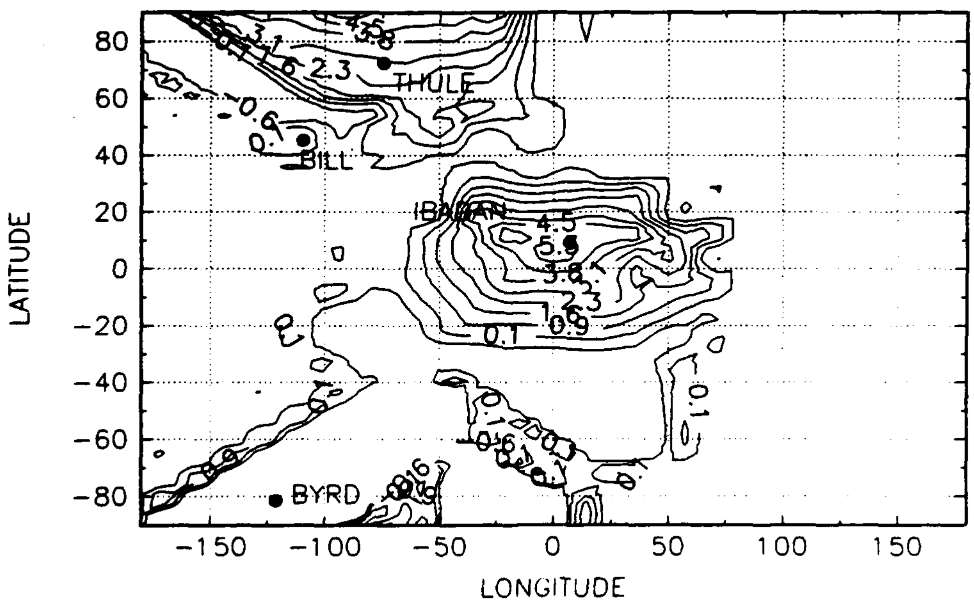

Figure 56. Geographical 1-MHz atmospheric noise model error, December, January, February, 0400–0800 hours.

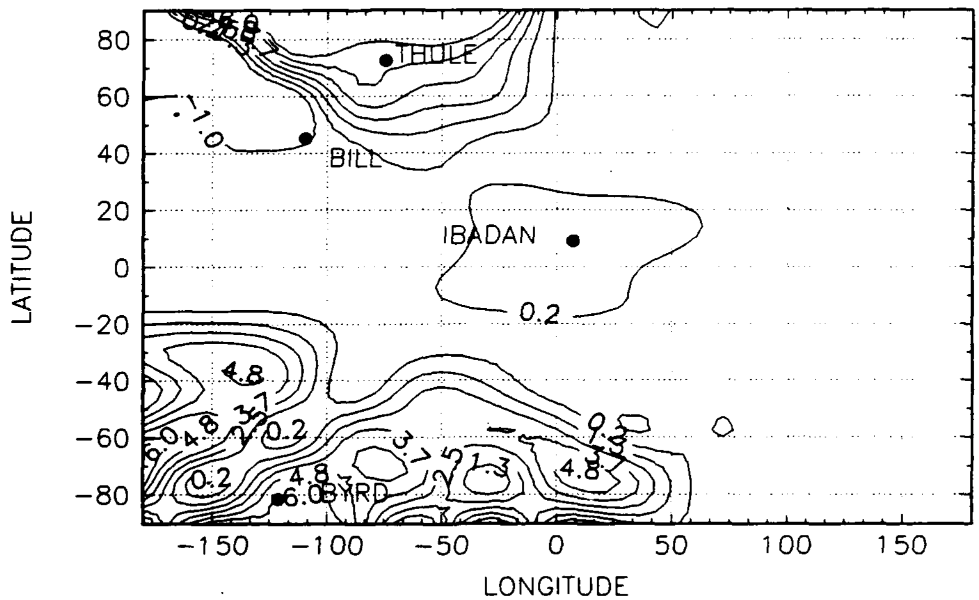

Figure 57. Geographical 1-MHz atmospheric noise model error, December, January, February, 0800–1200 hours.

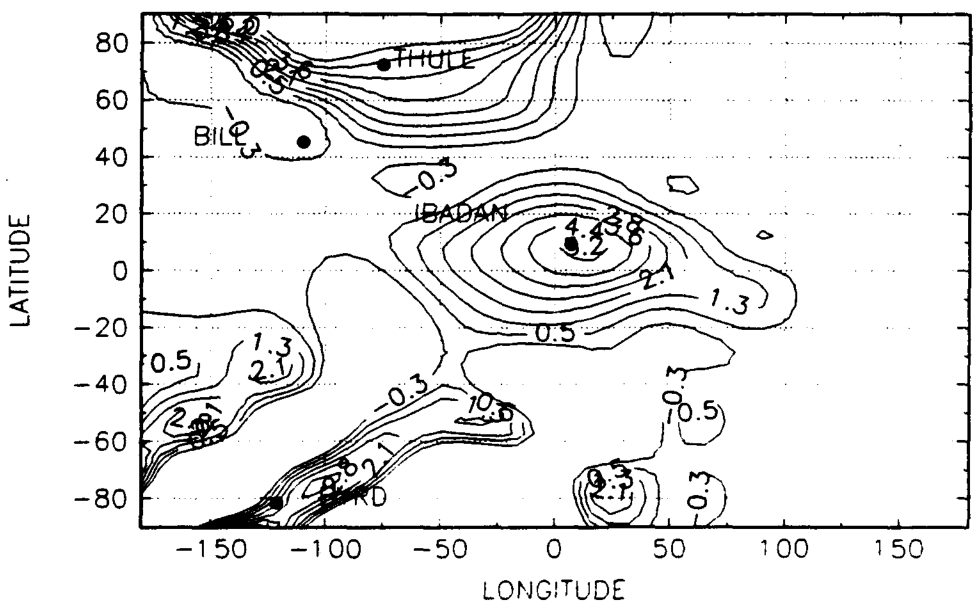

Figure 58. Geographical 1-MHz atmospheric noise model error, December, January, February, 1200–1600 hours.

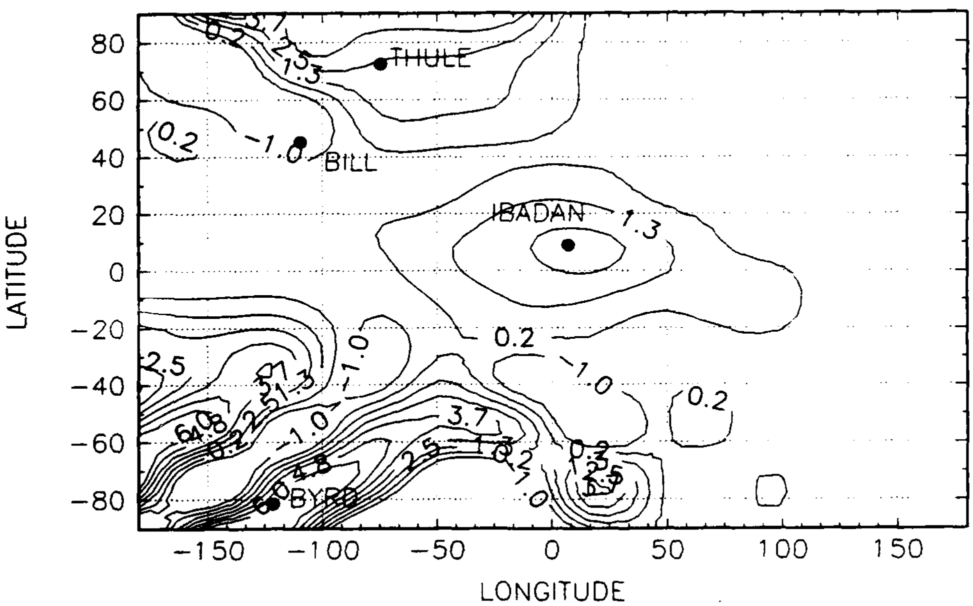

Figure 59. Geographical 1-MHz atmospheric noise model error, December, January, February, 1600–2000 hours.

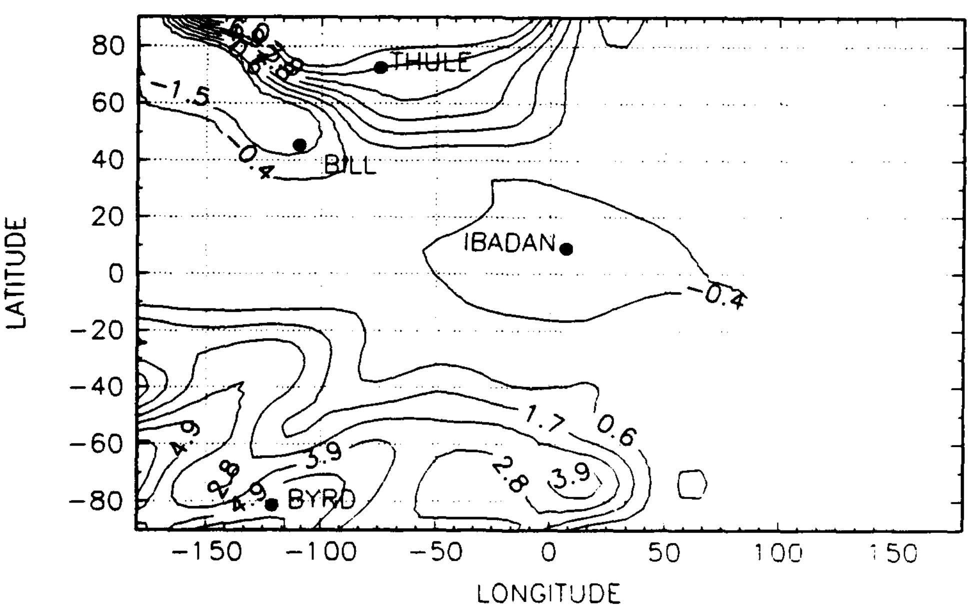

Figure 60. Geographical 1-MHz atmospheric noise model error, December, January, February, 2000–2400 hours.

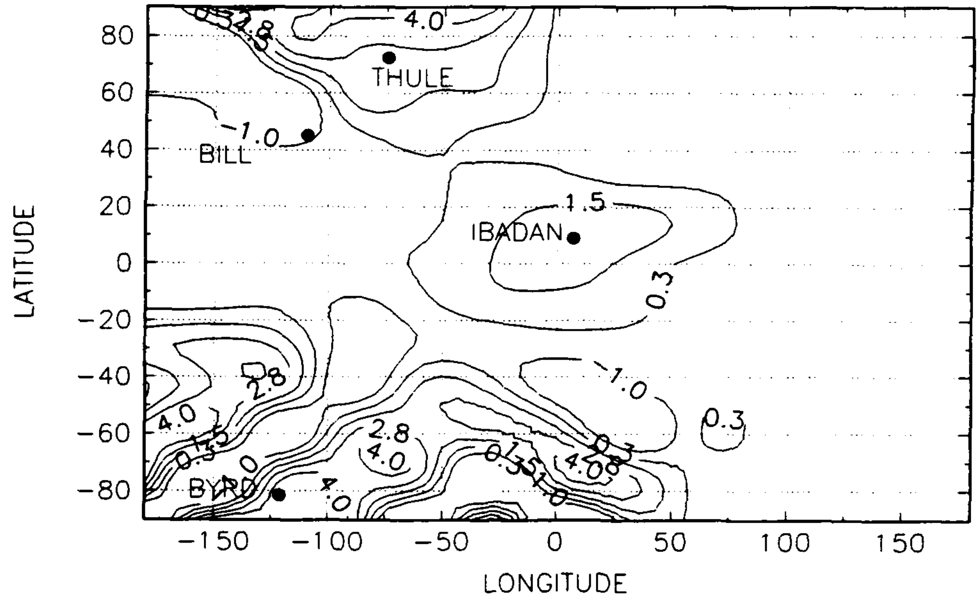

Figure 61. Geographical 1-MHz atmospheric noise model error, March, April, May, 0000–0400 hours.

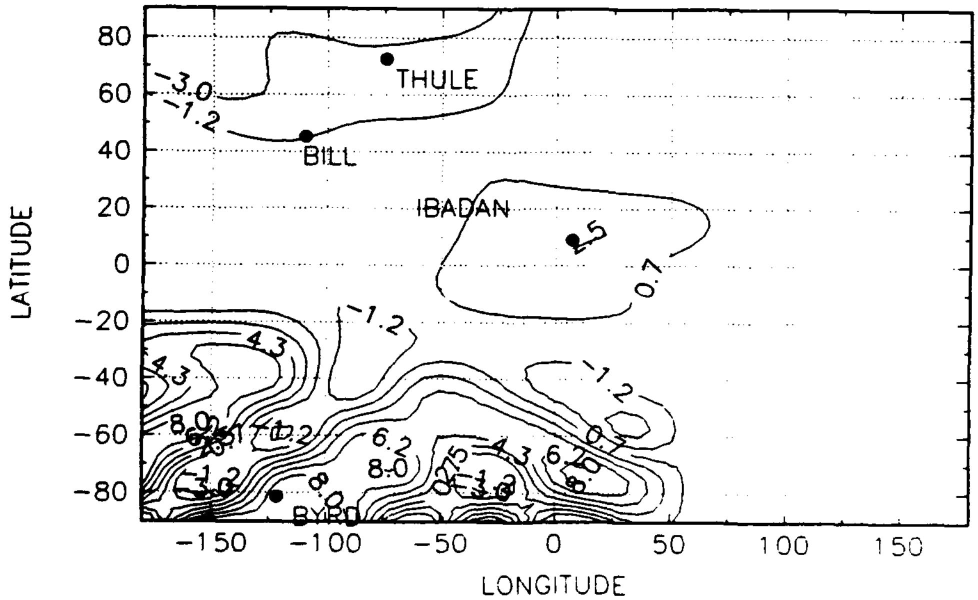

Figure 62. Geographical 1-MHz atmospheric noise model error, March, April, May, 0400–0800 hours.

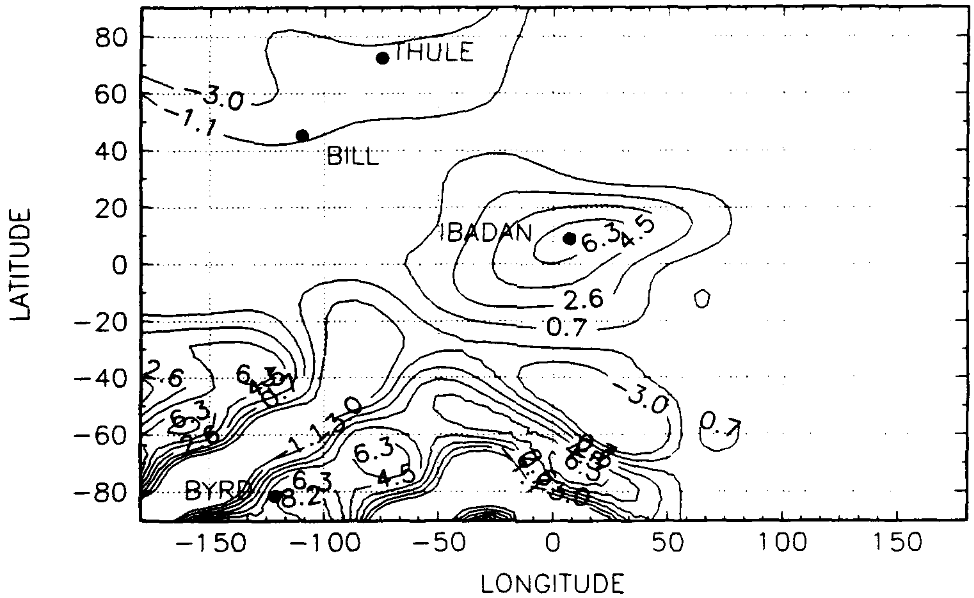

Figure 63. Geographical 1-MHz atmospheric noise model error, March, April, May, 0800–1200 hours.

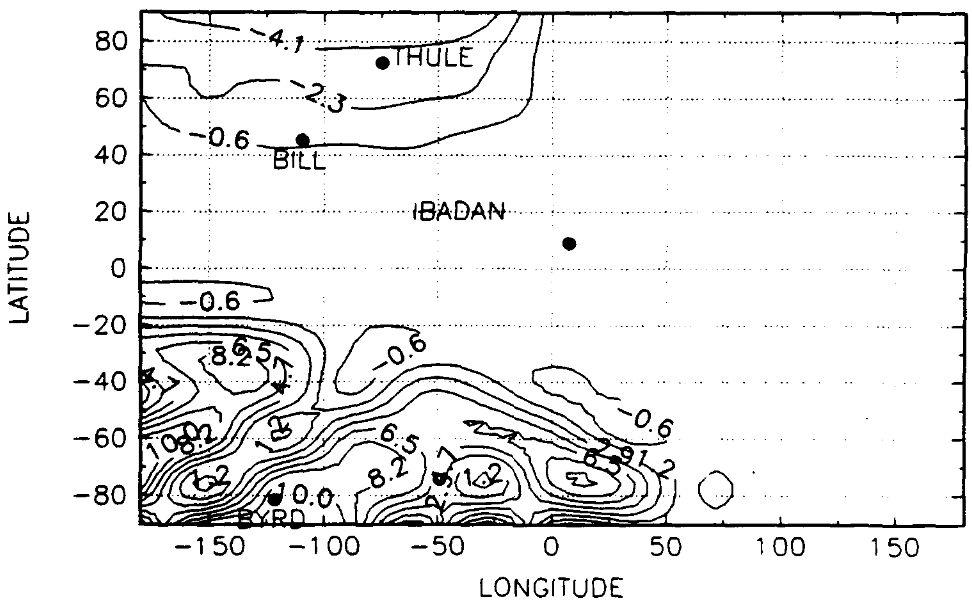

Figure 64. Geographical 1-MHz atmospheric noise model error, March, April, May, 1200–1600 hours.

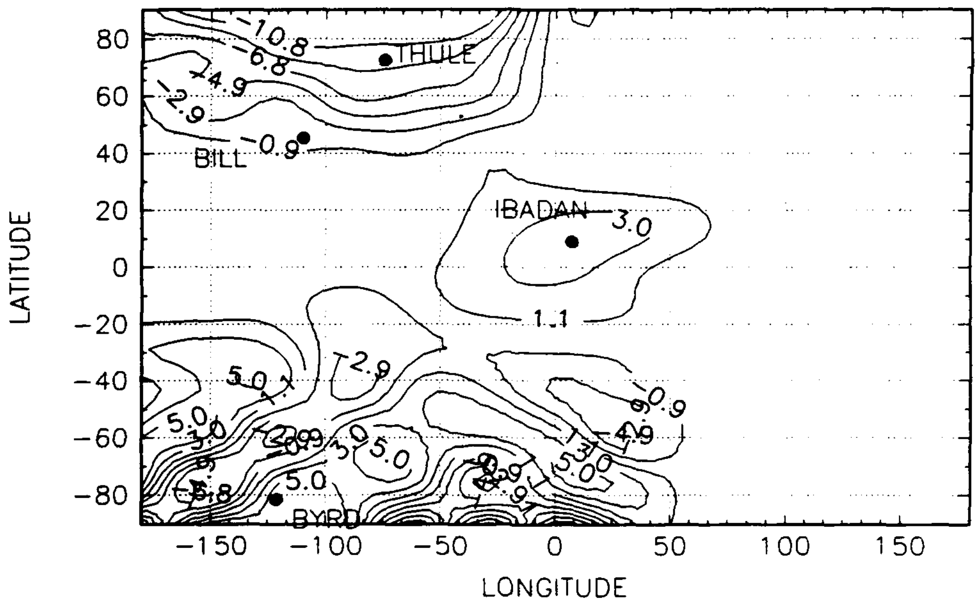

Figure 65. Geographical 1-MHz atmospheric noise model error, March, April, May, 1600-2000 hours.

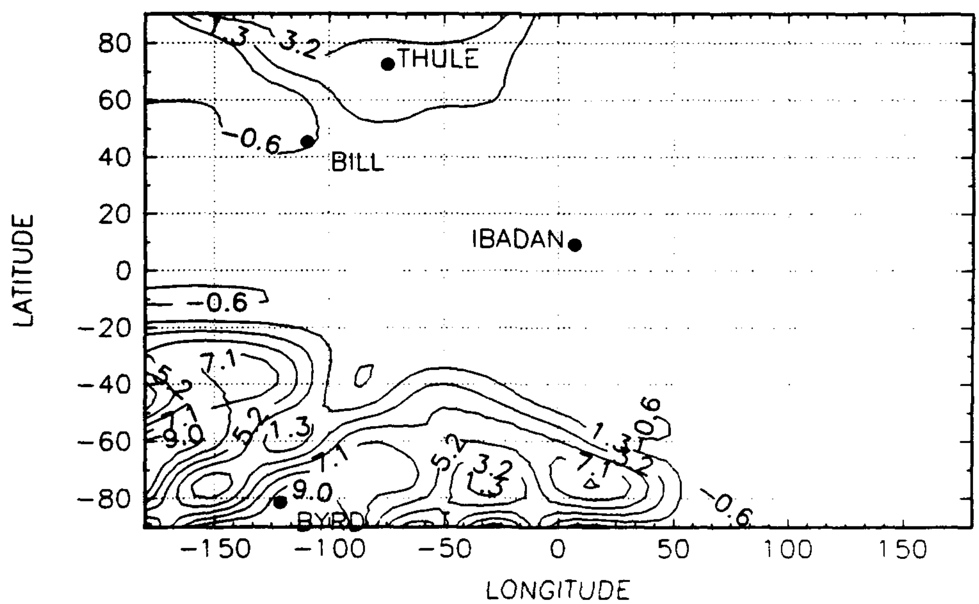

Figure 66. Geographical 1-MHz atmospheric noise model error, March, April, May, 2000-2400 hours.

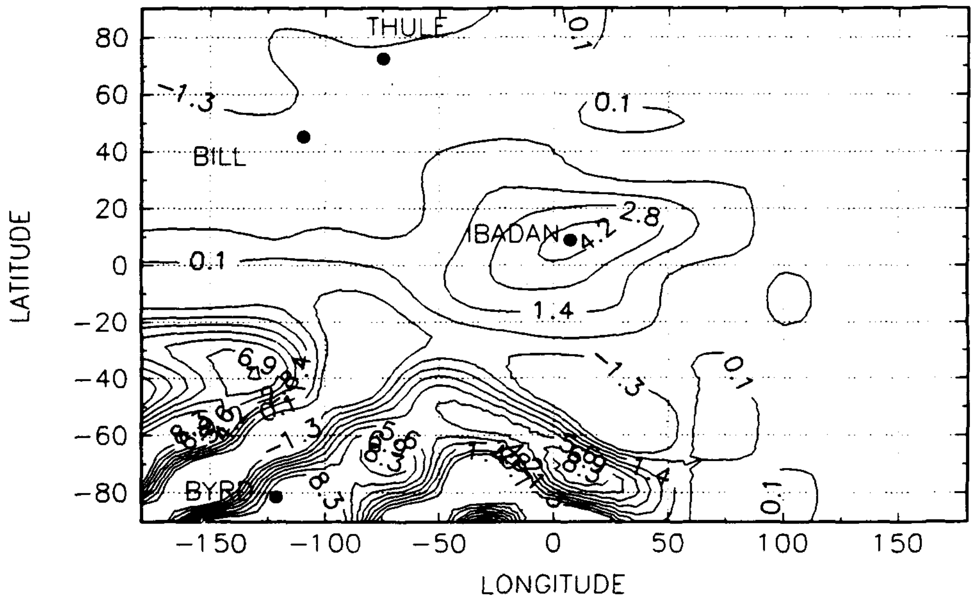

Figure 67. Geographical 1-MHz atmospheric noise model error, June, July, August, 0000-0400 hours.

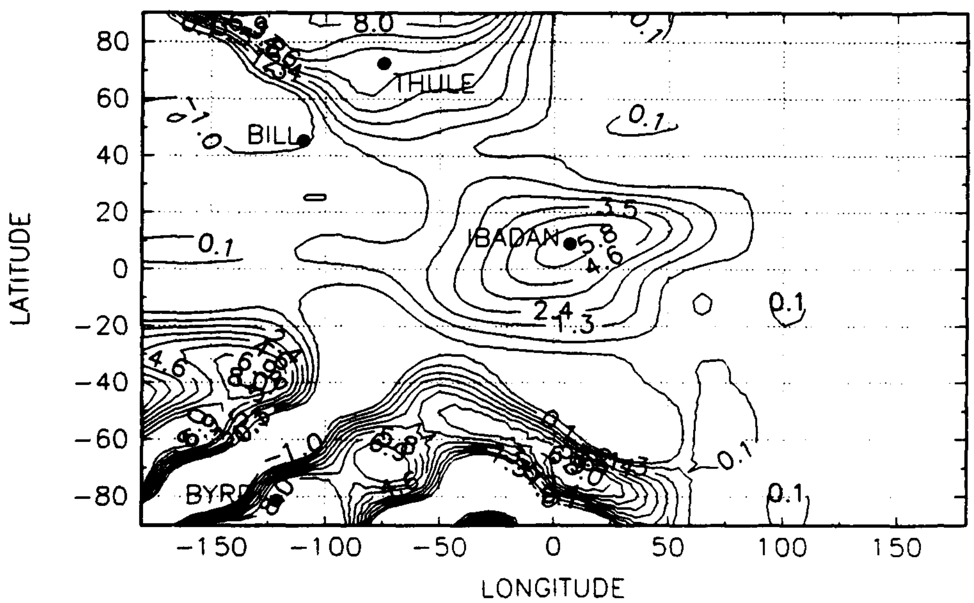

Figure 68. Geographical 1-MHz atmospheric noise model error, June, July, August, 0400-0800 hours.

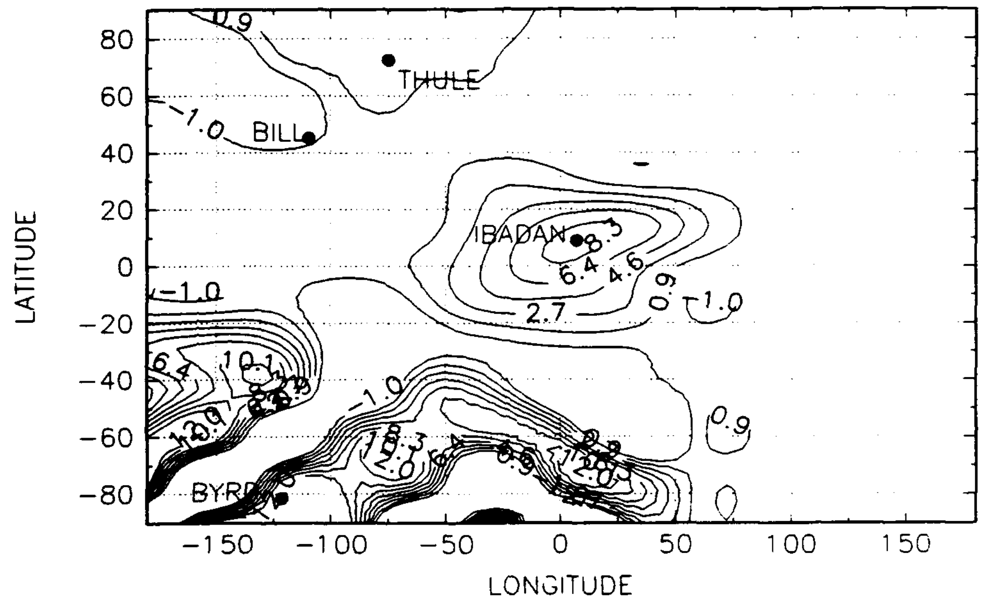

Figure 69. Geographical 1-MHz atmospheric noise model error, June, July, August, 0800–1200 hours.

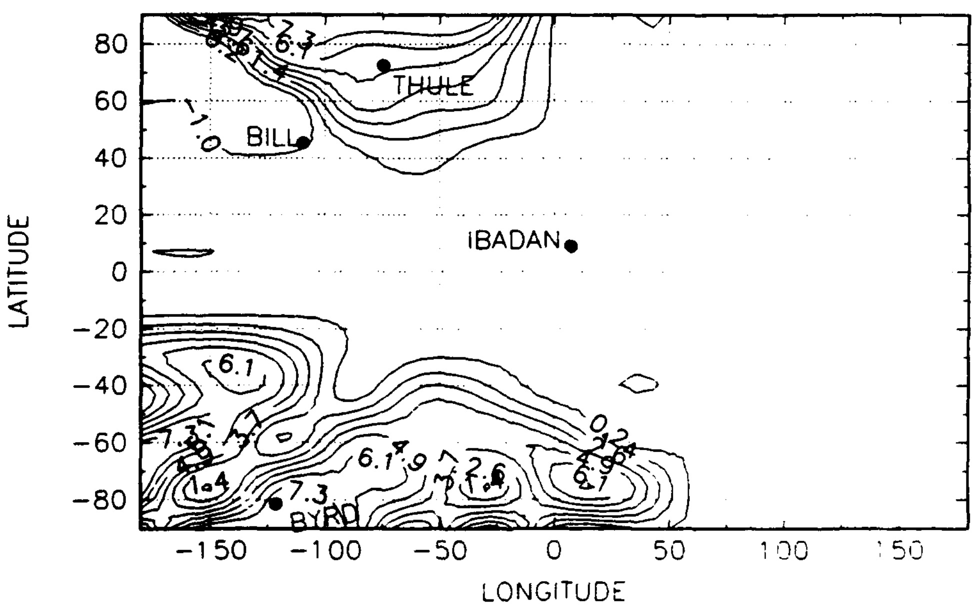

Figure 70. Geographical 1-MHz atmospheric noise model error, June, July, August, 1200–1600 hours.

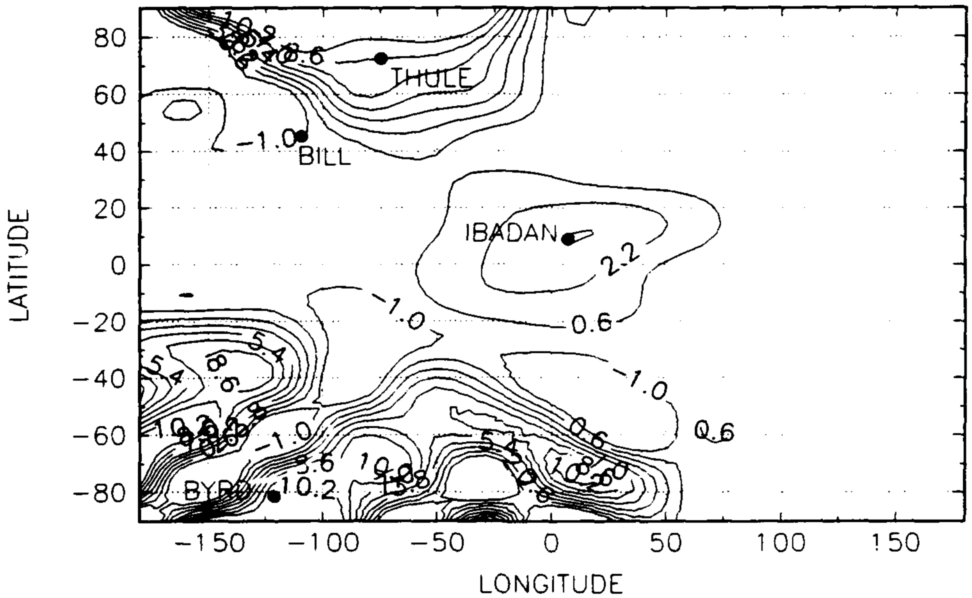

Figure 71. Geographical 1-MHz atmospheric noise model error, June, July, August, 1600–2000 hours.

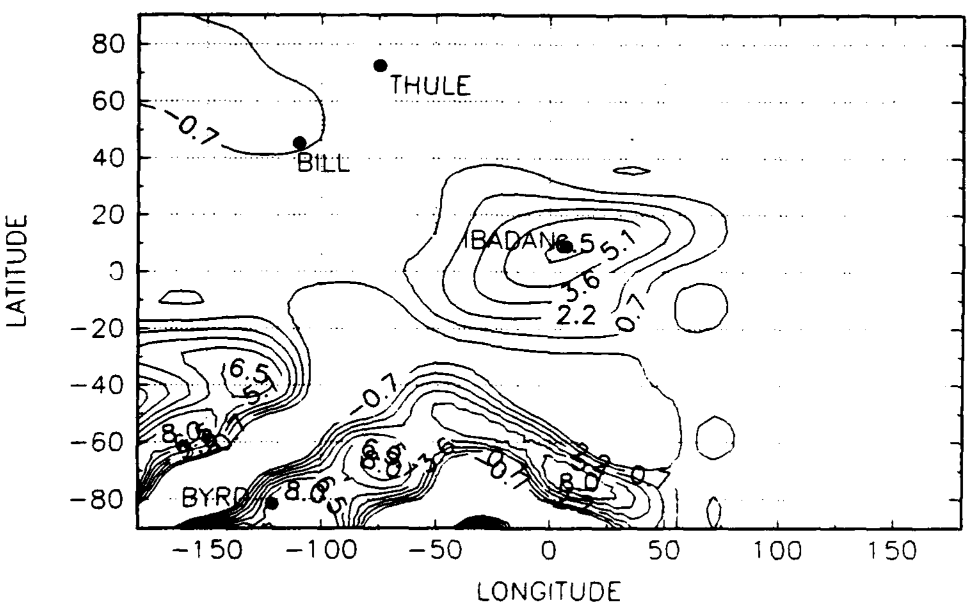

Figure 72. Geographical 1-MHz atmospheric noise model error, June, July, August, 2000–2400 hours.

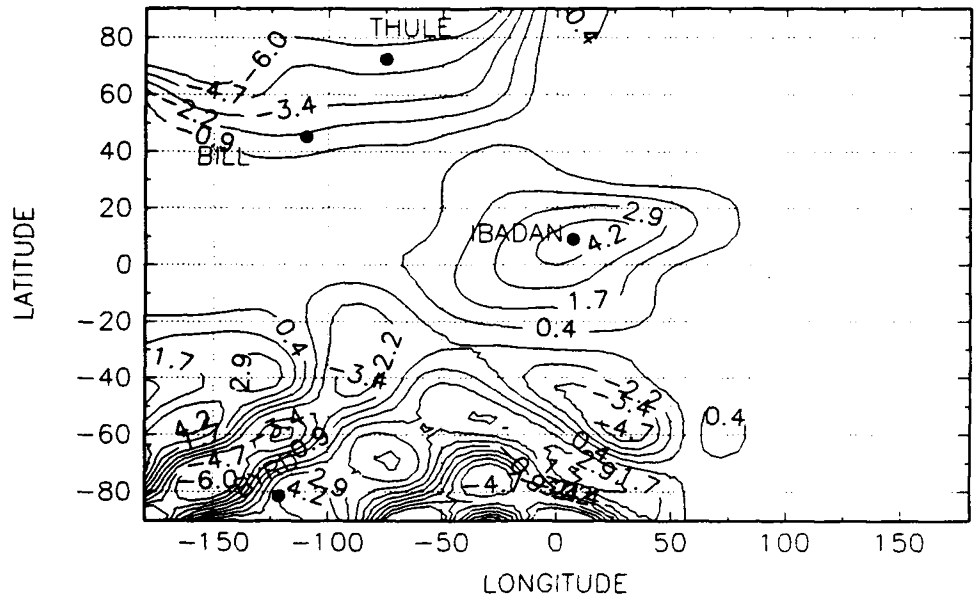

Figure 73. Geographical 1-MHz atmospheric noise model error, September, October, November, 0000–0400 hours.

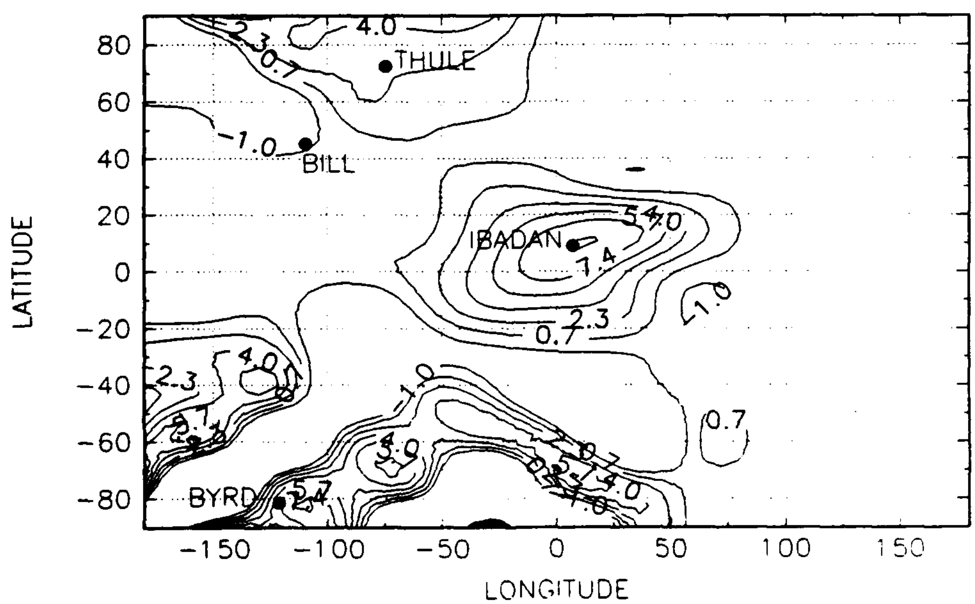

Figure 74. Geographical 1-MHz atmospheric noise model error, September, October, November, 0400–0800 hours.

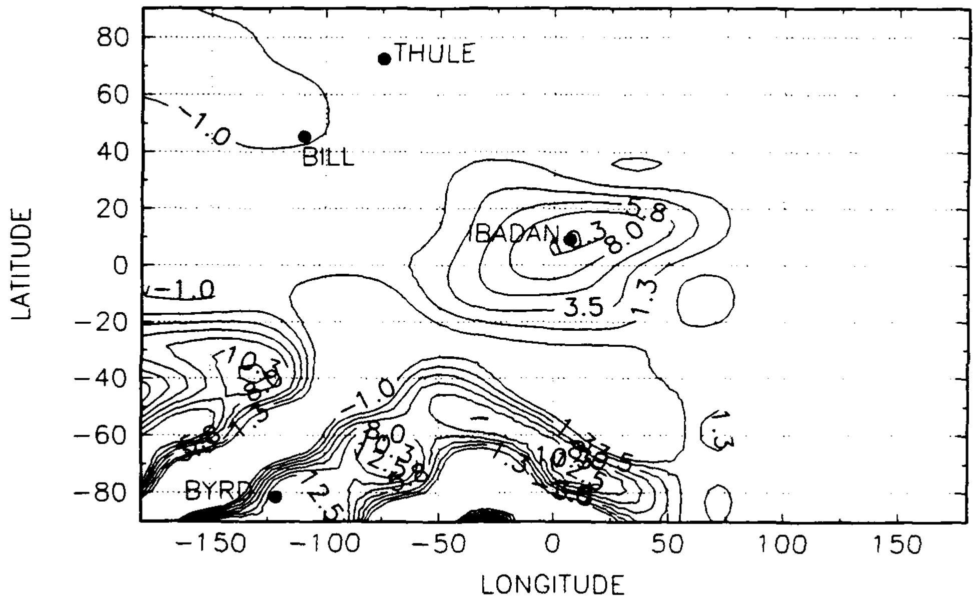

Figure 75. Geographical 1-MHz atmospheric noise model error, September, October, November, 0800–1200 hours.

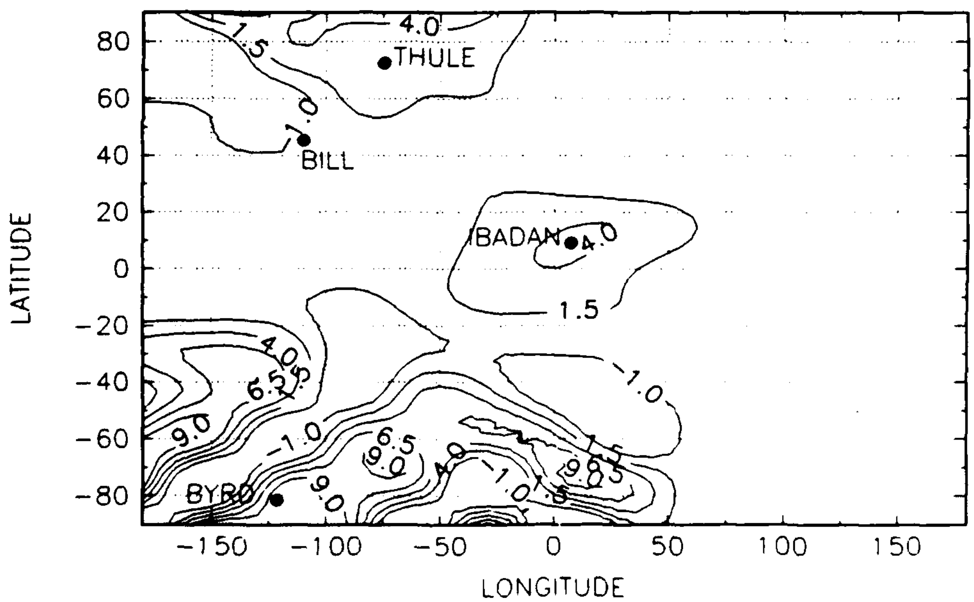

Figure 76. Geographical 1-MHz atmospheric noise model error, September, October, November, 1200–1600 hours.

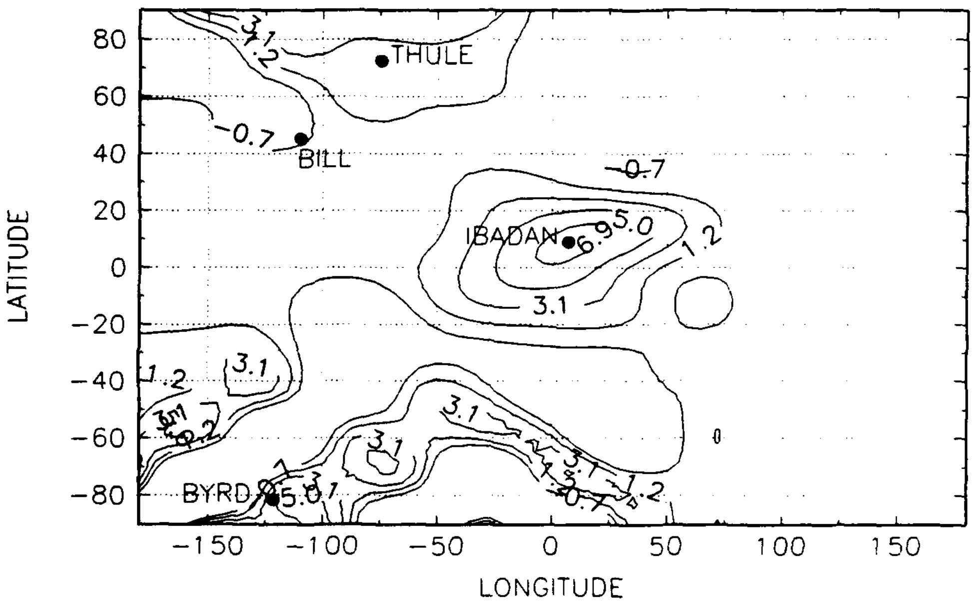

Figure 77. Geographical 1-MHz atmospheric noise model error, September, October, November, 1600-2000 hours.

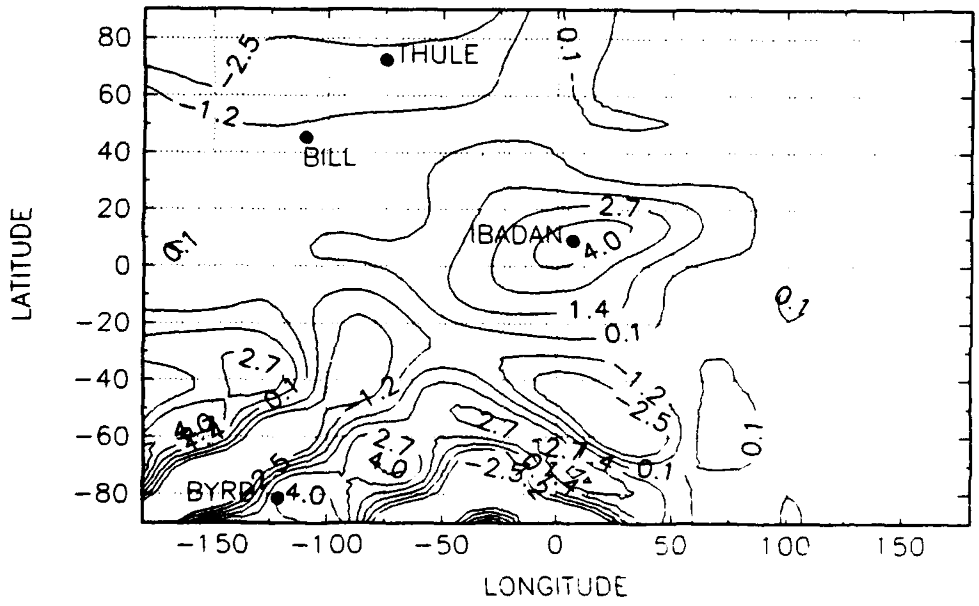

Figure 78. Geographical 1-MHz atmospheric noise model error, September, October, November, 2000-2400 hours.

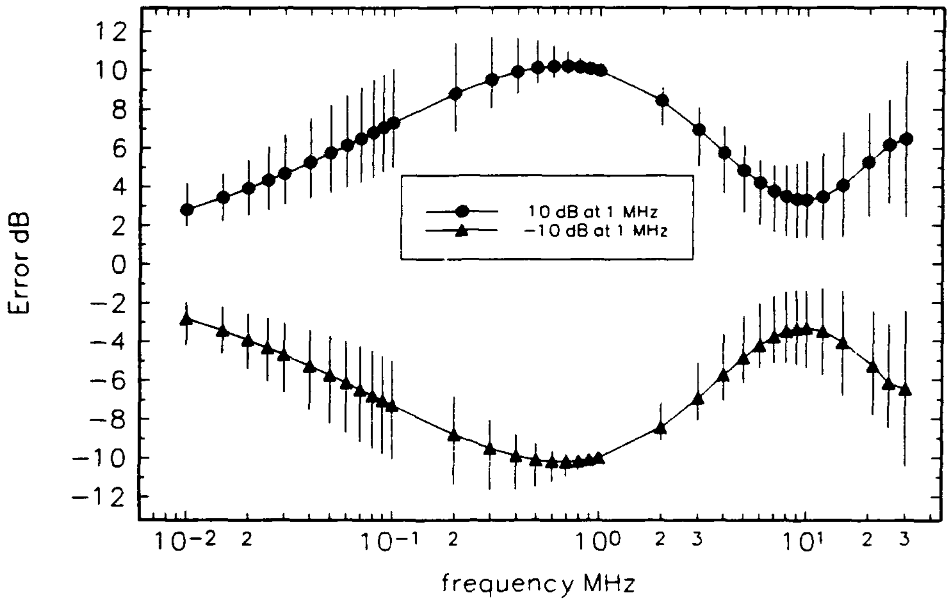

Figure 79. Error in atmospheric noise as a function of frequency for a given error at 1 MHz, mean, maximum, minimum for all time blocks.

4.3 INTERPOLATION EFFECTS

The accuracy of the interpolation itself is affected by the lack of inclusion of data from the four measurement locations. First, the number of triangles and number of edges of these triangles is reduced. From Lawson (1977), the number of triangles is

$$n_t = n_b + 2\,(n_i - 1) \leq 2n \tag{2}$$

and the number of edges is

$$n_e = 2n_b + 3\,(n_i - 1) \leq 3n \tag{3}$$

where n is the number of distinct points in the set S; n_b denotes the number of points in S on the boundary of the convex hull of S; and n_i denotes the number of points in the interior of the convex hull of S so that $n = n_b + n_i$. In the case of data points on a sphere, $n_b = 0$ (i.e., there are no boundary points). For $n = 19, n_t = 36$ and $n_e = 54$. For $n = 23$, $n_t = 44$ and $n_e = 66$. Thus there is a 122.22-percent increase in triangle edges by adding the four points. Second, the number of input data points affects how the C^1 surface interpolation determines the triangles themselves. Each pair of triangles forms a quadrilateral. The Lawson criterion gives the preferred triangulation of a quadrilateral (Ripley, 1981). Lawson required that the smallest of the six angles in the two triangles be larger for this division of a convex quadrilateral than that given by the other

diagonal, as shown in figure 80. The left-hand triangulation is chosen because angle A is larger than angle B. Thus when the four data measurement locations are not used in the model development, then the triangulation is considerably changed and may not be optimum. Further, Akima (1984) has shown that poor estimates of partial derivatives usually occur when a thin (or slim) triangle is involved in the interpolation, which affects the accuracy of the interpolation. This is more likely to have occurred when the four data locations, particularly the two high latitude sites, are left out.

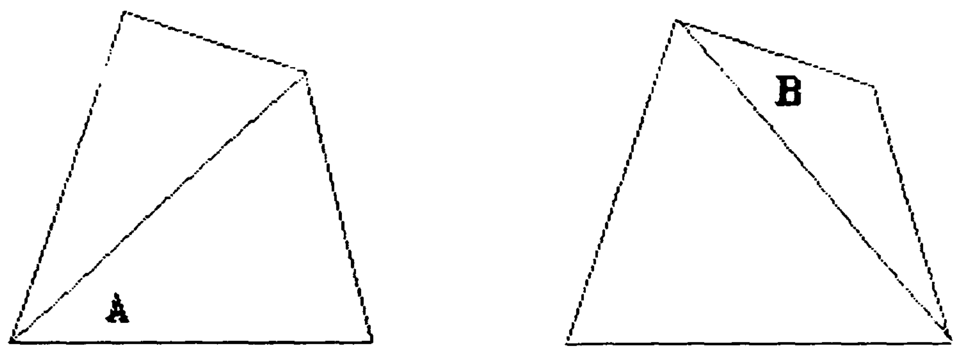

Figure 80. The Lawson criteria. The left-hand triangulation is chosen because angle A is greater than B.

Several of the contour plots giving the correction factors in figures 7 through 30 have values larger or smaller than the extreme values used in the interpolation to obtain these figures. The figures with the minimum extreme less than the input minimum extreme usually had this extreme occurring at one or two of the same locations. These two locations are either in the very most Eastern part of Asia or in the North Atlantic just south of Greenland. These extremes likely would not have occurred had the data at Thule, Greenland, been used; in this case the triangulation would have been considerably different. The figures with the maximum extreme greater than input maximum extreme usually had this extreme occurring at one or two of the same locations. The first location was usually in the vicinity of Guam. The second location was in the South Atlantic between South America and Africa. This latter location would have been affected by the triangulation if the data from Ibadan, Nigeria, and Byrd Station, Antarctia, had been included. However, the extreme occurring in the vicinity of Guam is due to the gradients occurring in the input data in eastern Asia. The data there goes from large negative corrections in the north to large positive corrections at Singapore. The interpolation program extrapolated to obtain the large positive correction factors in the vicinity of Guam. Further, in this case the triangulation would not have changed if the data for the other four locations had been included in the model development. Whether this correction is valid or not is unclear. Additional input data in the vicinity of Guam would have been useful.

5.0 PROPOSED PROCESS TO DEVELOP A CORRECTED 1-MHz RADIO NOISE MODEL

A three-step process is proposed to develop a new 1-MHz noise model. The first step is to obtain correction factors for additional locations to increase the accuracy of the interpolation. This includes adding data measured at Thule, Greenland; Byrd Station, Antarctica; Ibadan, Nigeria; and Bill, Wyoming. Attention will be given to the elimination of man-made noise at these locations. The second step is the interpolation of the data to a 100-latitude by 84-longitude grid for each time block/season for numerical mapping. Consideration will be given to using the interpolation method used by Spaulding and Washburn (1985). However, a two-dimensional method of interpolation (Akima, 1978a, 1978b, 1979) and more recent algorithms (Cline & Renka, 1984; Renka 1984a, 1984b, 1984c; Renka & Cline, 1984) will be examined for possible use. The final step is the numerical mapping of the data itself to produce the final model. A numerical mapping technique from Zacharisen and Jones (1970) will be used. However, the mapping will be done in local time rather than in universal time as applied by Zacharisen and Jones.

5.1 ADDITIONAL DATA LOCATIONS

There are nine possible locations for which additional data might be used to increase the accuracy of the 1-MHz atmospheric noise model. The first four are the four original 1-MHz measurement locations not used to obtain correction factors. These are Thule, Greenland; Byrd Station, Antarctica; Ibadan, Nigeria; and Bill, Wyoming. For Thule and Byrd Station, the effects of man-made noise will be removed by techniques described below. For Ibadan, a correction factor of zero will be used since there is no new data available for this site from that already used in the original CCIR 322 model. For Bill, the correction factors for Boulder will be used as Spaudling and Washburn indicate that they differ little from those at Bill. If data from the four Soviet Union locations (Simferopol, Sverdlovsk, Tbilisi, and Kiev) not used in the development of CCIR Report 322-3 can be used, the accuracy in the northern latitudes would be increased. These data will be reexamined for that purpose. The latter three sites are located close to either Moscow or Ashkabad and may not provide as much improvement as would Sverdlovsk. One additional site is at Ping-Cheng, Taiwan, China, about 33 km from Taipei. Atmospheric noise measurements have been made at this location using the ARN-2 atmospheric noise measurement equipment from 1967 through 1973 (Huang, 1977). If that data can be obtained, then the need for data in the vicinity of Guam may not be necessary. The locations of these nine sites are noted in table 10.

Table 10. Additional atmospheric noise measurement locations.

Bill, Wyoming	105.2W,	43.2N
Byrd Station, Antarctia	120.0W,	80.0S
Ibadan, Nigeria	3.9E,	7.4N
Kiev, USSR	30.3E,	50.72N
Ping-Cheng, Taiwan	121.23E,	24.95N
Simferopol, USSR	34.03E,	45.02N
Sverdlovsk, USSR	61.07E,	56.73N
Tbilisi, USSR	40.0E,	41.72N
Thule, Greenland	68.7W,	76.6N

Data measured on board the ship USNS *Eltanin* might be of use in verifying the accuracy of the interpolation method chosen to interpolate the correction factors to a 100-longitude by 84-latitude grid. This ship made measurements from April 1962 through November 1964 at various locations off the coast of South America. The ship usually made measurements at 5 locations during a month, repeating some locations during another month of the same season. As a result, more than a dozen locations were used to make measurements.

Atmospheric noise data being collected by Stanford University might be of use in verifying the accuracy of the atmospheric noise model at VLF frequencies. Stanford University is presently operating a global network of eight computer-controlled receiving systems for the measurement of radio noise in the 10 to 32,000 Hz (ELF/VLF) frequency band (Fraser-Smith et al., 1987). Data are being recorded on 16 frequencies, including 10.2 and 32 kHz. The locations of the sites are given in table 11 and figure 81. Several of these locations are in areas for which no other data exists.

Table 11. Geographical coordinates of ELF/VLF noise measurement sites.

Station	Coordinates
Thule, Greenland	77°N, 69°W
Søndre Strømfjord, Greenland	67°N, 51°W
New Hampshire	44°N, 72°W
L'Aquilla, Italy	42°N, 13°E
Stanford, California	37°N, 122°W
Kochi, Japan	33°N, 133°E
Dunedin, New Zealand	46°S, 170°E
Arrival Heights, Antarctica	78°S, 167°E

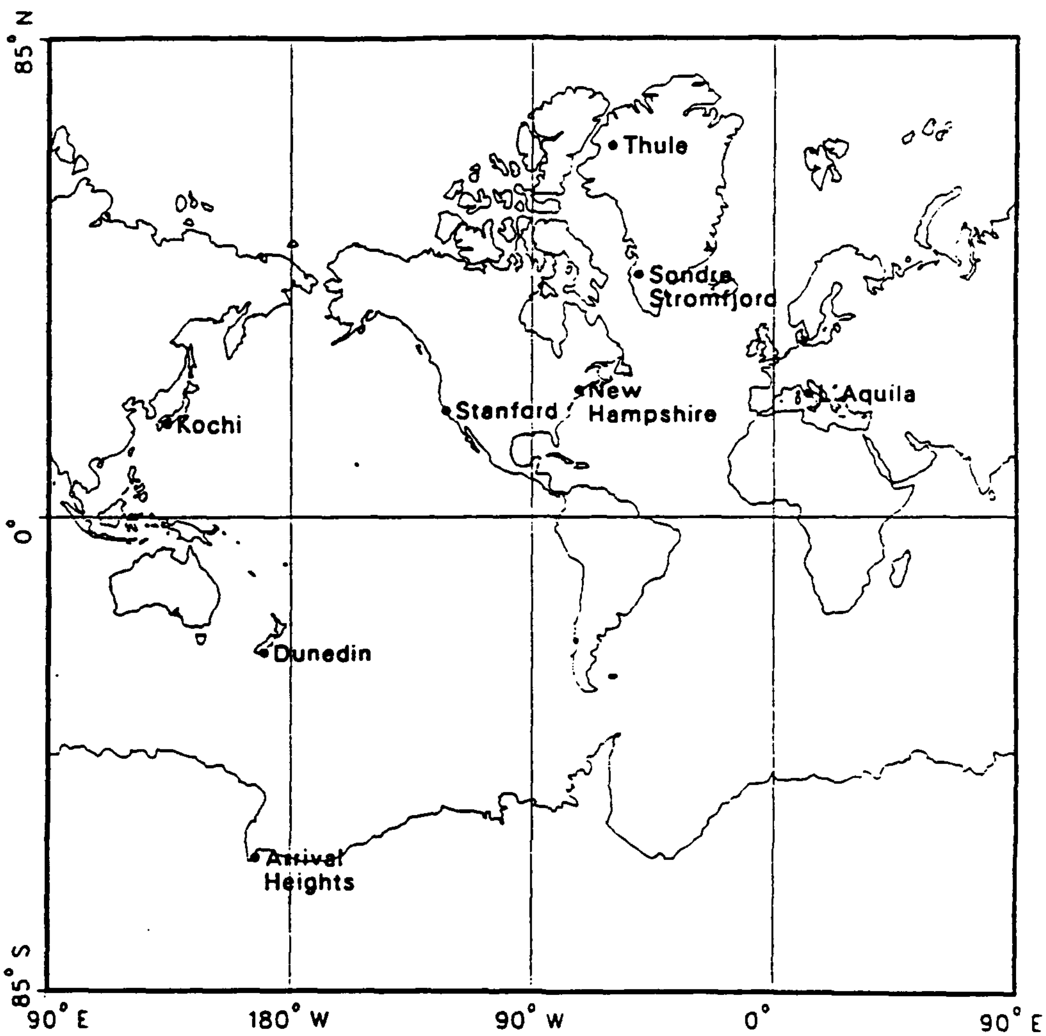

Figure 81. Locations of the eight ELF/VLF radiometer locations on a world map.

5.2 REMOVAL OF THE EFFECTS OF MAN-MADE NOISE

Basically, three methods are available for processing the measured data to remove the effects of man-made noise in the determination of the noise at 1 MHz at each measurement location. These methods can be used together or alone depending on the particular case. Having obtained the noise value at 1 MHz, the correction factors are determined as described in section 3.3.

5.2.1 Extrapolation up to 1 MHz

This method was described in section 3.2. The measured noise values for each time block and season are graphed as a function of frequency. Then the atmospheric noise frequency-dependence curves for this same time block/season and the noise curves for quiet rural and rural man-made noise are superimposed on this curve. By examining

the results, it can be determined whether the measured values at the HF frequencies are contaminated by man-made noise. This can be determined by comparing the slope of the values at HF to that of the man-made curves and by comparing the magnitude of the noise relative to that of the man-made curves. If it appears that there is no contamination, then the frequency-dependence curves can be used to interpolate the data to 1 MHz. If it appears that there is contamination, then the data points below 1 MHz can be used to extrapolate up to 1 MHz. Only those data points not having a slope the same as the man-made curve are used. The frequency-dependence curve that fits the data points is determined. Then this curve is used to extrapolate up to 1 MHz. Examples are given in figures 5 and 6, which are discussed in section 3.2.

A graphics package such as Axum for personal computers could be used to real advantage for this purpose. Each of the sets of frequency-dependence curves for both atmospheric and man-made noise for each time block/season can be stored as an image graph to be used later. Then, after the data for a site for a time block/season have been graphed, the appropiate image graph can be superimposed. Having determined the particular frequency-dependence curve to use to extrapolate to 1 MHz, Axum's capability to zoom in on a portion of a graph while in the "VIEW" mode can be used to determine an accurate estimate of the 1-MHz value.

The method described here has the disadvantage of only using the frequencies below 1 MHz. Thus, in most cases half the data set is lost. If this method is used with the methods described below, it may be possible to use the data above 1 MHz.

5.2.2 Use of V_d and L_d

If the parameters V_d and L_d are available for a particular measurement value of noise, they can be used to determine if the measured noise value is contaminated by man-made noise. If the procedure described below is used, and it is determined that the measurement is contaminated, then the measured value should be eliminated from the set of data unless some other procedure is used to remove the effects of man-made noise.

The measured noise parameter that will reflect any contamination by man-made noise will be the logarithmic parameter, L_d (Crichlow et al., 1960b). This contamination generally will cause the value of L_d to be less than it would have been, had the recorded value been only atmospheric noise. In determining the amplitude-probability distribution (APD) from the three measured statistical moments, F_a, V_d, and L_d (Crichlow, Disney, & Jenkins, 1960a; Crichlow et al., 1960c), contaminated values of L_d may be found that will not give a solution of the APD. That is, for a given V_d only a certain range of values of L_d will result in an APD representative of atmospheric noise. The combination of a given V_d and a minimum allowable L_d results in a nonunique solution (i.e., there is an infinite number of solutions all with the same V_d and L_d combination). In figure 82 the lower curve on the graph indicates the minimum value of L_d that will give an APD by the method of Crichlow et al. (1960a) for a given value of V_d. It can therefore be used to determine if the measured noise value is

contaminated. The upper curve in the graph is a curve of the most probable value of L_d for a given V_d determined as the best fit for the integrated moments from over 60 measured APDs of uncontaminated atmospheric radio noise.

5.2.3 Estimates of Man-Made and Galactic Noise

If estimates or measurements of man-made noise and galactic noise are available, it should be possible to remove the effects of these noise sources by using the inverse of the normal procedure used to combine the estimates of noise from the three main sources of noise used in prediction programs. In the case of Byrd Station, Enkoping, and Thule measurement locations, Herman (1962, 1963, 1964) has determined the man-made noise environment. For galactic noise, which is only received at frequencies above the vertical critical frequency of the F-region, it is necessary to know the critical frequency of the F-region for the hour and month of the measurement. F-region critical frequency data are available on computer media for this purpose for the following noise measuremnt sites: Alma Alta, Ashkabad, Boulder, Byrd Station, Ibadan, Irkutsk, Khabarovsk, Moscow, Murmansk, New Delhi, Ping-Cheng, Pretoria, Rabat, Simferopol, Singapore, Sverdlovsk, Tbilisi, and Thule. This includes all but two entries in table 10.

5.2.4 Use of High-Latitude Absorption Events to Determine Man-Made High-Latitude Man-Made Noise Environments

In both northern and southern Arctic regions, Herman (1962, 1963, 1964) has shown that atmospheric noise decreases during polar cap absorption (PCA) events, most markedly in the HF band. He has estimated the probable magnitude of man-made noise in the HF band from data taken when atmospheric noise is absent. He estimated the man-made noise level during PCA events at both Thule, Greenland, and at Byrd Station, Antarctica.

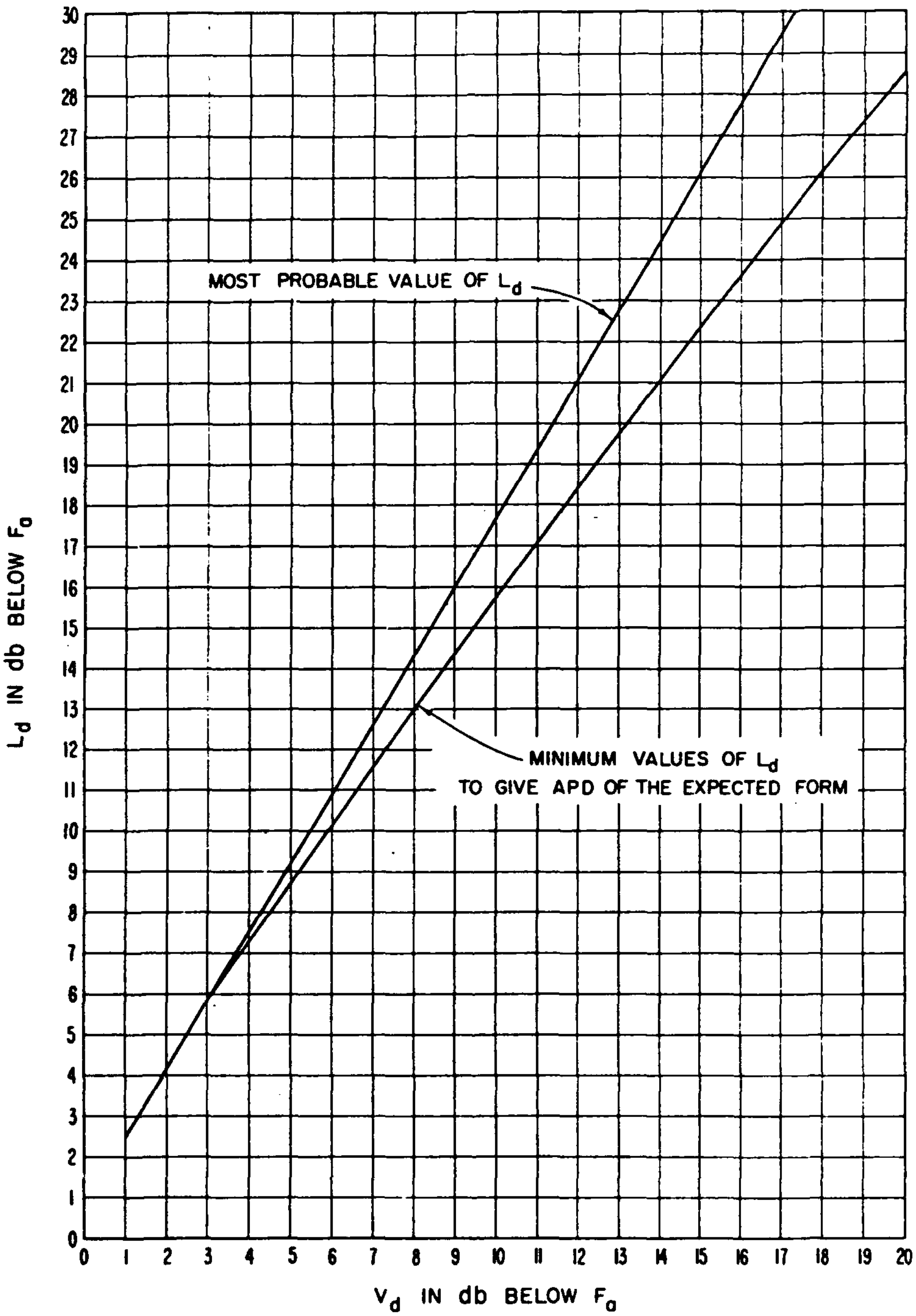

Figure 82. Most probable and minimum values of L_d versus V_d for atmospheric radio noise.

Herman used a noise index, defined as the daily average fractional departure of the measured noise from the month-hour median, to select anomalous absorption periods between March 1958 and December 1959. Both polar cap and auroral zone absorption events were detected with this index. At Byrd Station, 14 PCA events were identified that correspond to previously reported Nothern Hemisphere PCAs. It was shown that PCA has a remarkable effect on HF atmospheric radio noise. The noise level is severely depressed, especially on 5.0 and 10 MHz, and remains so during the entire PCA event. The noise level is depressed as much as 25 dB below the median during PCA.

Figure 83 shows the mimimum noise on each frequency during all PCAs for Byrd Station averaged together and plotted as a function of frequency. (The minimum noise recorded during absorption events in all cases was the the minimum recorded in the month without regard to ionospheric conditions.) The average deviation is ±3 dB or less on all frequencies. Curve B shows the minimum radio noise level that can be expected at any time at Byrd Station, regardless of the source. Because ionospheric absorption is maximum at the gyro-frequency, Herman felt that the measured noise power on 2.5 and 5.0 MHz during intense absorption events consisted entirely of man-made noise. Therefore, he estimated a man-made noise curve (curve C), with the same slope as used in CCIR for man-made noise. At 10 and 20 MHz, the noise power is above the indicated man-made noise level because the absorption of the distant atmospheric noise changes inversely as the square of the frequency and because of a large contribution from cosmic noise at frequencies near and above the F-layer critical frequency. Below 2.5 MHz, the noise power becomes increasingly greater than the man-made level because complete absorption of the atmospheric noise does not take place on the frequencies that do not penetrate completely throughout the D-region before reflection. Curve A is the median autumn 00–04 time block curve for Byrd Station for comparison.

Of all the atmospheric noise measurement sites, only Murmansk is far enough north to experience a PCA event. The geomagnetic latitude there is 64.1 degrees north. This means reprocessing the noise data for this location, but likely will improve the values of 1-MHz atmospheric noise estimates for this site. It does require the daily noise measurements to determine the noise index to establish the days for which PCA events occured while noise measurements were underway.

5.3 INTERPOLATION OF CORRECTION FACTORS TO THE STANDARD GRID

After obtaining the correction factors, the next step is to interpolate these data to a standard 100-latitude by 84-longitude grid. Once this has been accomplished, then the correction factors are added to noise values for the original CCIR Report 322 also given at these same grid locations for each time block and season.

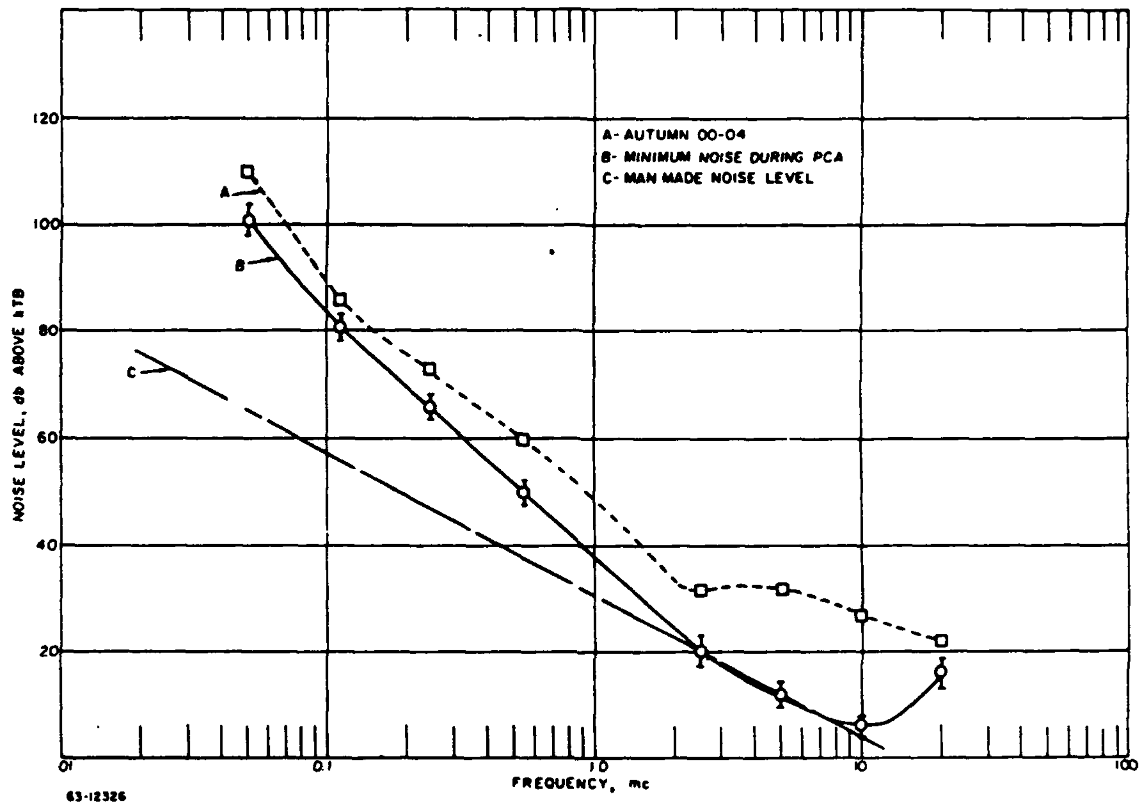

Figure 83. Minimum noise level observed at Byrd Station during PCA.

To interpolate the data to a standard 100-latitude by 84-longitude grid it is necessary to choose an accurate interpolation method. The available methods seem to fall into two categories. The first category includes methods that interpolate data in a plane. Methods that could be used that fall into this category include Akima (1978a, 1978b, 1979), Cline and Renka (1984), Renka (1984c), and Renka and Cline (1984). Additional methods are described by Franke (1982). The disadvantage to these methods is that the interpolation is affected by the boundary imposed by the available data points. This affects both the number of triangles and the choices themselves of the triangles chosen for the interpolation. The second category eliminates the boundary by interpolating the data on a sphere. There are two methods available for this purpose (Lawson, 1982; Lawson, 1984; Renka, 1984a; Renka, 1984b). The method due to Renka is available from the Association for Computing Machinery. As the atmospheric noise data was measured on a sphere, these two methods would be applicable. It will be necessary to test the accuracy of these two methods against a benchmark. One such benchmark might be computed results from a model of the Earth's magnetic field.

5.4 NUMERICAL MAPPING OF THE NOISE DATA

The final step in the development of an improved atmospheric noise model is the numerical mapping of the 100-by-84 grid data sets for use in computer programs. Two numerical mapping techniques are available for this purpose (Lucas and Harper, 1965; Zacharisen and Jones, 1970). The Zacharisen and Jones method results in a considerable reduction of coefficients but was originally designed to be used with data given as a function of universal time. The reduction in coefficients significantly reduces the computation time of models produced by the technique. Sailors (1985) found that the local-time Lucas and Harper model was not always more accurate than the universal-time Zacharisen and Jones model. Moreover, Sailors reported the development of a 1-MHz minicomputer atmospheric noise model in local time using a modification of the Zacharisen method. He found that for each and every case, the local-time map had a lower error than the corresponding universal-time map. This occurs because the gradients of atmospheric noise as a function of longitude are much smaller than those in universal time. Hence, it appears that the Zacharisen and Jones numerical mapping technique applied in local time is more accurate than the Lucas and Harper method and would be the method to use.

One major problem exists with numerical mapping techniques. That is the tendency to smooth out physical properties of the atmospheric noise, particularly at low latitude where the gradient in atmospheric noise maximizes due to concentration of noise sources in that region. As the number of harmonics in the numerical map is reduced to make the model efficient, the high-level contours begin to disappear, enhancing the problem. Sailors (1983) showed that an improvement can be made by making a transformation so that the latitude input into the latitude function in the numerical mapping process is spread further away from the equator than the actual latitude. This transformation resulted in a more uniform variation of atmospheric noise as a function of the modified latitude than for the actual latitude. The transformations used preserved the stability of the latitude function at the poles. One problem was that the transformations were applied with the universal-time version of the Zacharisen and Jones mapping technique. The gradients in longitude had a tendency to introduce errors at other longitudes removed from the atmospheric noise storm centers. When used with the local-time Zacharisen and Jones technique, it can be expected to work even better in improving the atmospheric noise model.

6.0 CONCLUSIONS AND RECOMMENDATIONS

This report has presented the probable cause and a recommended solution for a discrepancy in the CCIR Report 322-3 radio noise model. This report has not determined whether there is a discrepancy between the new CCIR model and the data values used to develop it. Nor has there been an attempt to determine the validity of the measured data values used to develop the model or to validate the model against any other data.

The basis for this discrepancy was found to be in the procedure used to prepare the measured noise data for the determination of a global numerical representation of the 1-MHz data. The procedure followed in the development of the model was to determine correction factors to the old CCIR model for each measurement site, to interpolate these corrections to a 100-latitude by 84-longitude grid for each time block/season, to add the correction factors at each grid point to corresponding values for the old CCIR model, and finally to numerically map the resulting data for each time block and season. Nineteen locations were used in the final model. Four sites used in the original CCIR model were not used. These include Bill, Wyoming; Byrd Station, Antarctica; Ibadan, Nigeria; and Thule, Greenland. As no correction factors were obtained for these locations or a correction factor of zero was used, the interpolation algorithm used to obtain the 100-latitude by 84-longitude grid of correction factors supplied other values. For Bill, Wyoming, the result is not too serious, but for the other three sites the error is at some seasons and time of day serious. For Thule, Greenland, the maximum and minimum errors in the correction contours were 10.1 and –10.8 dB, respectively. For Ibadan, Nigeria, the maximum and minimum errors were 12.5 and –1.5 dB, respectively. For Byrd Station, Antarctica, the maximum and minimum errors were 12.0 and 3.0 dB, respectively. Examination of the geographical extent of these errors reveals that the error is not confined to the measurement location but in fact is very large. It was found that the error as a function of frequency was diurnally dependent. An error of 10 dB at 1 MHz was more serious at another frequency during local daytime than at night. Finally, the absence of the data locations affected the accuracy of the interpolation itself.

Because of the errors in the CCIR Report 322-3 atmospheric noise model, it is recommended that it be used with caution. It is most accurate in Europe, Asia, the Indian Ocean, the western Pacific from Asia to the date line, and Australia. It is most inaccurate in both the northern and southern high latitudes, the Arabian Peninsula, northern Africa, and the mid-Atlantic Ocean area. For applications in the latter list of areas, the user should consider using the original CCIR Report 322 model.

A three-step process was proposed to develop a new 1-MHz atmospheric noise model. The first step was to obtain correction factors for additional locations to increase the accuracy of the interpolation. Nine additional locations were identified as locations for which there might be sufficient data to obtain correction factors.

Three methods were presented that might be used in removing the effects of man-made noise from the noise data. Second, two alternate methods of interpolation were

identified. It was proposed that the accuracy of these methods be examined against a benchmark to be determined. Finally, it was proposed that the local time version of the Zacharisen and Jones (1970) numerical mapping technique be used to develop the final model. In addition, it was proposed that a latitude transformation be used to increase the accuracy of the numerical mapping itself.

It is recommended that the U.S. counterpart to CCIR Study Group 6 take a lead role in submitting a corrected model to the CCIR.

7.0 REFERENCES

Akima, H. 1978a. "A method of bivariate interpolation and smooth surface fitting for irregularly distributed data points," *ACM Trans. Math. Software*, Vol. 4, pp. 148–159.

Akima, H. 1978. "Algorithm 526 bivariate interpolation and smooth surface fitting for irregularly distributed data points[E1]," *ACM Trans. Math. Software*, Vol. 4, pp. 160–164.

Akima, H. 1979. "Remark on Algorithm 526," *ACM Trans. Math.* Software, Vol. 5, pp. 242–243.

Akima, H. 1984. "On estimating partial derivatives for bivariate interpolation on scattered data," *Rocky Mountain J. Math.*, Vol. 14, pp. 41–52.

Bowen, N. M. and A. C. Fraser-Smith. 1992. "A comparison of measured 32 MHz radio noise amplitudes with CCIR model predictions," National Radio Science Meeting, 7–10 Jan 1992, Boulder, CO.

CCIR Xth Plenary Assembly. 1964. "Geneva, World Distribution and Characteristics of Atmospheric Radio Noise," Report 322c, Geneva, Int. Telecommun. Union.

CCIR XVth Plenary Assembly, Dubrovnik. 1988. "Characteristics and Applications of Atmospheric Radio Noise Data" Report 322-3c, Geneva, Int. Telecommun. Union.

Chindahporn, R. and E. L. Younker. 1968 (May). "Analysis of medium- and high-frequency atmospheric radio noise in Thailand," Stanford Research Institute Special Tech., Report 37, Contract DA 36-039 AMC-00040(E).

Cline, A. K. and R. J. Renka. 1984. "A storage-efficient method for construction of a Thiessen triangulation," *Rocky Mountain J. Math.*, Vol. 14, pp. 119–139.

Crichlow, W. Q., C. A. Samson, R. T. Disney, and M. A. Jenkins. 1959. "Radio noise data for the International Geophysical Year July 1, 1957 - December 31, 1958," National Bureau of Standards Tech. Note 18, 27 July 1959.

Crichlow, W. Q., C. J. Roubique, A. D. Spaulding, and W. M. Beery. 1960a. "Determination of the amplitude-probability distribution of atmospheric radio noise from statistical moments," *J. Research NBS*, Vol. 64D.

Crichlow, W Q., R. T. Disney, and M. A. Jenkins. 1960b. "Quarterly Radio Noise Data - June, July, August 1959," National Bureau of Standards Tech. Note 18-3, 9 September 1960.

Crichlow, W. Q., A. D. Spaulding, C. J. Roubique, and R. T. Disney. 1960c. "Amplitude-Probability Distributions for Atmospheric Radio Noise," National Bureau of Standards Monograph 23, 4 November 1960.

Crichlow, W. Q., R. T. Disney, and M. A. Jenkins. 1967. "Quarterly radio noise data September, October, November 1966," Environmental Science Services Administration Tech. Report IER 18-ITSA 18-32, October 1967.

Franke, R. 1982. "Scattered data interpolation: tests of some methods," *Math. Comput.*, Vol. 38, pp. 181–200.

Fraser-Smith, A.C., R. A. Helliwell, B.R. Forthnam, P.R. McGill, and C.C. Teague. 1987. "A new global survey of ELF/VLF radio noise," AGARD Conf. Proc., CP 420 on Effects of Electromagnetic Noise and Interference on Performance of Military Radio Communication Systems.

Herman, J.R. 1962. "Polar-cap and auroral-zone absorption effects on 2.5 and 5.0–megacycles per second atmospheric radio noise," J. Geophys. Res., Vol. 67, pp. 2299–2308.

Herman, J.R. 1963. "Atmospheric radio noise at Byrd Station, Antarctica," Avco Corporation Antarctic Research and Data Analysis Sci. Report 9, Tech. Report RAD–TR–63–46, Contract NSF–C255, 27 December 1963.

Herman, J.R. 1964. "Radio noise problems in arctic regions,"Arctic Communications, AGARDograph No. 78, edited by B. Landmark, Pergamon Press, Oxford.

Huang, Y. 1977. "Variations of atmospheric noise at Ping-Cheng, Taiwan, China," *Radio Sci.*, Vol. 12, pp. 239–247.

Lawson, C.L. 1977. "Software for C1 surface interpolation," Mathematical Software III, edited by J.R. Rice, Academic Press, New York.

Lawson, C.L. 1982 (July). "C1 surface interpolation for scattered data on a sphere," Proc. of the Surfaces Symposium, Stanford Univ.

Lawson, C.L. 1984. "C1 surface interpolation for scattered data on a sphere," *Rocky Mountain J. Math.*, Vol. 14, pp. 177–202.

Lucas, D. and J.D. Harper, Jr. 1965. "A numerical representation of CCIR Report 322 high frequency (3–30 mc/s) atmospheric radio noise data," National Bureau of Standards Tech. Note 318, 5 August 1965.

Renka, R.J. 1984a. "Interpolation of data on a sphere," *ACM Trans. Math. Software*, Vol. 10, pp. 417–436.

Renka, R.J. 1984b. "Algorithm 623 Interpolation on the surface of a sphere," *ACM Trans. Math. Software*," Vol. 10, pp. 437–439.

Renka, R.J. 1984c. "Alogorithm 624 Triangulation and interpolation at arbitrarily distributed points in the plane," *ACM Trans. Math. Software*, Vol. 10, pp. 440–442.

Renka, R.J. and A.K. Cline. 1984. "A triangle-based C1 interpolation method," *Rocky Mountain J. Math.*, Vol. 14, pp. 223–237.

Ripley, B.D. 1981. *Spatial Statistics*, John Wiley & Sons, New York.

Sailors, D.B. 1983. "Advances in atmospheric noise mapping by numerical methods," National Radio Science Meeting, Boulder, CO, 5–7 January 1983.

Sailors, D.B. 1985. "Development of a minicomputer 1 MHz atmospheric noise model in local time," North American Radio Science Meeting, Vancouver, Canada, 17–21 June 1985.

Sailors, D.B. and R.P. Brown. 1982 (May). "Development of a minicomputer atmospheric noise model," Naval Ocean Systems Center Tech. Report 778.

Sailors, D.B. and R.P. Brown. 1983. "Development of a minicomputer atmospheric noise model," *Radio Sci.*, Vol. 18, pp. 625–637.

Spaulding, A.D. and J.S. Washburn. 1985. "Atmospheric radio noise: worldwide levels and other characteristics," National Telecommun. and Information Administration Report 85–173.

Zacharisen, D.H. and W.B. Jones. 1970 (October). "World maps of atmospheric radio noise in universal time," Institute for Telecommun. Sciences Res. Report 2.

REPORT DOCUMENTATION PAGE

Form Approved OMB No. 0704-0188

1. AGENCY USE ONLY *(Leave blank)*	2. REPORT DATE	3. REPORT TYPE AND DATES COVERED
	May 1993	Final

4. TITLE AND SUBTITLE

A DISCREPANCY IN THE CCIR REPORT 322–3 RADIO NOISE MODEL
The Probable Cause and a Recommended Solution

5. FUNDING NUMBERS

PE: 0601153N, OMN
AN: DN307, 513, DN303046
PROJ: MP82, CM20

6. AUTHOR(S)

David B. Sailors

7. PERFORMING ORGANIZATION NAME(S) AND ADDRESS(ES)

Naval Command, Control and Ocean Surveillance Center (NCCOSC)
RDT&E Division
San Diego, CA 92152–5001

8. PERFORMING ORGANIZATION REPORT NUMBER

TD 2496

9. SPONSORING/MONITORING AGENCY NAME(S) AND ADDRESS(ES)

Space and Naval Warfare Systems Command
Washington, DC 20363

Office of Naval Research
800 N. Quincy Street
Arlington, VA 22217

10. SPONSORING/MONITORING AGENCY REPORT NUMBER

11. SUPPLEMENTARY NOTES

12a. DISTRIBUTION/AVAILABILITY STATEMENT

Approved for public release; distribution is unlimited.

12b. DISTRIBUTION CODE

13. ABSTRACT *(Maximum 200 words)*

The cause of a reported discrepancy in the CCIR Report 322–3 radio noise model was determined, and a course of action to overcome the discrepancy is recommended.

The source of the discrepancy was found to be in the procedure used to prepare the measured noise data for the determination of a global numerical representation of the 1-MHz data. In the development of the model, correction factors to the old CCIR model were determined for each measurement site. These corrections were interpolated to a 100-latitude by 84-longitude grid for each time block/season. The correction factors at each grid point were then added to corresponding values for the old CCIR model, and finally the resulting data for each time block and season were numerically mapped. Nineteen locations were used in the final model. Four sites used in the original CCIR model were not used, including Bill, Wyoming; Byrd Station, Antarctica; Ibadan, Nigeria; and Thule, Greenland. As no correction factors were obtained for these locations or a correction factor of zero used, the interpolation algorithm used to obtain the 100-latitude by 84-longitude grid of correction factors supplied other values. For Bill, Wyoming, the result is not too serious; but for the other three sites, the error is at some seasons and time of day serious. For Thule, Greenland, the maximum and minimum errors in the correction contours were 10.1 and −10.8 dB, respectively. For Ibadan, Nigeria, the maximum and minimum errors were 12.5 and −1.5 dB, respectively. For Byrd Station, Antarctica, the maximum and minimum errors were 12.0 and 3.0 dB, respectively. Examination of the geographical extent of these errors reveals that the error is not confined to the measurement location but in fact is very large. It was found that the error as a function of frequency was diurnally dependent. An error of 10 dB at 1 MHz was more serious at another frequency during local daytime than at night. The absence of the data locations affected the accuracy of the interpolation itself.

The recommended course of action includes (1) obtain correction factors for additional locations to increase the accuracy of the interpolation; (2) test the method of interpolation against a benchmark; (3) use the Zacharisen and Jones numerical mapping technique applied in local time to develop a new 1-MHz model; (4) consider using a latitude transformation to increase the accuracy of the numerical mapping technique; (5) submit a corrected model to the CCIR; and (6) use the CCIR Report 322–3 atmospheric model with caution, especially in the northern and southern high latitudes, the Arabian Peninsula, northern Africa, and the mid-Atlantic Ocean area. In these cases, consider using CCIR Report 322 instead until an improved model is available.

14. SUBJECT TERMS

atmospheric noise measurement
radio noise models

15. NUMBER OF PAGES

90

16. PRICE CODE

17. SECURITY CLASSIFICATION OF REPORT	18. SECURITY CLASSIFICATION OF THIS PAGE	19. SECURITY CLASSIFICATION OF ABSTRACT	20. LIMITATION OF ABSTRACT
UNCLASSIFIED	UNCLASSIFIED	UNCLASSIFIED	SAME AS REPORT

21a. NAME OF RESPONSIBLE INDIVIDUAL	21b. TELEPHONE (Include Area Code)	21c. OFFICE SYMBOL
David B. Sailors	(619) 553–3063	Code 542

INITIAL DISTRIBUTION

Code 0012	Patent Counsel	(1)
Code 50	H. O. Porter	(1)
Code 54	J. H. Richter	(5)
Code 542	J. A. Ferguson	(10)
Code 542	D. J. Sailors	(20)
Code 542	W. K. Moision	(1)
Code 542	R. Rose	(1)
Code 542	F. P. Snyder	(1)
Code 772	J. A. Audia	(1)
Code 772	N. Ai	(1)
Code 772	B. J. Satterlee	(1)
Code 832	P. A. Singer	(3)
Code 832	P. M. Hansen	(1)
Code 832	K. Grauer	(3)
Code 833	G. Crane	(1)
Code 961	Archive/Stock	(6)
Code 964B	Library	(2)

Defense Technical Information Center
Alexandria, VA 22304–6145 (4)

NCCOSC Washington Liaison Office
Washington, DC 20363–5100

Center for Naval Analyses
Alexandria, VA 22302–0268

Navy Acquisition, Research and Development Information Center (NARDIC)
Washington, DC 20360–5000

GIDEP Operations Center
Corona, CA 91718–8000

NCCOSC Division Detachment
Warminster, PA 18974–5000

Space and Naval Warfare Systems Command
2451 Crystal Drive
Arlington, VA 22245–5200

Naval Computer & Telecommunications Command
Washington, DC 20390

Office of Naval Research
Arlington, VA 22217–5000

Electromagnetic Compatability Analysis Center
Annapolis, MD 21402–1187 (3)

Defense Information Systems Agency
Arlington, VA 22203 (2)

Chief of Naval Operations
Washington, DC 20350–2000 (2)

U.S. Army HQDA
Washington, DC 20310–0107

U.S. Army Electronic Proving Grounds
Fort Huachuca, AZ 85613–7110 (2)

U.S. Army ISEC
Fort Huachuca, AZ 85613–5300 (2)

CECOM
Fort Monmouth, NJ 07703

Phillips Laboratory
Kirkland AFB, NM 87117

Institute for Telecommunication Sciences
Boulder, CO 80303–3328 (2)

National Telecommunications & Information Administration
Annapolis, MD 21401

Voice of America
Washington, DC 20024 (2)

Stanford University
Stanford, CA 94305 (2)

Pacific Sierra Researach Corporation
Santa Monica, CA 90025 (2)

SRI International
Arlington, VA 22209